Optimization of various procedures in terms of testing and manufacturing procedures for CERN's homemade force transducer – The capacitive gauge.

Πειραματική μελέτη για την βελτιστοποίηση του χειροποίητου αισθητήρα μέτρησης δύναμης και πίεσης επιφανείας – CERN'scapacitivegauge – σε θέματα εφαρμογής, μετρήσεων και παραγωγής.

Βελισσαρίδης Κωνσταντίνος - K. Velissaridis

Bachelor Thesis 03/12/2013

Technological Educational Institute Of Piraeus

Tutor

Κωνσταντίνος Στέφανος
Νίκας

Supervisor

Michael Guinchard

Αφιερωμένο με πολλή
αγάπη στον πατέρα μου.

Acknowledgments

Within these few paragraphs, I wantto try to express my sincere gratitude to all the people that provided me the opportunity to spend the last year of my bachelor studies, in such wonderful places as CERN, Switzerland and France.Thanks to you, not only have I learned great things for my future career as a mechanical engineer and was I introduced with the best possible way to this demanding field of engineering, but I have also had greatsocial moments that assembled the most memorable year of my life.

To begin with, I would like to thank my supervisor Michael Guinchard for accepting and making me a part of his team, treating me like a member of the MML "family" from the very first moment I stepped foot at CERN. He was there to guide me and teach me things that can be by no means learned only from reading books. Thank you Michael!

I would also like to thank Ofelia Capatina and Francesco Bertinelli the leaders of ES and MME groups accordingly. Moreover, a big thank you to all the people that helped me run all this measurements and write this thesis. AlexandreGerardin, AgostinoVacca, Miguel Gil Costa, Marina Malabaila and the people from the metrology section that helped me with the pre-stressing plates activity. Also Philippe for machining the pieces and for helping me with the hardness measurements.Robin Betemps that corrected and helped me with the mechanical drawings. Thank you all, you proved that by working as a team, great things can be achieved.

Additionally, I want to thank Raul and Tommi, the two previous technical students of MML that guided me during my first days and provided me the resources on which my work and this thesis are based on. Also all the people that shared a coffee break or a lunch break with me during this year, the Italian team Federico and Nicolas, Edyta and Harris.

The last people, I would like to thank from CERN are my laboratory colleagues. Angelina, Sergio, Antonin, Yan, Philippe, Diego, Oscar, Smurfus and of course Daniel. Specifically for Daniel, thank you for supporting my every move, thank you for transforming several working hours into funny and educative moments and finally thank you for being a great friend,colleague and teacher.

As for my Technological Institute, I would like to thank all the teachers that contributed to my knowledge and patiently taught me all the things that I know about the mechanical engineering field. I would also like to thank my two great classmates and friends Konstantinos Loukis and MichaelFotsalis that helped me get through countless hours of lectures and write all these laboratory exercise reports. The last person to thank from my institute is my tutor Konstantinos StefanosNikas. Not only did he manage to teach us some of the most difficult courses I had during my studies, in the most clear, professional and constructive way but he also stood by me in every difficulty I faced with my studies and showed so much interest to help me with my future.Δάσκαλε, thank you so much for everything and I hope that more teachers will follow your steps in the future leading the way for young students.

Concluding, I would like to thank my family and my friends for always supporting me and making me feel that they are right next to me even though 2500 Km of distance is separating us. Finally, Maria, my life partner, this was a difficult year but we made it thanks to the strong foundations we have built together all these years you are next to me. Thank you for making me the man I am today, for existing and for being you... Infinity times infinity.

Thank you all for everything!

Table of Contents

Purpose of the thesis

This thesis has been written keeping in mind that it will serve two purposes. The first purpose is to present the steps that have been followed in order to further progress the overall optimization of a force transducer called the capacitive gauge. The second purpose is to guide all the people that will work on this topic in the future, to become familiar with this sensor and to adapt to some of the procedures this thesis includes.

In order to achieve these goals, this document has been divided into three chapters. The first chapter is aiming to introduce someone to the capacitive gauges. It explains the working principals and describes the need for theirs production. The second chapter is aiming to present the steps that have been followed in order to improve the way they are being tested and calibrated and introduce the readers into newly adapted procedures to achieve these two. The third and final chapter is dedicated to the manufacturing procedure of the gauges. New ideas have been implemented and are presented in order to discover alternative ways to achieve better results, obtainable fasterand easier. Finally a sequence of the actions that have been followed to solve an existing problem with the manufacturing procedure of the capacitive gauges has been described, leading to some conclusion and suggestion paragraphs that should be followed, the problem will be resolved.

Chapter I
Introduction

Section I
CERN

The European Organization for Nuclear Research (French: ConseilEuropéen pour la Recherché Nucléaire), known as CERN, is the largestparticle physics centre.in the world. In CERN, scientists from all over the world come to explore what matter is made of and what forces hold it together. This becomes possible by running experiments utilizing the LHC, the world's largest and most powerful particle accelerator.
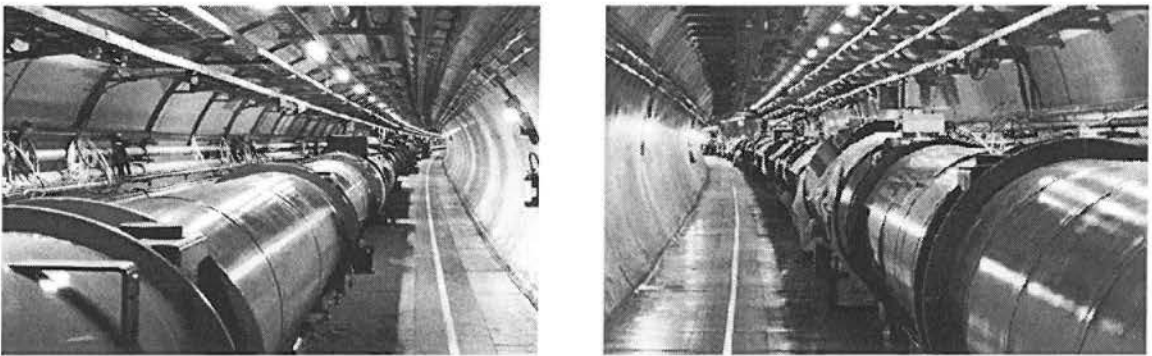
Figure 1: The LHC – Large Hadron Collider

The LHC mainly consists of a 27 km ring of superconducting magnets with a number of accelerating structures to boost the energy of the particles along the way. The main idea is to make two beams of particles circulate and accelerate in the LHC andwhen they have reached a certain amount of energy,having acquired almost the speed of light,they collide in the center of CERN's detectors. By doing so, new particles are beingcreated giving the chance to physicists to study them, confirm their theories and discover the reasons behind our very existence.

CERN was founded 1954 and nowadays it employs more than 10000 people from all around its 22 European member states, including Greece and various other people from external enterprises.
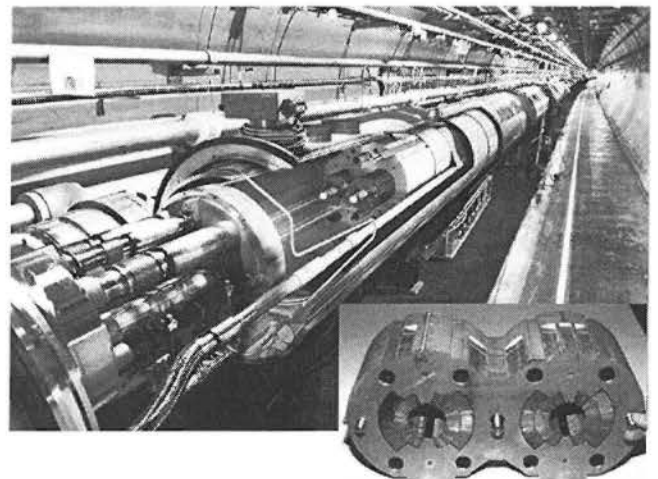
Figure 2: LHC dipole's core.

> ## *Mechanical Measurements Laboratory*

CERN is divided in departments and experiments. One of the departments, the Engineering Department (EN) has the purpose of providing CERN with the engineering competences, infrastructure systems and technical coordination required for the design, installation, operation, maintenance and dismantling phases of the CERN accelerator complex and its experimental facilities. A part of the EN department, the Mechanical & Materials Engineering Group (MME) provides to the CERN community specific engineering solutions, combining mechanical design, production facilities and material sciences. Inside the MME group, the Mechanical Measurements Lab (MML) [Ref: 6] is an entity which aim is to provide support in the measurement of mechanical (including deformations, vibrations, ground motion or modal analysis), electrical or thermal properties and effects. This includes everything from the design of each individual test to the data acquisition and the data analysis; as well as the design, manufacturing, installation and control of different kind of gauges. The goal of the MML is to provide mechanical measurement expertise to various on-going projects all around CERN facilities, both to validate theoretical models or mechanical assemblies and to assess whether the tested systems are functioning properly and most importantly safely.
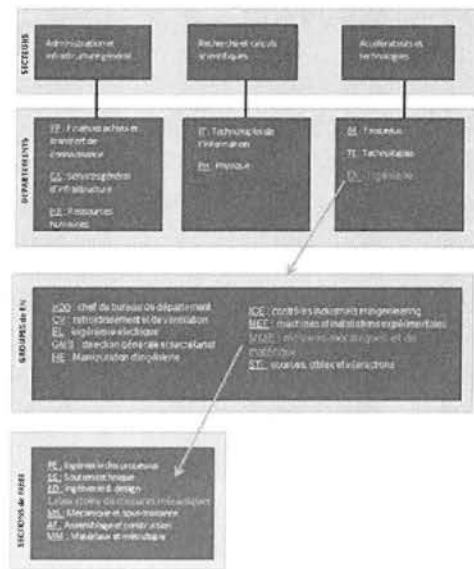

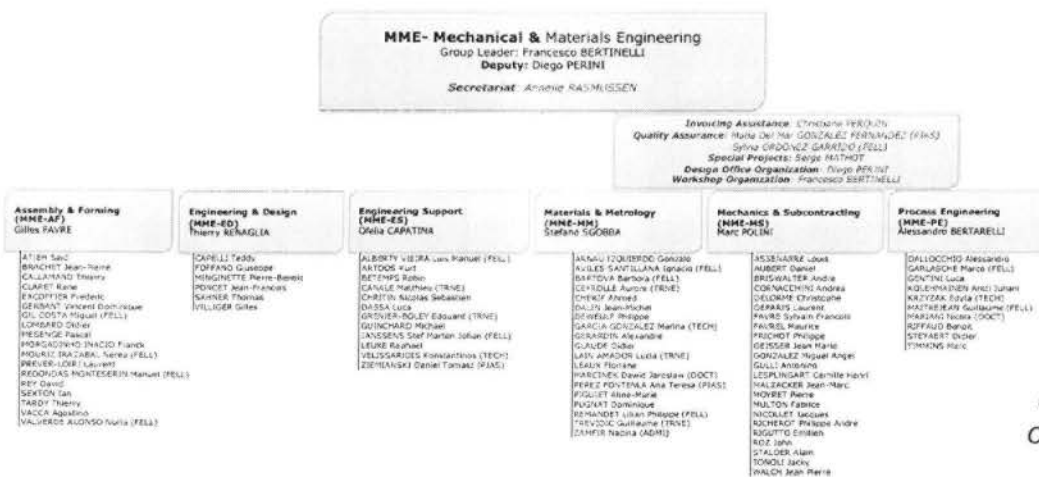*Figure 3: CERN's organization chart*

Figure 4: MME's organization chart

> ## *The need for a special sensor*

Inside the LHC, several kinds of superconducting magnets are used to provide the tangential acceleration to the beam and bend it to the mentioned orbit (dipoles) or to focus it (quadrupoles).LHC upgrades are directly linked to the development of these superconducting magnets. In order to raise the energy of the accelerator, upgraded, better and more powerful magnets have to be developed.

One of the consequences of raising the power of the magnets is that higher magnetic fields, cause higher magnetic Lorentz forces acting in the coils and one of the milestones of the development is to avoid the implosion of the assembly during the performance of the magnet in cryogenic environments. For this, a minimum compressing force has to be assured on the coils at all times. In order to apply this compressing force, an amount of pre-stress is applied tangentially and radially to the setup in room temperature, which needsto be both calculated and measured.

This is not a trivial task, as the assembly is rather complex: the core alone is formed by layers of collars of stainless steel that hold the copper coils, which are insulated by a layer of Kapton®, a polymer developed by DuPont. Such mix of materials and shapes are linked, in addition to the fact that all the setup has to be cooled down to 4.2K to provide superconducting properties to the cables. This change of temperature causes a decrement of volume in the materials which might greatly vary depending on the material. This change of volume causes a change in the internal stress state of the material, caused by the initial deformation applied to the setup. The main goal of this task is to guarantee a minimum force while, in the final conditions, without overstressing and causing plastic deformations on the materials during the assembly phase.
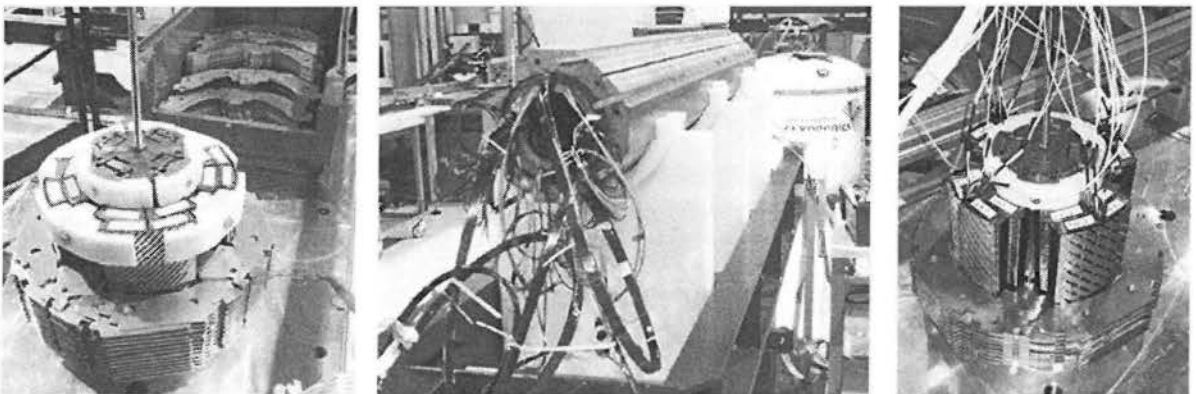
Figure 5: MQXC quadrupole mock-ups. Short model (Extremities) and full length (Center)

After a first phase of theoretical calculations to optimize the design, several tests are been made on different mock-ups in order to validate the FEA models and to optimize the mechanical parameters for the final model.One of the tests performed is the pressure monitoring of an interphase of the coil packs during the assembly and the cool-down to cryogenic temperatures. For this reason a special sensor has been developed at CERN in1995, named "the capacitive gauge".

Figure 6: A series of capacitive gauges monitoring the interface of the coil packs displayed in the CAD model.
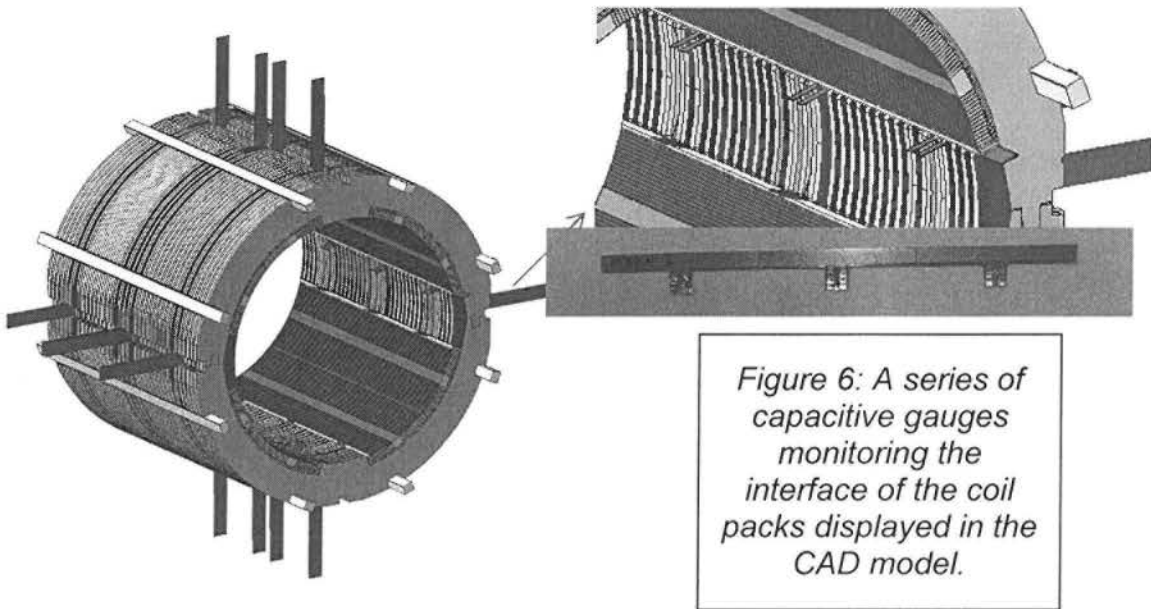
Figure 7: Preparation of a coil pack.
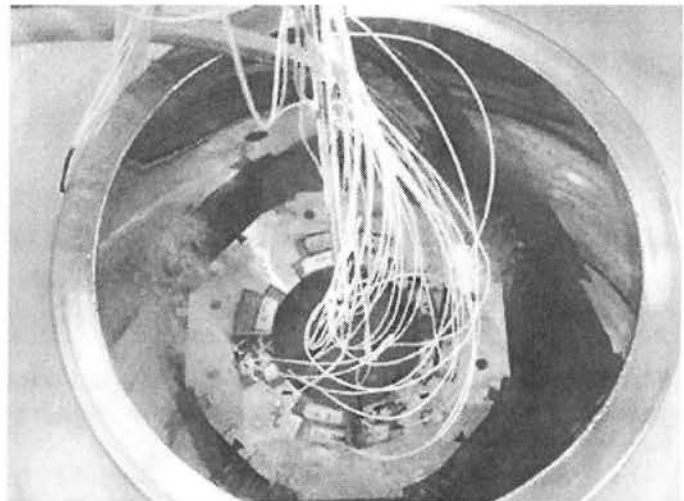
Figure 8: Pressure monitoring at 77K.

Section II
The capacitive gauges

Figure 9: The capacitive gauge.

The capacitive force transducers have been developed and used for monitoring the coil pre-stress during assembly and excitation of several magnet mock ups for the LHC. Typically these gauges are strip several tenths of millimetre thick that can be shaped to a large variety of geometries.
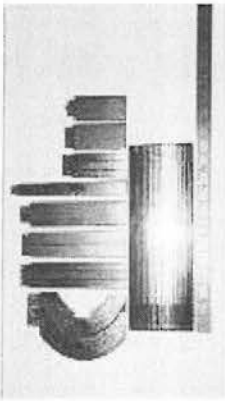
Figure 10: Various geometries depending on the request.
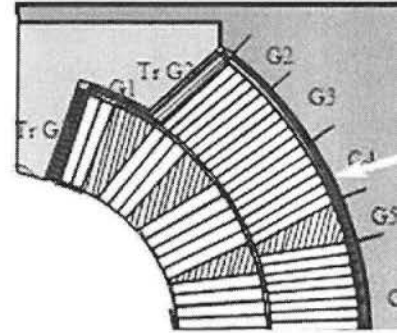
Figure 11: Capacitive gauges inside an LHC dipole

Inserted between two surfaces, they allow measuring the local distribution of contact pressures for up to 200 MPa,from room temperature to 1.9 K with in the presence of static magnetic fields. The sequence and the quality of the manufacturing steps are determining factors in terms of performance for this kind of gauges.

Each gauge consists of a "sandwich" of stainless steel foils interleaved with polyimide films glued together (Fig: 12 and 13).
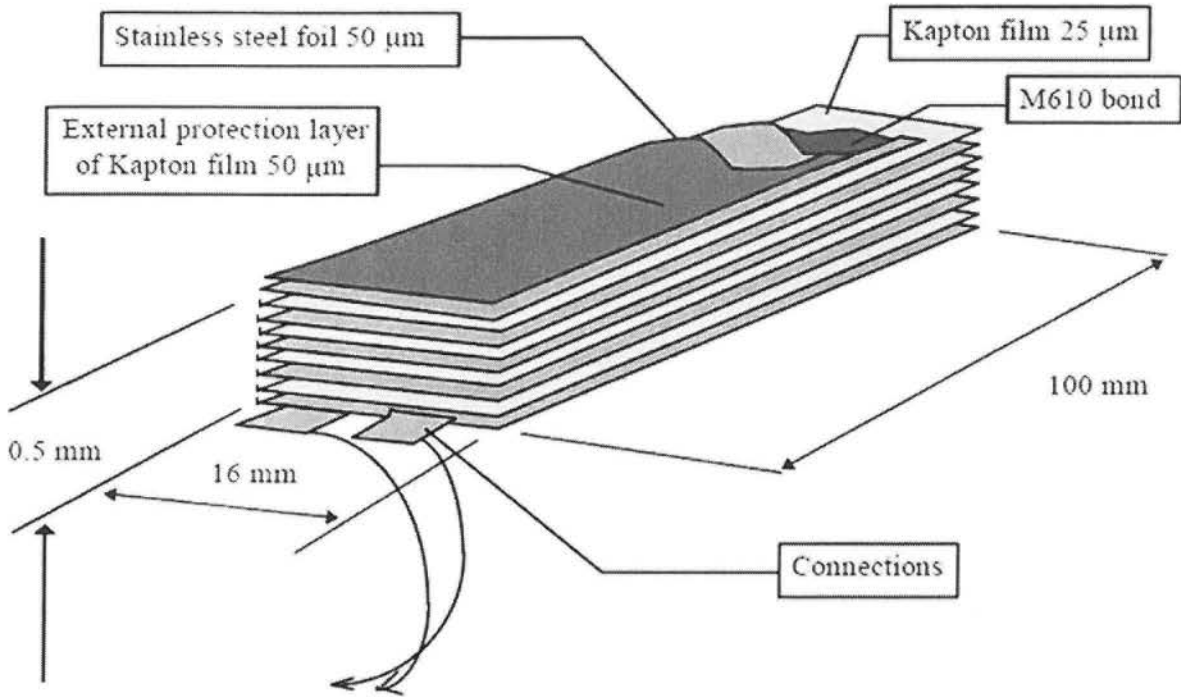
Figure 12: Typical capacitive gauge structure.
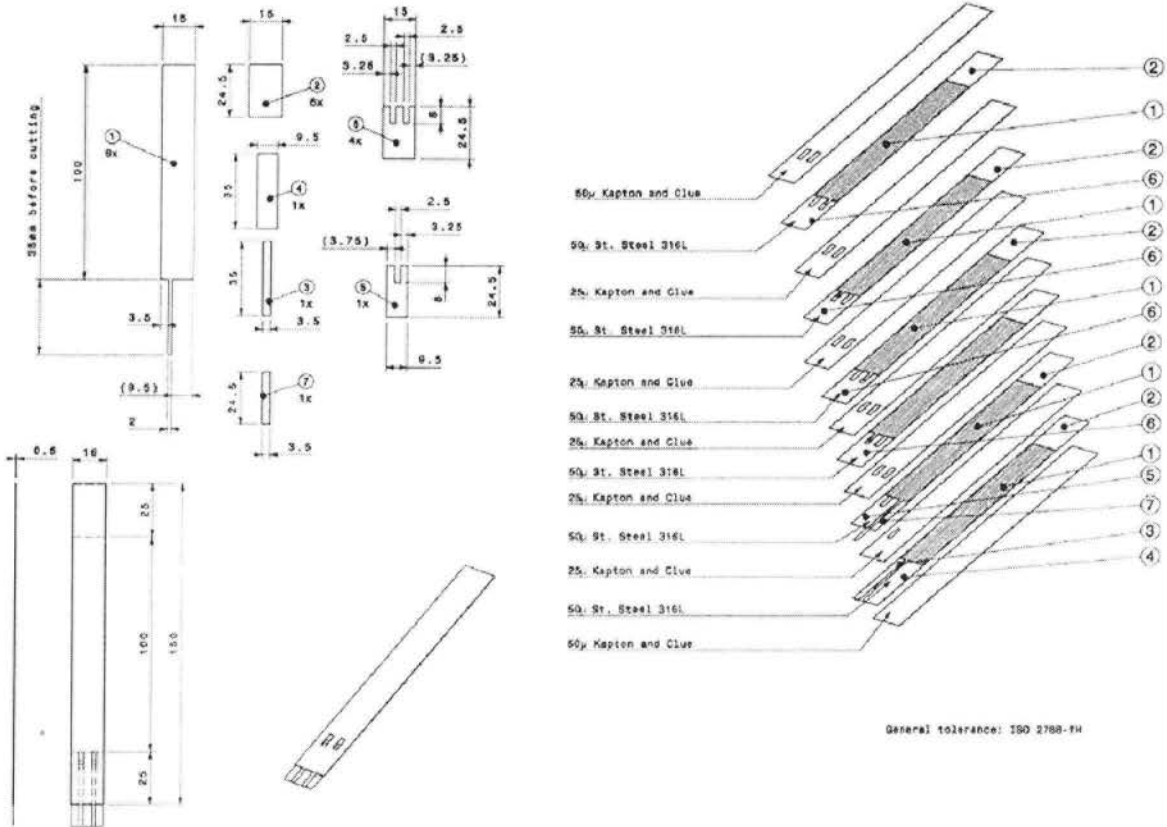
Figure 13: Type 57 capacitive gauge (Source: EDMS 1015738)

Much like a capacitor, the capacitance of each gauge is directly dependant on its geometry and the electrical permittivity of the dielectric. For conditions prevailing in superconducting magnet applications (high pressure cycling in a wide range of temperatures), polyimide tapes are well suited. The capacitive gauge is being consisted of layers of stainless steel separated by layers of DuPont Kapton®, acting as a condenser. When an external pressure compresses the Kapton, it changes the distance between steel layers and so, it changes the capacitance. The layers of conductor and dielectric are glued together by a specific epoxy resin adhesive (Vishay M-Bond 610), formulated specifically for gluing strain gauges. The adhesive works in the range of temperatures between -269 and 370°C and the curing is done by warming it up during two hours at 150°C and with a recommended pressure of up to 220 MPa. The reason why there is a need to make a sandwich with the stainless steel foils will become apparent in the analysis section.

The capacitive gauges are interesting from several points of view. First, its small thickness allows them to be placed in the interphase between two materials, barely affecting the morphology of the system in which they are placed, measuring directly the compressing force of the interphase. Besides, the shape of this gauge can be adapted to the surface in which they are going to measure without any problem. Another strong point is their flexibility, which makes them robust against bending forces. In addition, they are quite robust against shocks and falls, so they can be transported without problem.

Finally it has to be mentioned that the capacitive gauges are hand-made at the mechanical measurement laboratory. Being hand-made means intrinsically that the performance between each one of the gauges varies rather significantly depending on the gauge, due to the variations in the parameters of the manufacturing process.

In the next few pages the theoretical working principals of the gauges will be explained. By reading that, one will have acquired almost all the necessary information needed in order to start working with the capacitive gauges.

> ➤ *Theoretical analysis of the capacitive gauges' working principals*

Before progressing to the theoretical analysis of the working principals of the capacitive gauges, it is essential to introduce two very important concepts, milestones in the respective fields of electronics and measurements. First, from the electrical measurements point of view, the concept of a circuit bridge will be introduced called the Wheatstone bridge. Following this, the concept of a capacitor as a part of a simple circuit will be introduced and expand it to the case of a capacitive gauge which is based on the electromagnetism principles and the principles of elasticity of materials.

> ➤ *The Wheatstone bridge circuit*

Sir Charles Wheatstone (1802 - 1875), an English scientist, reported in 1843 on a circuit which made the accurate measurement of electrical resistances possible. This circuit has become known as the "Wheatstone bridge circuit". The Wheatstone bridge can be used in various ways to measure electrical resistances:

- For the determination of the absolute value of a resistance by comparison with a known resistance,

- For the determination of relative changes in resistance.

It has to become apparent that in most cases, mechanical measurements which are performed by reading electrical signal and values are in most cases really small in magnitude (less than mV or mΩ). A direct measurement of the potential difference either for an absolute value or a relative change of a resistance is not accurate and not possible most of the times due to the limitations of the measuring instrument. The connecting wires of the circuits alone may have a higher value of resistance that may vary from 10^3 to 10^6 times more than what one is trying to actually measure. That is why, bridge circuits such as the Wheatstone bridge have become an integral part of the mechanical measurement field.

> ➤ *Bridge analysis - Determination of an unknown resistance*

Consider an electrical circuit such as the one shown in figure 14.
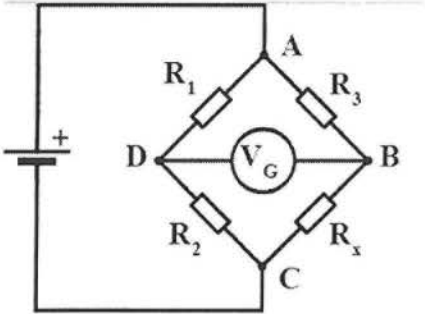
Figure 14: Wheatstone bridge circuit.

In this figure, Rx is the unknown resistance to be measured; R_1, R_2 and R_3 are resistors of known resistance and the resistance of Rx is adjustable. If the ratio of the two resistances in the known arm (R_2 / R_1) is equal to the ratio of the two in the unknown arm (Rx / R_3), then the voltage between the two midpoints (B and D) will be zero and no current will flow through the galvanometer V_G. If the bridge is unbalanced, the direction of the current indicates whether R2 is too high or too low. R_2 is varied until there is no current through the galvanometer, which then reads zero.

Detecting zero current with a galvanometer can be done to extremely high accuracy. Therefore, if R_1, R_2 and R_3 are known to high precision, then Rx can be measured to high precision. Very small changes in Rx disrupt the balance and are readily detected.

At the point of balance, the ratio is

$$\frac{R_2}{R_1} = \frac{R_x}{R_3} \leftrightarrow R_x = \frac{R_2}{R_1} * R_3$$

Alternatively, if R_1, R_2 and R_3 are known, but Rx is not adjustable, the voltage difference across or current flow through the meter can be used to calculate the value of Rx, using Kirchhoff's circuit laws (also known as Kirchhoff's rules). This setup is frequently used in strain gauge and resistance thermometer measurements, as it is usually faster to read a voltage level off a meter than to adjust a resistance to zero the voltage.

➤ *Bridge analysis – Principles of the voltage fed circuit*

If a supply voltage Vs is applied to the two bridge supply points 2 and 3 then this is divided up in the two halves of the bridge R_1, R_2 and R_4, R_3 as a ratio of the corresponding bridge resistances, i.e. each half of the bridge forms a voltage divider(Fig: 15).
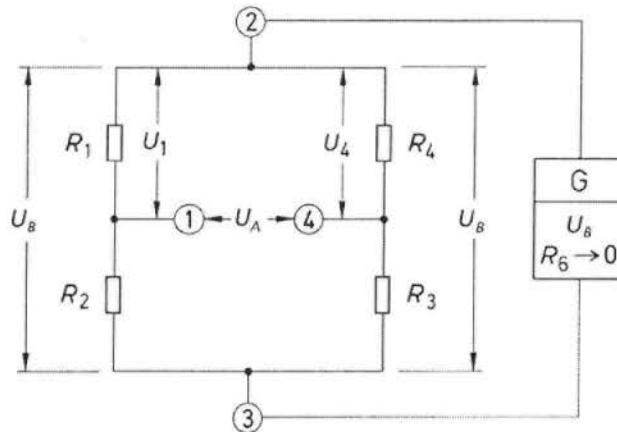
Figure 15: Principle of the voltage-fed Wheatstone bridge circuit.

The following treatment of the bridge circuit assumes that the source resistance R_6 of the voltage supply is negligibly small and that the internal resistance of the instrument for measuring the bridge output voltage is very high and does not cause any load on the bridge circuit.

If the bridge is not balanced, this is caused by the difference in the voltages from the electrical resistances on R_1, R_2 and R_3, R_4. This is calculated as:

$$V_o = V_S \left(\frac{R_1}{R_1 + R_2} - \frac{R_4}{R_3 + R_4} \right)$$

If the bridge is balanced meaning:

$$\frac{R_2}{R_1} = \frac{R_4}{R_3}$$

The bridge output voltage is zero.

With a small change of the resistances in the arm, this gives:

$$V_o = V_S \left(\frac{R_1 + \Delta R_1}{R_1 + \Delta R_1 + R_2 + \Delta R_2} - \frac{R_4 + \Delta R_4}{R_3 + \Delta R_3 + R_4 + \Delta R_4} \right)$$

For the purposes of the measurements with sensors such as the capacitive gauges and the strain gauges, the resistances are chosen to have the same nominal value meaning R=R1=R2=R3=R4. This gives:

$$V_o = V_S \left(\frac{R + \Delta_1}{R + \Delta_1 + R + \Delta_2} - \frac{R + \Delta_4}{R + \Delta_3 + R + \Delta_4} \right) =$$

$$= V_S \left(\frac{(R + \Delta_1) * (2R + \Delta_3 + \Delta_4)}{(2R + \Delta_1 + \Delta_2) * (2R + \Delta_3 + \Delta_4)} - \frac{(R + \Delta_4) * (2R + \Delta_1 + \Delta_2)}{(2R + \Delta_1 + \Delta_2) * (2R + \Delta_3 + \Delta_4)} \right)$$

For simplification while expanding these terms it can be observed that the terms containing only Δvalues or multiplications between them are very small whencompared to the other terms containing the initial resistance, therefore they can be neglected. By doing so the equation becomes:

$$\frac{V_o}{V_S} = \frac{\Delta_1}{4 * R} - \frac{\Delta_2}{4 * R} + \frac{\Delta_3}{4 * R} - \frac{\Delta_4}{4 * R}$$

Finally, keeping in mind that the resistances must have the same initial nominal value, the important equation that describes the voltage fed Wheatstone bridge circuit becomes:

$$\frac{V_o}{V_S} = \frac{1}{4} \left(\frac{\Delta R_1}{R_1} - \frac{\Delta R_2}{R_2} + \frac{\Delta R_3}{R_3} - \frac{\Delta R_4}{R_4} \right)$$

Further analysis and description on the subject that eventually lead to strain gauge measurements as well as more circuit bridges such as the kelvin bridge, are beyond the scope of this thesis and should the reader requires more information, it is advised to further consult other sources such as [Ref: 1].

> ➤ *The capacitor*

A capacitor is a passive two-terminal electrical component used to store energy electrostatically in an electric field. The forms of practical capacitors vary widely, but all contain at least two electrical conductors separated by a dielectric (insulator); for example, one common capacitor consists of two metallic foils separated by a thin layer of insulating film. Capacitors are widely used as parts of electrical circuits in many common electrical devices.

When there is a potential difference across the conductors, an electric field develops across the dielectric, causing positive charge to collect on one plate and negative charge on the other plate. Energy is stored in the electrostatic field. An ideal capacitor is characterized by a single constant value, capacitance. This is the ratio of the electric charge on each conductor to the potential difference between them. The SI unit of capacitance is the farad, which is equal to one coulomb per volt.
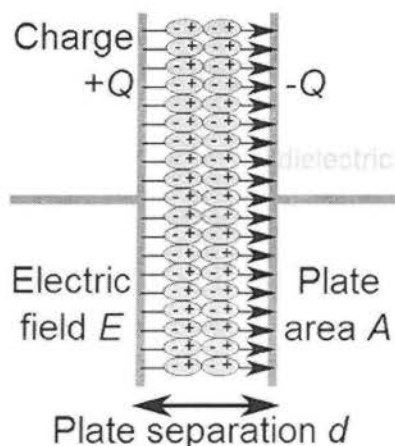
Figure 16: Simple capacitor modelling.

The equation describing it, is:

$$C = \frac{Q}{V}$$

Where C is the capacitance, Q is the charge stored in the plates and V the potential difference.

The value of the capacitance is only dependent on thedielectric properties of the insulator between the conductors and the geometry of the capacitor (the area of the plates and the separating distance between them). In other words:

$$C = \varepsilon_r * \varepsilon_0 * \frac{A}{d} \qquad (1)$$

Where:

- C: Capacitance, in Farads (F)

- A: Area of overlap of the two plates (m^2)

- ε_r: Relative static permittivity (sometimes called the dielectric constant) of the material between the plates (for Kapton, $\varepsilon r = 3.4$)

- ε_0: Electric constant ($\varepsilon 0 \approx 8.854 \times 10^{-12}$ F m^{-1})

- d: Separation between the plates (m)
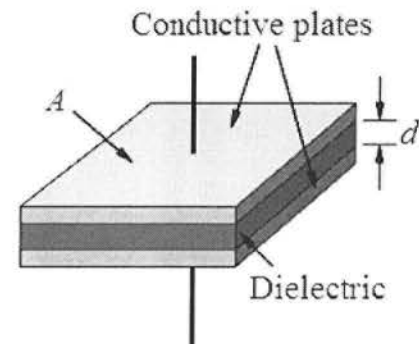
Figure 17: Geometry of a simple capacitor

Capacitors are widely used in electronic circuits for blocking direct current while allowing alternating current to pass. In analogue filter networks, they smooth the output of power supplies. In resonant circuits they tune radios to particular frequencies. In electric power transmission systems they stabilize voltage and power flow.

As it was mentioned before, the capacitive gauges are based in the electromagnetism principlesand the principles of elasticity of materials.Each capacitive gauge is in fact a "sandwich" of capacitors connected in parallel that when they are subjected to compressing load, its geometry is being affected (mainly the distance between the metallic foils is decreasing due to the elasticity of the dielectric that deforms), therefore the capacitance is changing providing an indication of the force applied. Of course the distance of the foils is not the only variable but if we assume that the area of the gauge remains constant, and the dielectric constant of the material is not altered by factors such as the tensional state, the humidity or the temperature, the capacitance of the gauges depends entirely by it.

The equation describing the value of the capacitance in a capacitive gauge under load can be acquired by combining Hooke's law and equation (1):

$$E = \frac{\sigma}{\varepsilon} = \frac{F_c/A}{\Delta d/d_0} \leftrightarrow \Delta d = \frac{F_c * d_0}{E * A} \qquad (2)$$

Where:

- E is the Young´s modulus of the dielectric, in Pa.
- σ is the stress of the material, in Pa.
- ε is the strain of the material.
- F_c is the compressing force applied to the gauge, in N.
- A is the area in which we apply the force, in m^2.
- Δd is the decrement of thickness due to the compressing force, in m.
- d_0 is the initial thickness of the dielectric layer.

Then:

$$(1) \overset{(2)}{\Leftrightarrow} C = \varepsilon_r * \varepsilon_0 * \frac{A}{d_0 - \Delta d} = \varepsilon_r * \varepsilon_0 * \frac{A}{d_0(1 - \frac{F_c}{E * A})} \qquad (3)$$

The capacitive gauges manufactured by MML are formed by layers of an electrical conductive material (stainless steel) separated by layers of a dielectric material (Kapton®), acting as a parallel plate condenser. The potential in the conductive layers is the same every two metallic plates.
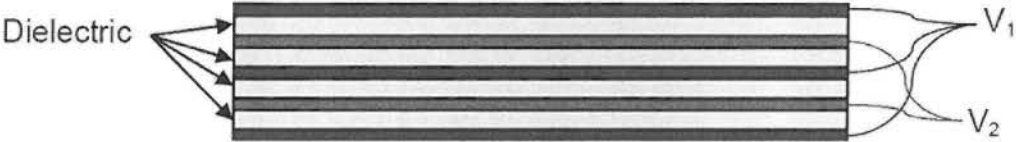
Figure 18: Five layer capacitive gauge (red and blue plates are charged differently)

When multiple capacitors are connected in parallel the capacitance adds up:

$$C_T = C_1 + C_2 + \cdots + C_n$$
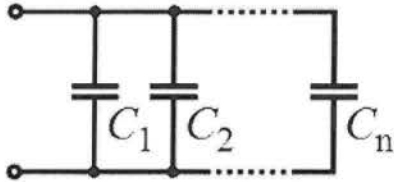
When a capacitive gauge is formed by 4 parallel plate capacitors connected in parallel, as the layers are placed in series, each one of these capacitors receives the same force along its surface. As the dielectric material is the same for all the capacitors (Kapton), the Young modulus of each capacitor is the same, so all the layers will have the same decrement of thickness and therefore the same change of capacitance. Eventually by stacking them together and connect them in parallel the value of the gauge's capacitance will be multiplied and become:

$$C_T = \sum_{i=1}^{4} C_i = \sum_{i=1}^{4} \varepsilon_r * \varepsilon_0 * \frac{A_i}{d_{0_i} * (1 - \frac{1}{E_i} \frac{F_{c_i}}{A_i})}$$

In the summation, ε_0 is a constant, so it can be extracted. Besides, as the material of all the layers is the same, ε_r and E are the same for all the dielectric layers. Apart from that, the quotient F_c/A (the pressure along the layer, that is constant along it) and the parameter d_0 are also the same for each layer. Besides, these parameters are not changing the capacitance with the increment of the number of layers, so they can also be extracted directly from the summation.

Finally, the A_i parameter (the area of each layer) is equal in all the layers, but the area of the layers adds up as the number of layers increases. Therefore, the capacitance of the 5-layers-of-steel gauge (4 single capacitors) can be expressed as:

$$C_T = \varepsilon_r * \varepsilon_0 * \frac{1}{d_0 * \left(1 - \frac{F_c}{E*A}\right)} * \sum_{i=1}^{4} A_i = \varepsilon_r * \varepsilon_0 * \frac{4*A}{d_0 * (1 - \frac{F_c}{E*A})}$$

Based on previous studies and experiments performed in the MML, the number of the metallic foils has been optimized to provide the best results in terms of signal and initial thickness. Alsothe odd number of layers providesthe advantage that the parasitic capacitance between the external layers of the gauge is zero, as both are of the same potential.

> ➤ *Analysis of the measuring setup using a capacitive gauge*

In most measuring cases using capacitive gauges,performed by the MML, the signal is being measured using either HBM's MGCPlus or HBM's QuantumX data acquisition systems [Ref: 5]. The measurements performed for the purposes of this thesis have been taken using QuantumX MX840, 8-channel universal amplifier connected with a modified Wheatstone-bridge circuit configuration (Fig 19).
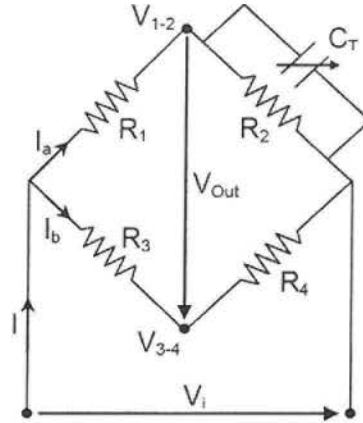
Figure 19: Modified Wheatstone bridge used for capacitive gauges' measurements.

The circuit is powered with AC of frequency 4800Hz (ω=2*Pi*4800rad/s). In this bridge, R_1, R_2 and C_T are part of the external circuit, where R_3 and R_4 are part of the internal electronics of the DAQ system. The circuit is powered by the DAQ system (V_{in}) with alternating current, so the output voltage (V_{out}) will be:

$$\overrightarrow{V_{Out}} = \overrightarrow{V_{1-2}} - \overrightarrow{V_{3-4}} = \overrightarrow{I_a} * R_1 - \overrightarrow{I_b} * R_3$$

Where:

$$\overrightarrow{I_a} = \frac{\overrightarrow{V_{in}}}{R_1 + \frac{1}{\frac{1}{R_2} + \frac{1}{Z_c}}} = \frac{\overrightarrow{V_{in}}}{R_1 + \frac{1}{\frac{1}{R_2} + j*\omega*C_T}} = \frac{\overrightarrow{V_{in}}}{\frac{R_1 * \left(\frac{1}{R_2} + j*\omega*C_T\right) + 1}{\frac{1}{R_2} + j*\omega*C_T}} == \overrightarrow{V_{in}} * \frac{\frac{1}{R_2} + j*\omega*C_T}{\frac{R_1}{R_2} + 1 + j*\omega*C_T*R_1} =$$

$$= \overrightarrow{V_{in}} * \frac{\left(\frac{1}{R_2} + j*\omega*C_T\right) * \left(\frac{R_1}{R_2} + 1 - j*\omega*C_T*R_1\right)}{\left(\frac{R_1}{R_2} + 1\right)^2 + \omega^2 * C_T{}^2 * R_1{}^2} =$$

$$= \overrightarrow{V_{in}} * \frac{\frac{R_1}{R_2{}^2} + \frac{1}{R_2} + \omega^2 * C_T{}^2 * R_1 - j*\omega*C_T*\left(\frac{R_1}{R_2} - \frac{R_1}{R_2} - 1\right)}{\left(\frac{R_1}{R_2} + 1\right)^2 + \omega^2 * C_T{}^2 * R_1{}^2}$$

$$= \overrightarrow{V_{in}} * \frac{\frac{R_1}{R_2{}^2} + \frac{1}{R_2} + \omega^2 * C_T{}^2 * R_1 + j*\omega*C_T}{\left(\frac{R_1}{R_2} + 1\right)^2 + \omega^2 * C_T{}^2 * R_1{}^2}$$

And:

$$\vec{I_b} = \frac{\vec{V_{in}}}{R_3 + R_4}$$

The ratio of output voltage by input voltage is:

$$\frac{\vec{V_{Out}}}{\vec{V_{in}}} = \frac{\vec{V_{1-2}} - \vec{V_{3-4}}}{\vec{V_i}} = \frac{\vec{I_a} * R_1 - \vec{I_b} * R_3}{\vec{V_i}} =$$

$$= \frac{\frac{R_1^2}{R_2^2} + \frac{R_1}{R_2} + \omega^2 * C_T^2 * R_1^2 - j * \omega * C_T * R_1}{\left(\frac{R_1}{R_2} + 1\right)^2 + \omega^2 * C_T^2 * R_1^2} - \frac{R_3}{R_3 + R_4}$$

The DAQ system only measures the part of the output signalthat is in phase with the excitation meaning:

$$Re\left(\frac{\vec{V_{Out}}}{\vec{V_{in}}}\right) = \frac{\frac{R_1^2}{R_2^2} + \frac{R_1}{R_2} + \omega^2 * C_T^2 * R_1^2}{\left(\frac{R_1}{R_2} + 1\right)^2 + \omega^2 * C_T^2 * R_1^2} - \frac{R_3}{R_3 + R_4}$$

When setting up the capacitive gauge, the value of the real part of the voltage gain for the initial capacitance of the gauge is taken as the zero. The signal of the transducer, after the balancing of the bridge with zero pressure will be:

$$Signal = Re\left(\frac{\overrightarrow{V_{out}}|_F}{\overrightarrow{V_{in}}}\right) - Re\left(\frac{\overrightarrow{V_{out}}|_{F=0}}{\overrightarrow{V_{in}}}\right)$$

$$= \left(\frac{\frac{R_1^2}{R_2^2} + \frac{R_1}{R_2} + \omega^2 * C_{T_F}^2 * R_1^2}{\left(\frac{R_1}{R_2} + 1\right)^2 + \omega^2 * C_{T_F}^2 * R_1^2} - \frac{R_3}{R_3 + R_4}\right)$$

$$- \left(\frac{\frac{R_1^2}{R_2^2} + \frac{R_1}{R_2} + \omega^2 * C_{T_{F=0}}^2 * R_1^2}{\left(\frac{R_1}{R_2} + 1\right)^2 + \omega^2 * C_{T_{F=0}}^2 * R_1^2} - \frac{R_3}{R_3 + R_4}\right) =$$

$$= \frac{\frac{R_1^2}{R_2^2} + \frac{R_1}{R_2} + \omega^2 * C_{T_F}^2 * R_1^2}{\left(\frac{R_1}{R_2} + 1\right)^2 + \omega^2 * C_{T_F}^2 * R_1^2} - \frac{\frac{R_1^2}{R_2^2} + \frac{R_1}{R_2} + \omega^2 * C_{T_{F=0}}^2 * R_1^2}{\left(\frac{R_1}{R_2} + 1\right)^2 + \omega^2 * C_{T_{F=0}}^2 * R_1^2}$$

In the actual bridge the resistors have the same nominal resistance value $R_1=R_2=R_3=R_4=R$ simplifying the last equation to:

$$Signal = \frac{2 + \omega^2 * C_{T_F}^2 * R^2}{4 + \omega^2 * C_{T_F}^2 * R^2} - \frac{2 + \omega^2 * C_{T_{F=0}}^2 * R^2}{4 + \omega^2 * C_{T_{F=0}}^2 * R^2}$$

Assuming a common measuring case where these parameters take the following values:

- R= 350 Ω

- ω= 4800*2*π rad/s

- n= 4 Layers of dielectric

- L= 0.150 m

- W =0.016 m

- d_0 =25*10^{-6} m

- ε_0= 8.85*10^{-12} F/m

- ε_r= 3.4

- E_{Kapton}= 200 GPa

The signal of the ideal capacitive gauge transducer would be:
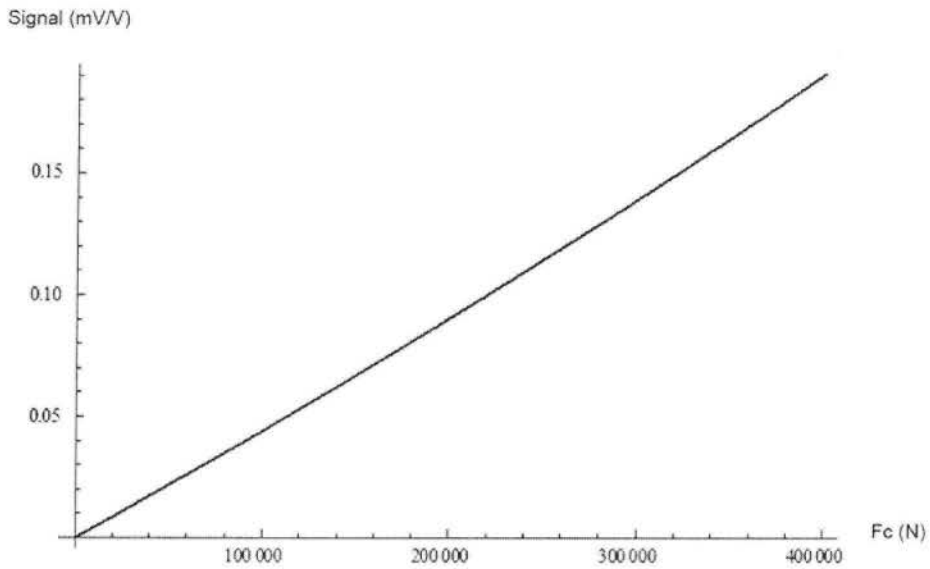
Figure 20: Signal vs Compressing Forceof the ideal transducer.

The analysis of the signal was performed by RaulMoronBallester former technical student of the MML and is included in his master thesis where the reader can obtain further information about the subject if needed [Ref:2].

Capacitive gauges' optimization

The creation of a new sensorfrom scratch that is meant to be used in measurements carried out in extremely hazardous environments involving most of the times cryogenic temperatures and high magnetic fields is not an easy task. The people working in the Mechanical Measurements Laboratory in CERN have already been performing this task for more than 8 years by studying, developing and effectively using these unique homemade sensors, the capacitive gauges. All this time the members of the MML have been focusing not only in the manufacturing of these sensors but also to improve them in every possible way by analysing their working principals, trying new things and ideas and of course improve the testing conditions and setups being used. Through experience and time, one thing have become apparent... several actions need to be performed so that the whole capacitive gauges optimization project will be eventually concluded with the sole purpose to deliver an accurate, reliable and nowhere else to be found force monitoring sensor.

In the next chapter, a number of actions taken have been documented mainly focusing in the testing procedures the capacitive gauges are being subjected to. In addition,a newly adopted calibration procedure along with instructions on how to perform it, includinga couple ofcalibration examples, is how the second chapter begins. This chapter also includes the steps that have been performed in order to integrate and utilize a new material testing machine,the laboratory has purchased,which will hopefully enhance the testing and measuring properties of the laboratory. Finally comparisons between the testing setups have been performed with a sole purpose of evaluating the progress made and plan the laboratory's next steps in this direction.

The third and final chapter of this thesis is focusing in the manufacturing and problem solving properties of the capacitive gauges. Some new ideas opening new manufacturing paths have been tested and are presented.

Chapter II
Optimization in terms of testing procedures

Section I
Calibration

When a capacitive gauge is being manufactured, before it is ready to start monitoring the existing force levels between component contacts as described in the introduction chapter, it needs to be calibrated. The calibration of a sensor is basically the mathematical link connecting the physical excitation of each sensor with the outcome signal that it provides. For this particular sensor, the calibration is usually performed by continuously loading and unloading a capacitive gauge in a press, for a defined number of cycles. For the analysis of the collected data, a least squared polynomial fitting is mainly being used and a number of statistical tools such as the mean values of a loading step, their standard deviation or the "goodness" of the fitting are finalizing the calibration. Of course for the capacitive gauges, which are being used in cryogenic environments, a second calibration in liquid nitrogen is being performed. Finally a certificate including all these results is being provided along with each gauge to the requestor of the measurement. An example of two resulting graphs from previous calibrations is being presented in the next figure.
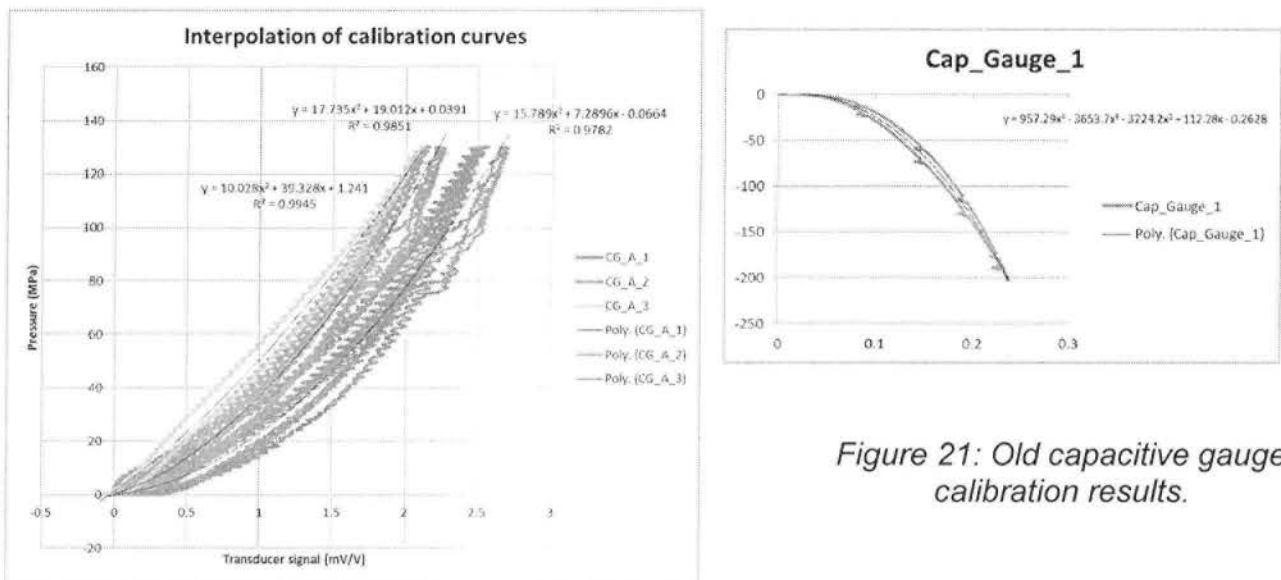
Figure 21: Old capacitive gauge calibration results.

The need for a more informative calibration procedure, led to the acquisition of International standards that include guidelines for such operations andinformation on how to perform them properly, minimizing the measurement errors. A detailed overview of the new procedure that has been implemented for the capacitive gauges is the main subject of the next section of this chapter.

> ## *Calibration procedure –ISO 376:2011*

1. Determination of deflection: A deflection is defined as the difference between a reading obtained under a load and a reading without force. The definition of the deflection applies to the output readings in electrical units taken from each measurement performed.

2. Overloading Test: According to the standards, at least one overloading test should be done by the manufacturer of the gauge before it is released for calibration or service. The overloading test shall be performed by subjecting the capacitive gauge to four successive applications of an overloading force that corresponds to 210 MPa of stress. Overloading shall be maintained for a period of 75 seconds for each individual repetition.

3. Preload: The maximum calibration force (corresponding to 200 MPa) should be applied three times before each calibration. The duration of the application of each preload is 75 sec.

4. Calibration: The calibration procedure should be performed by carrying out the following steps:

    *   Step 1: The calibration should begin by applying two series of calibration forces (explained below) onto the instrument with increasing values only, without disturbing the device.
    *   Step 2: The cryostat should be rotated 120° clockwise and two additional series of calibration forces should be applied.
    *   Step 3: Finally, the cryostat should be rotated another 120° clockwise reaching an angle of 240° overall with respect to the initial position. Two final series of calibration forces should be applied on the gauge.

    Overall, there will be six loading cycleseach involving a total of ten (including zero and release) loading steps, starting from 0 N to the value of the force corresponding to 200 MPa of pressure with a step of 25 MPa. The following figure shows the position and the names of each individual series as the calibration steps are being executed.

X1 , X2

120 Degrees steps

X5 , X6

X3 , X4
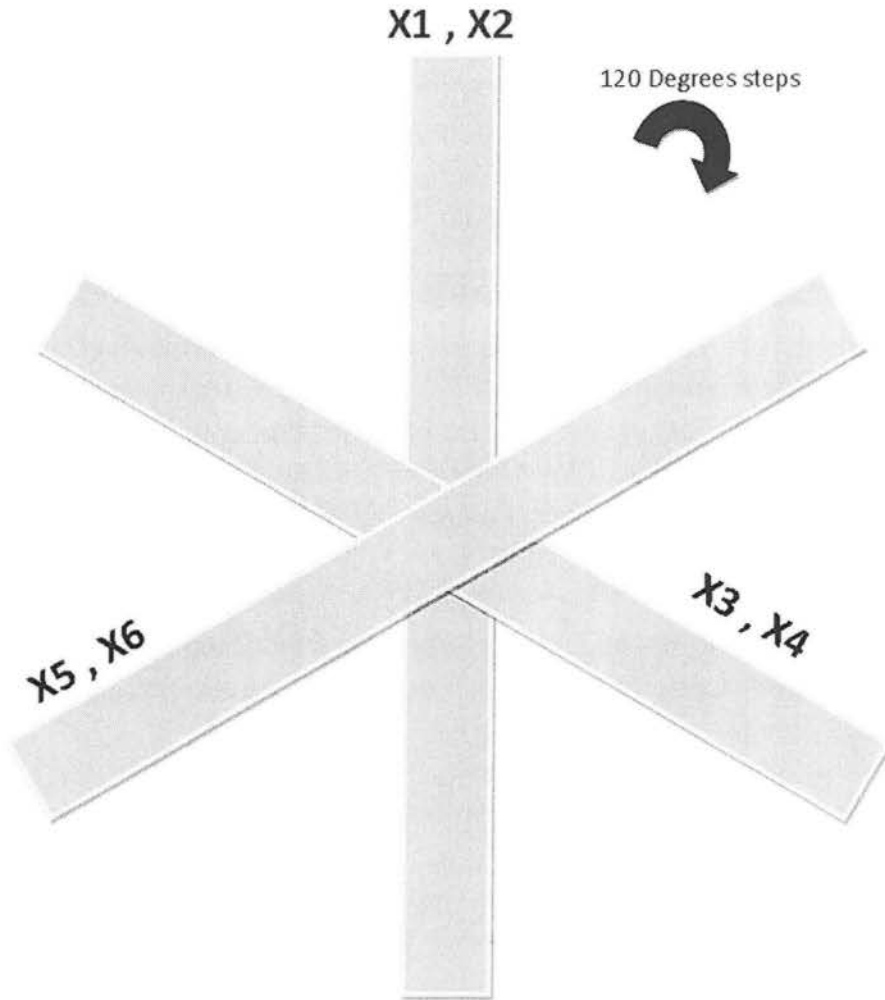
Figure 22: Three calibration steps, each with two series of loadings. X1 stands for loading series 1, X2 for loading series 2 and so on.

5. Loading conditions: Each loading step will last 40 seconds and no measurements will be taken for the first 30 seconds after a loading condition / step has been reached. After this period of 30 seconds, the deflection values of the gauge will be recorded for each given load. When a loading series has been completed the load will be removed and after the same period of 30 seconds, the zero value will be recorded and a new cycle will begin after 3 minutes have passed.

For convenience, it is advised to create a matrix of the measuring values that will be acquired from each individual step and series/cycle of force application. An example of such a matrix can be seen in the following figure.

Capacitive Gauge Calibration - Measurement Values							
Force (KN) Series	X1	X2	X3	X4	X5	X6
Release - 0 KN						
Creep test deflections						
$i_{30} =$				$i_{300} =$		

Figure 23: Calibration's measurement data matrix.

6. Creep test: The creep evaluation test of the gauge should begin at the end of the sixth cycle 'X6' and when the period of 30 seconds after the zero value has been achieved and stabilized. From that point on, two gauge's output values should be recorded and copied to the calibration matrix; the first value i_{30} shall be acquired directly after the beginning of the creep test and the other i_{300} after 300 seconds have passed.

7. Test parameters: The sampling frequency in the data acquisition software should be set at 5 Hz. The time window between each individual loading step has already been defined to be 40 seconds. The values that should be considered corresponding to each loading deflection are only the ones recorded the six seconds between 32" and 38" of each step. Having a recording window of 6 seconds with a 5 Hz sampling frequency , 30 samples will be acquired for each step and each cycle that will be later statistically analysed (mean values and standard deviation) and used to fill up the table in figure 23 (mean values only).

Calibration duration: 90 minutes.

8. Interpolation Curve: The interpolation curve should be determined from the average values of the deflections with rotation, $\overline{Xr}$(X1,X3,X5). These values are the outcome of the statistical analysis of the data gathered from step 7. The whole procedure is advised to be performed in MATLAB®, in which an algorithm covering the whole procedure will be provided in [Annex A] of this thesis.

➤ *Classification and assessment of the gauge*

1. According to the standards, in order to determine the range in which the gauge is classified, every relative error computed from the gauge response, for each loading step (see below), should be compared with the classification requirements (Table 2 – ISO 376:2011). The comparison starts with the maximum load and decreases until the lowestforce step. The classification range ceases and becomes defined at the last loading step for which the classification requirements are satisfied. This range should at least cover 50% to 100% of the F_N (Maximum calibration force – 200 MPa).

The capacitive gauges are classified, according to paragraph 8.2.4, as "case C" and the criteria which shall be only considered are:

- The relative reproducibility, repeatability and zero errors

- The relative interpolation error

- The relative creep error

2.1 Relative reproducibility and repeatability errors, b and b1

These errors are calculated for each calibration loading step using the following equations:

$$b = \left| \frac{X_{max} - X_{min}}{\overline{X_r}} \right| * 100\%$$

Where

$$\overline{X_r} = \frac{X_1 + X_3 + X_5}{3}$$

X_{max} & X_{min} correspond to the maximum and minimum deflections from the cycles 1,3,5 for each loading step accordingly.

$$b1 = \left| \frac{X_2 - X_1}{\overline{X_{wr}}} \right| * 100\%$$

Where

$$\overline{X_{wr}} = \frac{X_1 + X_2}{2}$$

2.2 Relative zero error, f_0

The zero reading should be recorded before and after each series/cycles of testing, after 30 seconds have passed since the zero value has been reached. Therefore the values of the first raw of the matrix shown in figure 22 will be used to fill up the values of i_f and i_o (deflections after the removal and before the application of the force accordingly). The relative zero error is calculated from the equation:

$$f_0 = \frac{i_f - i_0}{X_N} * 100\%$$

The maximum relative zero error evaluated should be considered.

2.3 Relative interpolation error, f_c

In order to calculate this error, a least square curve fitting - polynomial (maximum three degrees) must have been calculated (step 8). The relative interpolation error, as a function of each loading step, is then calculated by the following equation:

$$f_c = \frac{\overline{X_r} - X_a}{X_a} * 100\%$$

Where X_a are the calculated values interpolated from the fitting polynomial.

2.4 Relative creep error, c

This error can be calculated by using the following equation:

$$c = \left|\frac{i_{300} - i_{30}}{X_N}\right| * 100\%$$

Where X_N is the deflection corresponding to the maximum calibration force, taken from X_1 to X_6.

➢ *Measurement Uncertainty*

The combined standard uncertainty u_c should be calculated for each calibration force F from the readings obtained during the calibration. These combined standard uncertainties should be plotted against force and a linear least square fit should be used followed by the calculation of its coefficients. The equation that should be used is the following:

$$u_c = \sqrt{\sum_{i=1}^{7} u_i^2}$$

Where u_1-u_7 are the following uncertainties:

1. Calibration force uncertainty – u_1:

Is the standard uncertainty associated with the forces applied by the calibration machine, which in this case is 0.02%*F

2. Reproducibility uncertainty – u_2:

It is calculated by the following equation:

$$u_2 = \left|\frac{F_N}{X_N}\right| * \sqrt{1/6 * \sum_{i=1,3,5} (X_i - \overline{X_r})^2}$$

3. Repeatability uncertainty – u_3:

It is calculated by the following equation:

$$u_3 = \frac{b1 * F}{100 * \sqrt{3}}$$

4. Resolution uncertainty – u_4:

It is calculated by the following equation:

$$u_4 = \frac{r}{\sqrt{6}}$$

Where r is the resolution of the gauge that can be defined as the slope of a linear interpolation from the signal data gathered vs the force reference.

5. Creep uncertainty – u_5:

It is calculated by the following equation:

$$u_5 = \frac{c * F}{100 * \sqrt{3}}$$

6. Zero drift uncertainty – u_6:

It is calculated by the following equation:

$$u_6 = \frac{f_0 * F}{100}$$

7. Interpolation uncertainty – u_7:

It is calculated by the following equation:

$$u_7 = \left| \frac{\overline{X_r} - X_a}{\overline{X_r}} \right| * F$$

For convenience, it is advised to create a second matrix that this time will contain all the calculated values. An example of such a matrix can be seen in the following table.
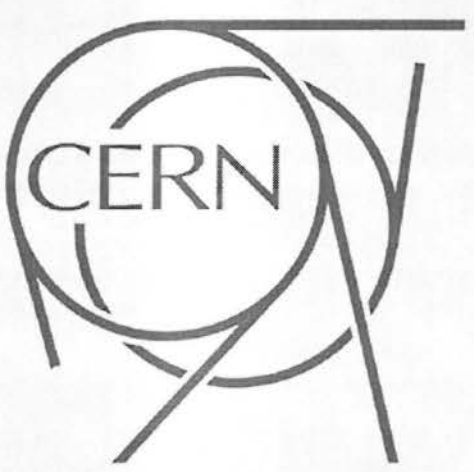
Capacitive Gauge Calibration - Calculated Values								
Force (KN)	Xr	Xwr	Xmax	Xmin	b	b1	Xa	fc
Force (KN)	Xn	f0	c	u1	u2	u3	u4	u5
Force (KN)	u6	u7	uc					

Figure 24: Calibration's calculated data matrix.

> ### Calibration - software instructions

The calibration procedure explained in the previous chapter might seem long and complicated, that is why this chapter is aiming to simplify it by providing useful information and instructions that will cover the full procedure. For starters, it has to be mentioned that all the "tools" one might need to use in order to perform a calibration, are located in the dfs folder EDMS_1304901. All these tools correspond to four different software programs that are required to be used to run the procedure. These software packages are:

- TestXpert II –is the software controlling the materials testing machine (Z400E – Zwick // Roell) with which the Mechanical Measurements Laboratory isequipped with.

- HBM's Catman Easy – is the data acquisition software that is needed to record all the measurement values obtained during the calibration. Moreover using Catman all these raw data values, can be exported into an ASCII or XLSX file that later will be imported to Matlab.

- MathWorks' Matlab – is the software used to analyse and post process all the calibration data, calculate and plot the results and finally export all the information to an XLSX premade certificate template (Fig: 41).

- Microsoft Excel – is the software used to visualize and print the calibration certificate.

The followingsectionscontain the necessary instructions required for a calibration procedure to be performed correctly byoperating these softwares accordingly.

> *TestXpert II - HBM's Catman Easy*

Caution

TestXpert II is the software controlling a machine that is able to compress with more than 40 tons, thus extra attention must be paid by the operator to whatever adjustments he chooses to apply.

- Start by running the TestXpert II and load the file named "Overloading.zp2" included in the "Calibration Tools"dfs folder. The parameters that need to be definedin this program are the dimensions of the capacitive gauge that is to be calibrated (provided they are different from the defaults) and the grip space and starting position.Those parameters can be set from the Wizard panel. Also run the Catman file "Testing.MEP" to monitor the procedure. Zero the channels"Force Reference" and "Capacitive Gauge" and hit start on both programs to let the overloading phase begin.
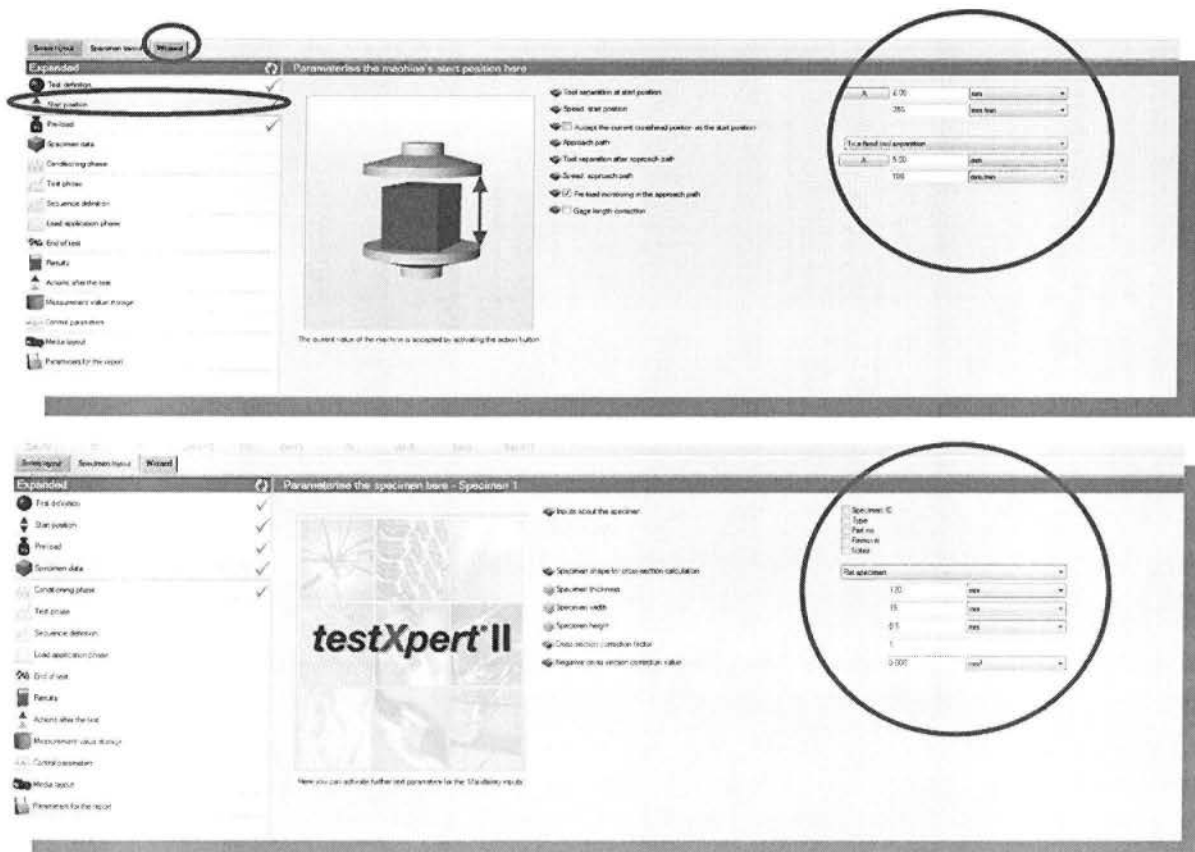

Figure 25: Setting the parameters in TestXpert II (the values vary in each calibration occasion, so if the operator is unaware of the correct values he should consult someone more experienced).

The next step is the preloading phase. Load the file named "Preloading Test.zp2" included in the calibration tools folder. Redefine the dimensions of the capacitive gauge, set the grip space and starting position again(if needed) and hit start.The machine will automatically perform three preloading cycles. When this phase has finished, stop Catman and save the recorded values both for the overloading and preloading phases.

- After the preloading cycles have finished, the Catman file "Calibration.MEP" should be loaded along with the TestXpert II filenamed "Calibration.zp2". From this point on, the main phase of thecalibration is taking place therefore all the values must be recorded by Catman. In Catman the only parameter that needs to be defined is the area of the gauge. Edit the "area" computation channel and set a new and final zero for the measuring channels "Force Reference" and "Capacitive Gauge". In the dfs you should create two folders where all your measurements (cryo and RT separately) will be saved. Catman by default saves the raw data in the local drive in"C:\Capacitive Gauges\calibration". It is suggested to save them locally and transfer them in the new folders created in the dfs, at the end of each procedure.
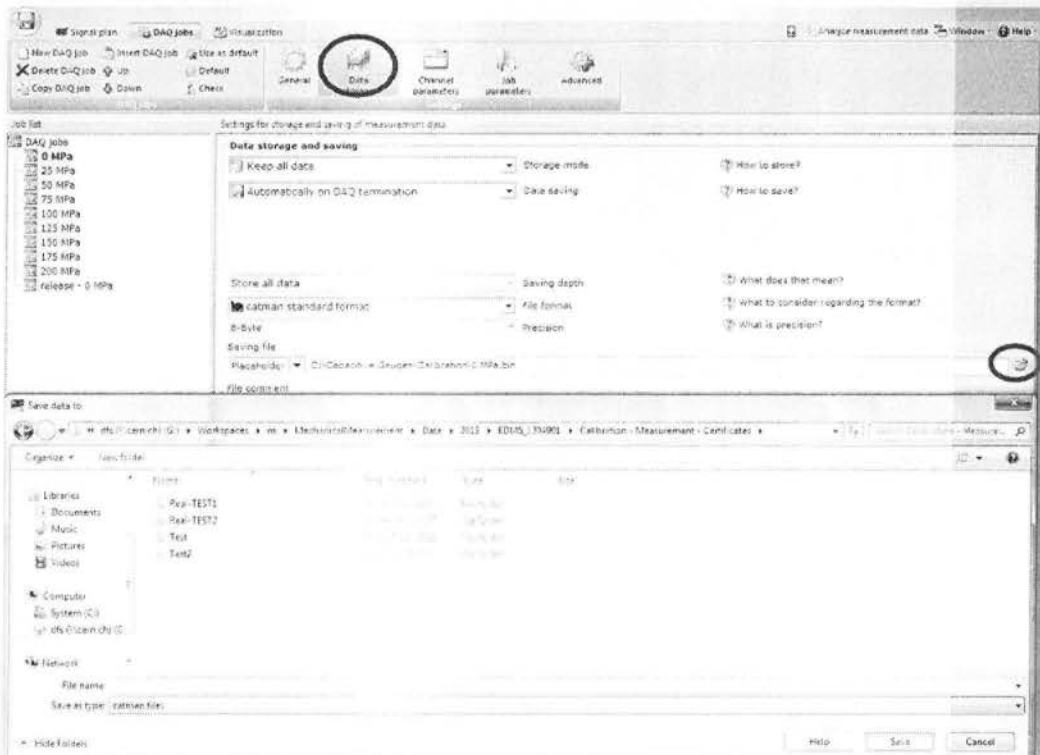
Figure 26: Defining a placeholder for the raw data of the calibration.

- Hit the start button and "executeall jobs" in Catman.

- The "0 MPa" will begin automatically and will keep recording values for 40 seconds. After this particular job has finished switch to TestXpert II and start the program. Wait until all loading steps/jobs have finished and make sure the last Catman job "release – 0 MPa" will record at least 40 seconds before you will have to manually stop the procedure (although it is advised to keep recording for at least 1 minute). Make sure that in the folder were the data are stored (by default at the C drive), there are 10 ".bin" files, each for every loading step including the release.

- From this point on wait three minutes and then repeat the same process 5 more times. After the second and fourth time the process has been repeated, the cryostat in the testing area needs to be twisted 120° clockwise.

- On the sixth and final cycle, the last Catman job "release – 0 MPa" should be let running for six minutes minimum (one or two minutes more won't hurt) and then stopped manually. This step is actually a creep test performed on the capacitive gauge. When the final cycle - creep test has been completed, there must be 10 loading steps * 6 cycles = 60 ".bin" files in the local drive that should be moved to their corresponding folder in dfs.

10 files per each cycle

6 cycles overall

Figure 27: Catman's measurement data after the 6 calibration cycles.

Data exportation:

- Run Catman from the beginning and select "New Analysis project". Move the ".bin" raw data files from the local drive to theircorresponding folder in dfs. In the "Test Explorer" panel locate and select that folder and hit "Load all tests" (Fig: 28).

Figure 28: "Test explorer and Load all tests panels" location in Catman analysis project. If everything was done correctly 60 tests should be loaded.

- Go to "Export" panel and hit "Load export list". In the "Calibration Tools" folder in dfs, select the "SIGNAL – Exportation List.EXP".

- In the "Select export format" select the "MS Excel Office 2007 XML" option and hit "Export". Name the file (name not important) and save it in a new folder keeping in mind that in this folder the certificate and the results will automatically be created (the exported XLSX files for both cryogenics and room temperature calibrations should be placed there, soMatlab will recognize the exported files and will modify the certificate twice for both temperatures).

Data analysis:

✓ The data analysis is performed using Matlab software. In the "Calibration Tools" folder in dfs run the file named "CG_Calibration.m". When the Matlab editor shows up either hit f5 on the keyboard to run the algorithm or press the run button. Select change folder and normally the analysis should begin.
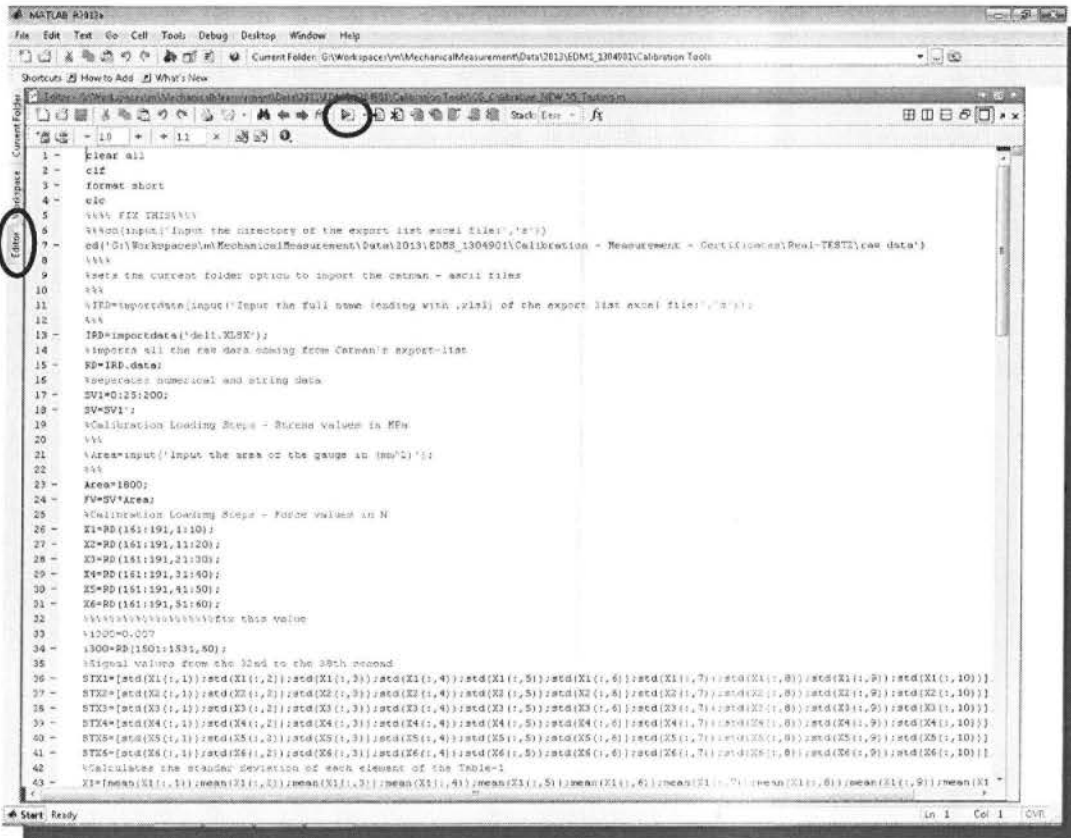
Figure 29: Run the algorithm by pressing run or f5 on the keyboard or the icon highlighted. Switching between the editor and command panel, can be achieved by using the second highlighted icon.

✓ The Matlab editor will be minimized and switch to the command window. Follow the instructions provided and input the necessary information for the calibration to be completed.

✓ Matlab will automatically perform the analysis and will create the "Certificate.xlsx" file (same folder as the export lists). After the first results have been acquired (RT or cryo), repeat the analysis for the other environmental condition measurement for the certificate to include both results.

Troubleshooting:

✓ In case there is a problem with the procedure it will most probably be a mistake in the operation of the softwares used. To fix this problem, the operator must check that the exported data from Catman are correctly listed and read from the rest of the softwares (wrong input means wrong or no results). There are three steps that should be followed to ensure this action.

1. Make sure that after every cycle, all ".bin" files corresponding to that particular cycle have been created. If any problem occurs and one file is missing, it is advised to repeat the whole cycle from the beginning.

2. While exporting the raw data, make sure that the measuringchannels from Catman'sexportation list are correctly listed. An example for the correct listing of the measuring channels can be seen in the next figure.
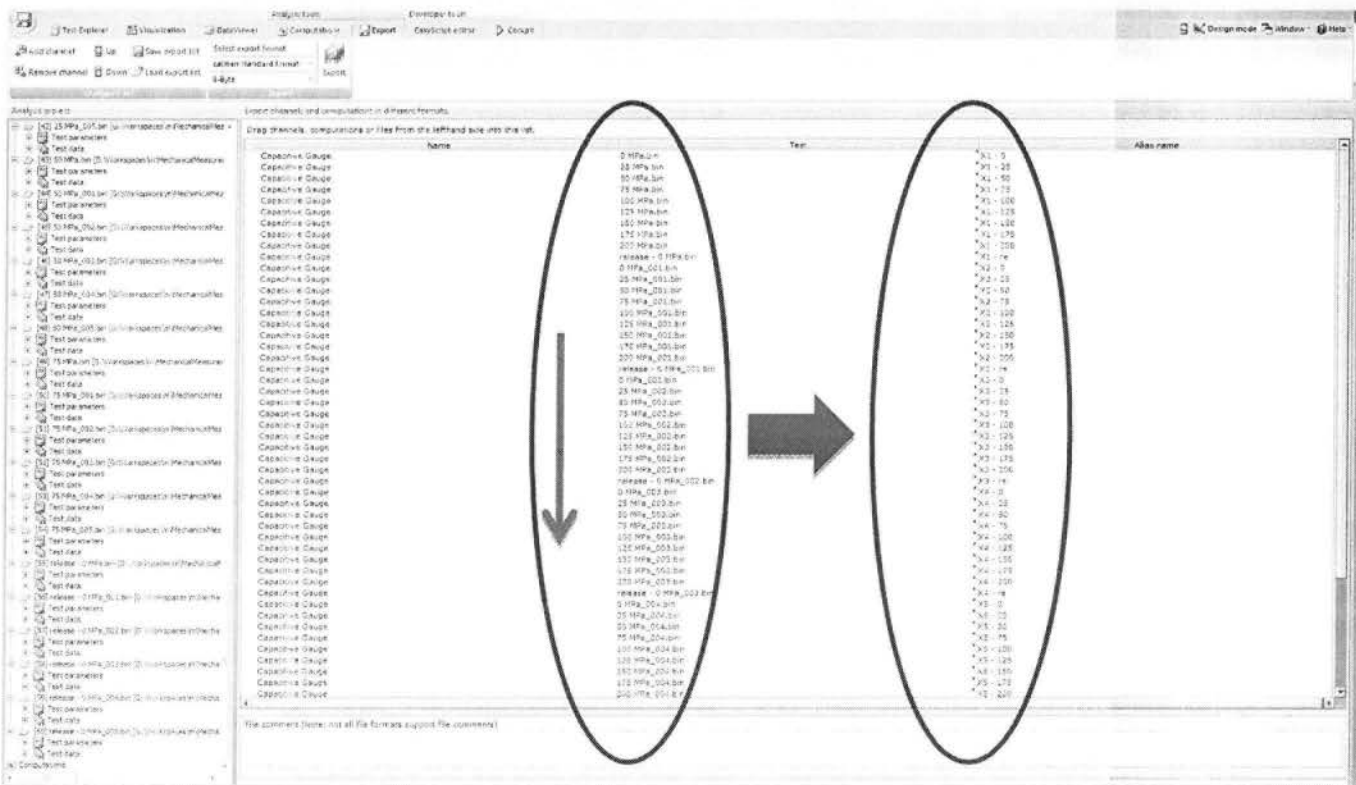
Figure 30: Verify the correct order of the channels of the exportation list. Normally all files in the left column correspond to the description located in the right column automatically.

3. The last step to verify that everything works as intended is performed by running the exported ".xlsx" file and checking the order of the exported measurement channels (first column X1 0 load, second column X1 25 MPa and so on up to X6 release). These steps are advised to be followed to ensure the validity of the results.

✓ Afterhaving finished checking the order of the channels, make sure that for every raw-data channel/column in Excel, there are at least 200 recorded values (since in Excel the values start from the row 50, all channels must contain values at least up to the 249th row). Furthermore, there must be more than 1530 recorded values (up to 1559th row)in the last column which corresponds to the creep test.

Note: These numbers are not random. Having a sampling frequency of 5 Hz while calibrating and by measuring the capacitive gauge's signal values for 40 seconds between each loading step, there must be 5*40=200 recorded values. Same things applies for the creep test with the only difference that the values that will be processed are starting after the 300th second and finishing 30 seconds afterwards: 5*300 + 5*6 = 1530 recorded values at least.

✓ After each calibration either in RT or cryogenics, move the 60 ".bin" files to the dfs (separate folders for RT and cryo). In order for the certificate to be automatically fulfilled and thus the calibration to finish, this file mustnot be opened during the analysis of Matlab, because Matlab will not be able to modify it and give a warning message (in case this happens the algorithm should be started over).

Closing RT &Cryogenic calibration notes:

- If you receive a warning for short-circuited values while making the analysis, follow the instructions given by Matlab.
- While filling up the cryostat with liquid nitrogen, it is advised to apply some small amount of load in the structure, in order to keep everything in position. Also since the machine's displacement resolution is of μm and the nitrogen will shrink the assembly, a new adjustment in the wizard panel of TestXpert (grip distance and starting position) should be made after the cool down has been achieved.

➤ *Calibration example*

In this section of this thesis, an example of a calibration procedure is being presented, mainly focused on the results and what to anticipate from such a procedure. For the purpose of this section, a capacitive gauge has been created (1800 mm^2 compression area) and has followed all the steps of a calibration procedure. The calibration took place in both room temperature and in liquid nitrogen at 77 K.
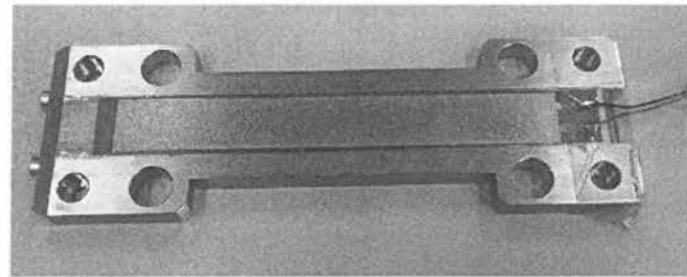
Figure 31: Capacitive gauge 1800 mm^2 compression area.

Overloading:

The capacitive gauge has been subjected to four successive overloading cycles in room temperature. The results obtained can be viewed in the next figure.
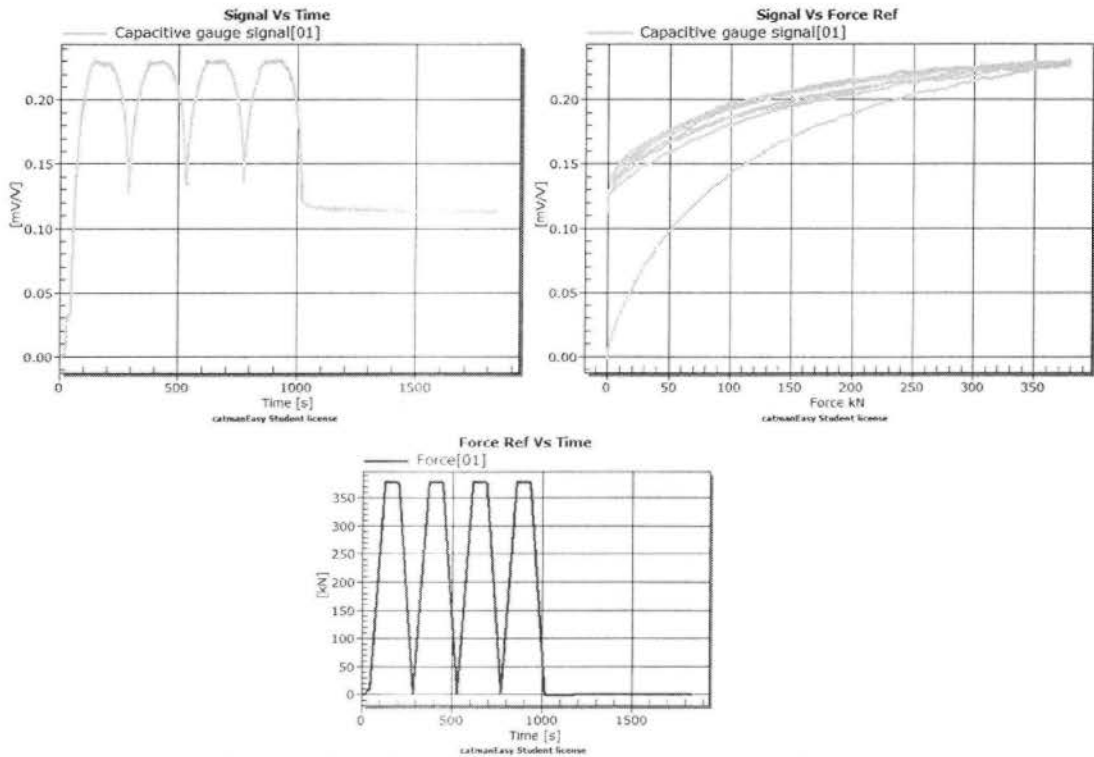
Figure 32: Overloading phase - four loading cycles.

Preloading:

Prior to each calibration three preloading cycles to the max loading capacity (200 MPa) should be performed. In the next graphs, both preloading steps for room temperature and cryogenics tests are being presented.
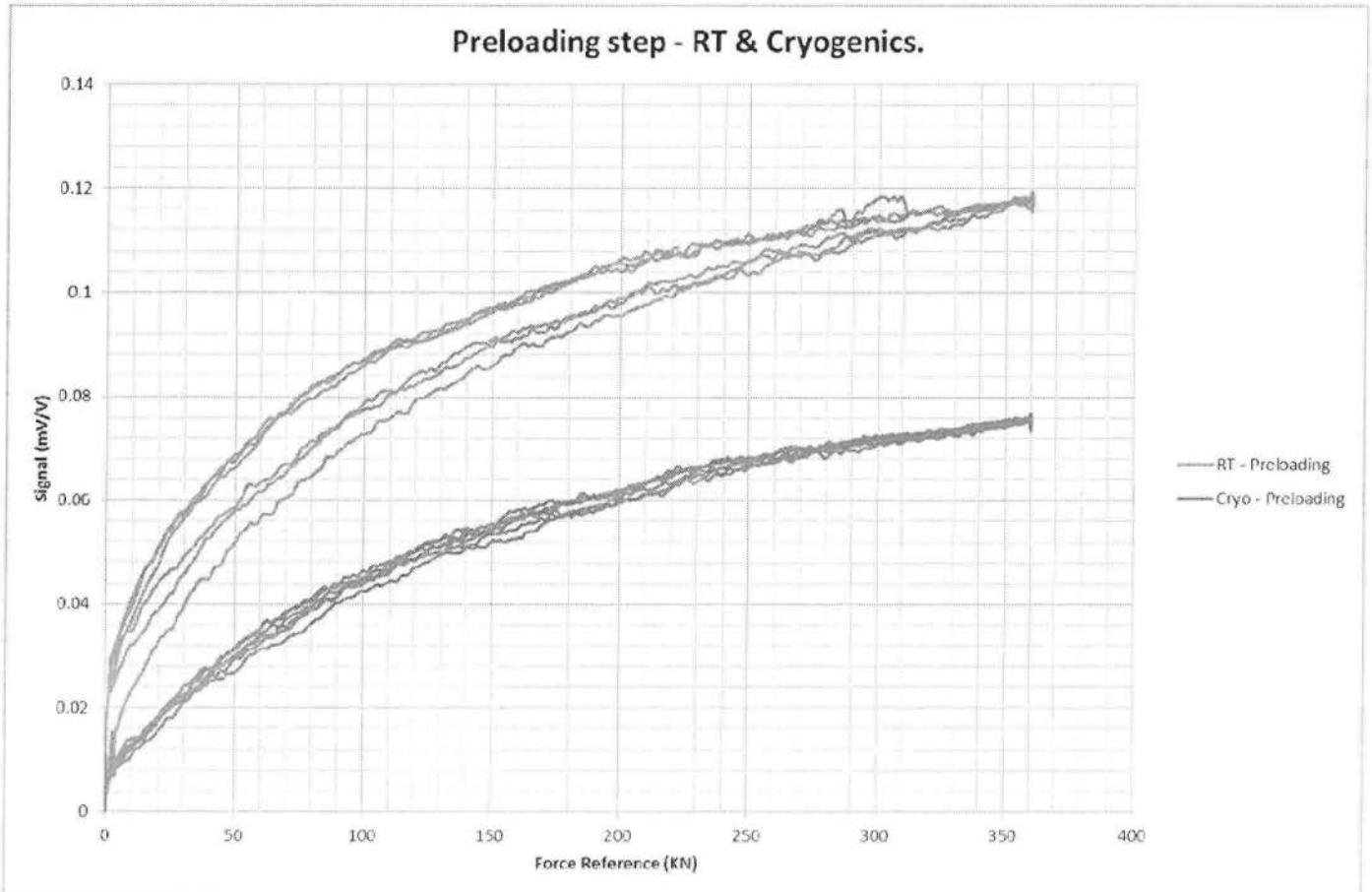
Figure 33: Three preloading cycles performed before each calibration procedure.

After each preloading step the main calibration took place to define the polynomial coefficients for the interpolation curves, the third degree curve fitting of the signal and the first degree polynomial of the measurement uncertainty, both as a function of the applied reference force. The calibration analysis was performed using the matlab algorithm [Annex A] and the results can be observed in the following tables.

Calibration:

Room Temperature

Capacitive Gauge Calibration - Measurement Values						
Force (KN) Series	X1	X2	X3	X4	X5	X6
0	-0.000518507	-0.000228096	-0.0002623	0.000185555	0.000704987	0.001453033
45	0.049969898	0.051263607	0.036621285	0.041299162	0.03828204	0.040366989
90	0.069238554	0.069901242	0.057809697	0.058865057	0.057466546	0.060714199
135	0.081582489	0.08201945	0.075516593	0.075323401	0.07142958	0.073490655
180	0.089076832	0.091191324	0.085019059	0.085935445	0.08269602	0.08390971
225	0.098507859	0.098765546	0.093137328	0.09488614	0.09136992	0.092581409
270	0.103667773	0.105546318	0.100458076	0.10128456	0.099153516	0.099976915
315	0.108775564	0.108421946	0.106402819	0.107970754	0.105045846	0.105345758
360	0.112286174	0.112708438	0.109771593	0.112127643	0.110129916	0.11036543
Release - 0 KN	0.001735753	0.002083521	0.002108422	0.002097545	0.002992216	0.003525992
Creep test deflections						
$i_{30}=$			$i_{300}=$			
0.003525992			0.00176511			

Figure 34: Deflection values for six calibration cycles with ten loading steps each. Deflection values in mV/V.

Capacitive Gauge Calibration - Calculated Values							
Force (KN)	Xr	Xwr	Xmax	Xmin	b	b1	Xa	fc
0	-2.5274E-05	-0.000373302	0.000705	-0.000518507	4841.003613	77.79528834	0.00245865	-101.0279
45	0.04162441	0.050616752	0.04997	0.036621285	32.0691956	2.555890899	0.03699161	12.52391
90	0.06150493	0.069569898	0.069239	0.057466546	19.13994268	0.952548938	0.06137376	0.213726
135	0.07617622	0.08180097	0.081582	0.07142958	13.32818654	0.534175733	0.07770933	-1.972879
180	0.0855973	0.090134078	0.089077	0.08269602	7.454453922	2.345940238	0.08810256	-2.843568
225	0.09433837	0.098636702	0.098508	0.09136992	7.566315222	0.261249309	0.09465768	-0.337329
270	0.10109312	0.104607046	0.103668	0.099153516	4.465444287	1.795811317	0.09947892	1.622661
315	0.10674141	0.108598755	0.108776	0.105045846	3.494161639	0.325618184	0.10467051	1.978492
360	0.11072923	0.112497306	0.112286	0.109771593	2.270928441	0.375354178	0.1123367	-1.430939

Force (KN)	Xn	f0	c	u1 (Load cell)	u2 (reproducibility)	u3 (repeatability)	u4 (resolution)	u5 (creep)
0				0	1.189941166	0	0.00044651	0
45				0.009	13.41576955	0.664039934	0.00044651	0.405906
90				0.018	12.3549638	0.494958947	0.00044651	0.811813
135				0.027	9.420596788	0.416348779	0.00044651	1.217719
180	0.11270844	2.103411693	1.562334	0.036	5.955475508	2.43797261	0.00044651	1.623625
225				0.045	6.855360193	0.339372807	0.00044651	2.029532
270				0.054	4.28415662	2.799392798	0.00044651	2.435438
315				0.063	3.481246955	0.5921866	0.00044651	2.841344
360				0.072	2.50836174	0.780159008	0.00044651	3.247251

Force (KN)	u6 (zero drift)	u7 (intepolation)	Uc
0	0	0	1.189941
45	0.94653526	5.008499169	14.37253
90	1.89307052	0.191943112	12.53675
135	2.83960579	2.716989887	10.28834
180	3.78614105	5.268227366	9.281053
225	4.73267631	0.761558881	8.614543
270	5.67921157	4.31122789	9.108513
315	6.62574683	6.111336513	10.0894
360	7.57228209	5.226164108	10.10458

Figure 35: Calculated values after the data analysis. Uncertainty values in KN.
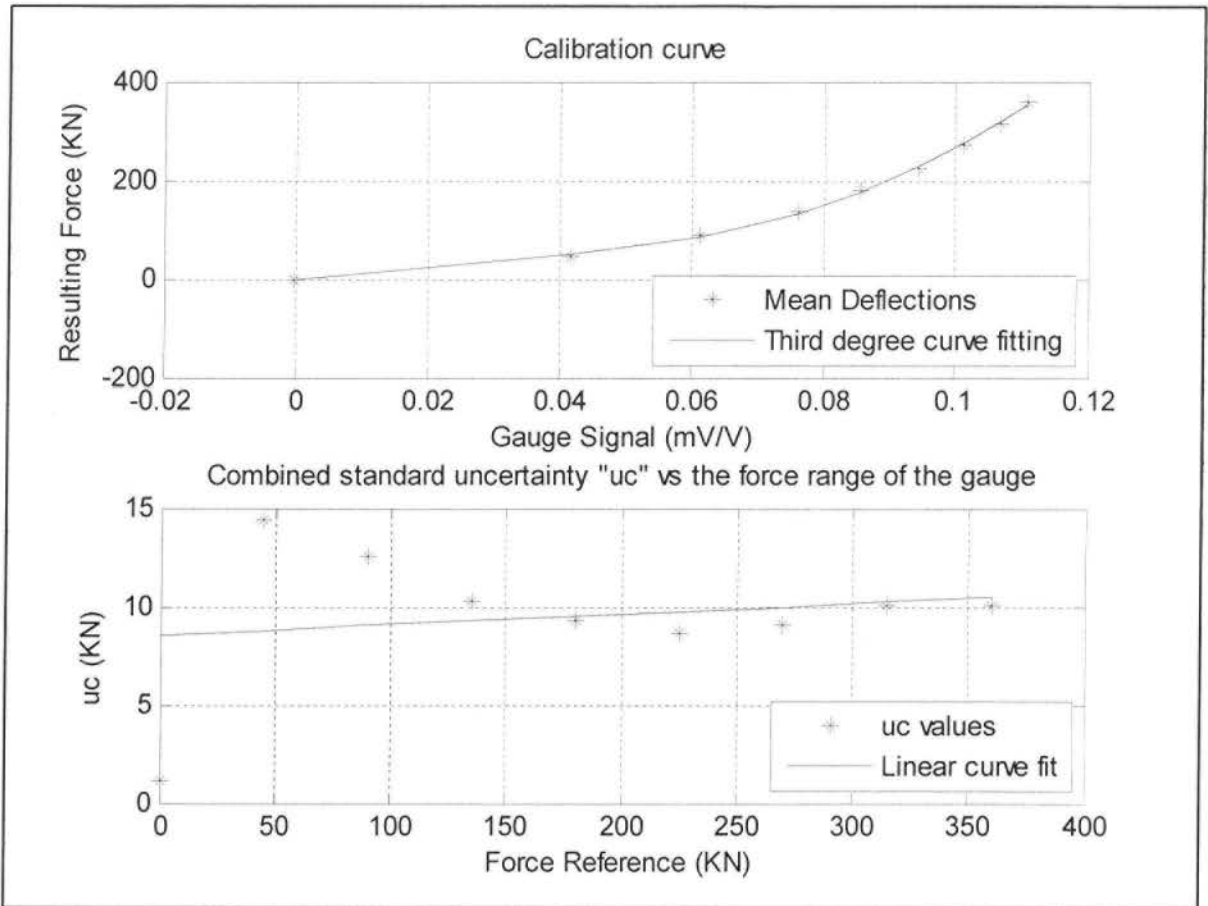
Figure 36: Room temperature calibration results.

- The coefficients of the third degree polynomial fitting are:

3.49e+05   -2.38e+04   1.56e+03   -3.92e-01

- The linear coefficients for the standard uncertainty of the gauge are:

5.29e-03   8.56

Cryogenics at 77 K.

Capacitive Gauge Calibration - Measurement Values							
Force (KN)	Series	X1	X2	X3	X4	X5	X6
0		-3.72674E-05	0.000420083	0.001016553	0.003728238	0.001378688	0.004673121
45		0.025109619	0.025882812	0.016570092	0.018524453	0.02252706	0.024148636
90		0.039578646	0.039690096	0.024235868	0.025952289	0.031949937	0.032904869
135		0.049385278	0.048608082	0.033450591	0.035001592	0.040396092	0.040539505
180		0.055501595	0.05611972	0.043581122	0.043889965	0.047996397	0.047919343
225		0.062494725	0.062051162	0.05043768	0.051366303	0.053248379	0.052181298
270		0.067091125	0.067387731	0.057382589	0.057800375	0.059216621	0.057327648
315		0.069834122	0.069838817	0.064029419	0.064532629	0.064355842	0.063906846
360		0.073662528	0.073404598	0.069273449	0.069772402	0.068403409	0.067596194
Release - 0 KN		0.000507809	-0.000439298	0.003193297	0.002410785	0.004340898	0.003249799
Creep test deflections							
i_{30} =				i_{300} =			
0.003249799				0.004075308			

Figure 37: Deflection values for six calibration cycles with ten loading steps each. Deflection values in mV/V.
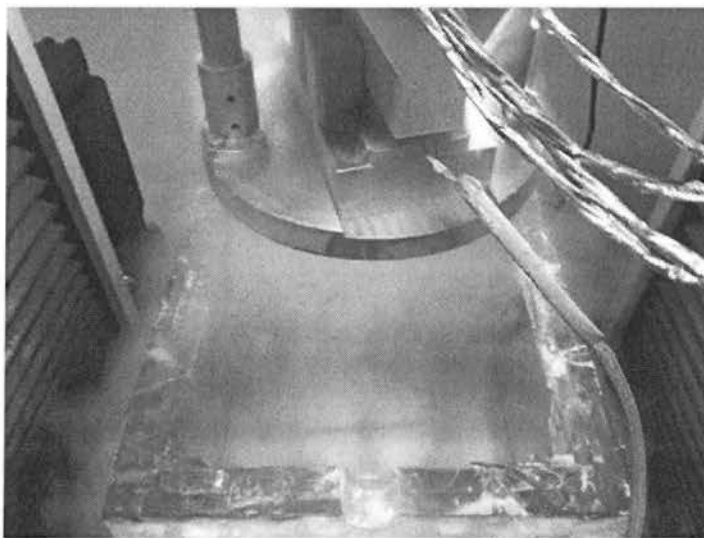
Figure 38: Cryogenic bath – Cryostat filled up with liquid nitrogen

Capacitive Gauge Calibration - Calculated Values							
Force (KN)	Xr	Xwr	Xmax	Xmin	b	b1	Xa	fc
0	0.000785991	0.000191408	0.001379	-3.72674E-05	180.1490142	238.9403978	0.00195318	-59.75842
45	0.021402257	0.025496216	0.02511	0.016570092	39.90012317	3.032580442	0.01903455	12.43901
90	0.031921484	0.039634371	0.039579	0.024235868	48.06411286	0.281193486	0.03215974	-0.740847
135	0.04107732	0.04899668	0.049385	0.033450591	38.79193387	1.586222534	0.04209993	-2.428998
180	0.049026371	0.055810658	0.055502	0.043581122	24.31441119	1.107538575	0.04962628	-1.208859
225	0.055393594	0.062272943	0.062495	0.05043768	21.76613549	0.712288264	0.05550998	-0.209663
270	0.061230112	0.067239428	0.067091	0.057382589	15.85581834	0.44112013	0.06052218	1.1697
315	0.066073128	0.06983647	0.069834	0.064029419	8.785270298	0.006722257	0.06543407	0.976643
360	0.070446462	0.073533563	0.073663	0.068403409	7.465412492	0.350765279	0.07101681	-0.803116

Force (KN)	Xn	f0	c	u1 (Load cell)	u2 (reproducibility)	u3 (repeatability)	u4 (resolution)	u5 (creep)
0				0	2.075556803	0	0.0006765	0
45				0.009	12.35711004	0.78788751	0.0006765	0.291157
90				0.018	21.64569335	0.146112421	0.0006765	0.582314
135				0.027	22.54219308	1.236338109	0.0006765	0.87347
180	0.073662528	4.02132503	1.120663	0.036	17.00468214	1.150987849	0.0006765	1.164627
225				0.045	17.79946796	0.925289597	0.0006765	1.455784
270				0.054	14.55368558	0.68763823	0.0006765	1.746941
315				0.063	9.201807106	0.012225455	0.0006765	2.038097
360				0.072	7.953982839	0.729051942	0.0006765	2.329254

Force (KN)	u6 (zero drift)	u7 (intepolation)	uc
0	0	0	2.075557
45	1.809596263	4.978304483	13.47078
90	3.619192527	0.671739232	21.96467
135	5.42878879	3.36078071	23.47785
180	7.238385054	2.202572577	18.68387
225	9.047981317	0.472733935	20.04714
270	10.85757758	3.121674616	18.51943
315	12.66717384	3.04667015	16.08013
360	14.47677011	2.91462633	16.94992

*Figure 39: Calculated values after the data analysis. Uncertainty values in KN.*
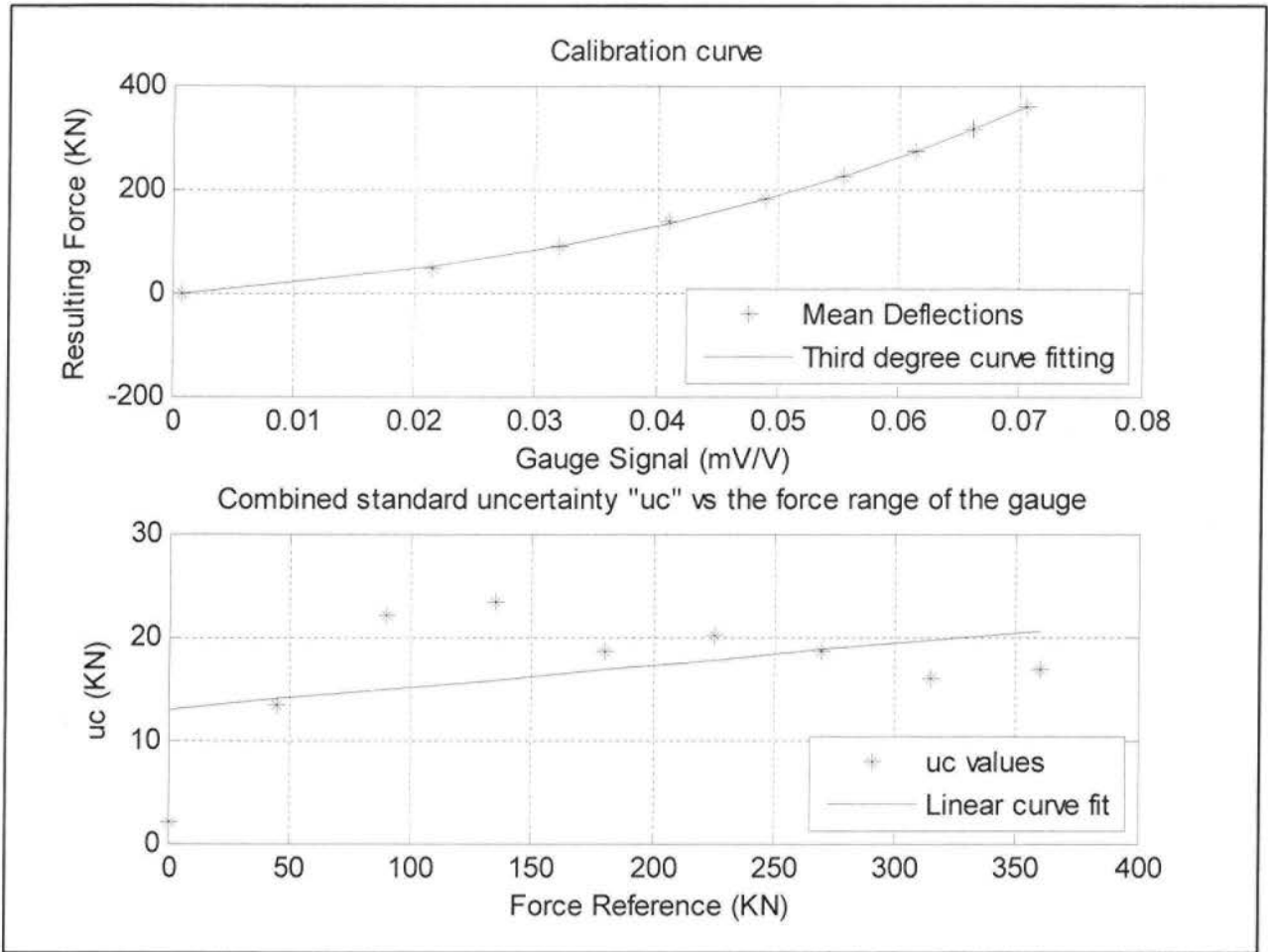
Figure 40: Cryogenics calibration results.

- The coefficients of the third degree polynomial fitting are:

  3.07e+05   2.84e+04   1.59e+03 -1.85

- The linear coefficients for the standard uncertainty of the gauge are:

  2.11e-02   1.30e+01

Finally after each calibration procedure for room and cryogenic temperatures, the gauge should be delivered to the requestor, accompanied by a laboratory official certificate form that has been modified to match the new process. This new certificate form, filled with information derived from the calibration process of a capacitive gauge, can be observed in the following figure.

Engineering Department

EN/MME

Laboratoire de Mesures Mecaniques / Mechanical Measurements Laboratory

Certificat d'etalonnage / Calibration Certificate

EDMS number	1304901		Gauge type	11 Tesla 1800 mm^2
Date	24/10/2013		Gauge serial number	Yan-03

Measurement Setup

Measuring Device	QuantumX MX840A		Force providing instrument	400 KN Load cell - Class 0.5 EN 10002-2
Zero balancing in RT	0.698881 mV/V		Calibrated according to	EN ISO 7500-1
Zero balancing in Cryo	0.545714 mV/V		Date of last calibration	06/02/2013
Acquisition speed	5 Hz		Examiner	K. Velissaridis
Calibration machine	Zwick Roell Z400E		Calibration according to	ISO 376:2011
Apparent strain	0.05105 mV/V		Notes	

Measurement Results

Curve fitting polynomial coefficients					Combined standard uncertainty coefficients	
349090.004	-23810.651	1555.184	-0.392	RT	0.005	8.558
KN / (mV/V)^3	KN / (mV/V)^2	KN / (mV/V)	(KN)		-	(KN)
Curve fitting polynomial coefficients					Combined standard uncertainty coefficients	
306617.596	28401.711	1588.915	-1.845	Cryo	0.021	13.007
KN / (mV/V)^3	KN / (mV/V)^2	KN / (mV/V)	(KN)		-	(KN)
RT curves				Cryogenic curves		

For specific request or questions about the capacitive gauges, please to contact M. Guinchard (michael.guinchard@cern.ch)
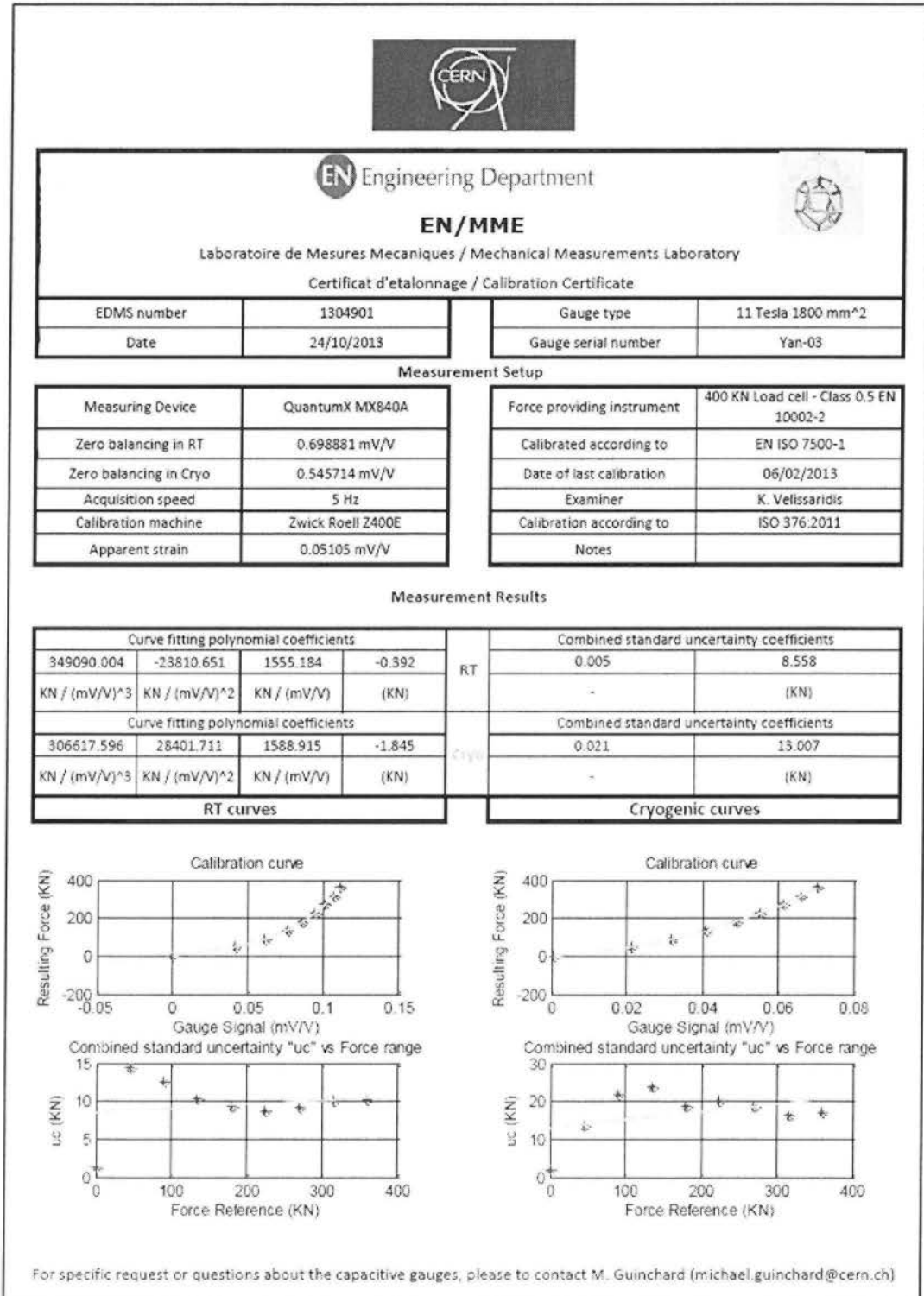
Figure 41: Official certificate form based on the instructions of ISO 376:2011.

Section II
Integration of a new testing set up.

Various studies have been made in the past about the compression machine that the Mechanical Measurement Laboratory is equipped with. This machine is a home-made press made at CERN for various uses (capacitive gauges testing and calibration not included) that was given to the MML more than 15 years ago when it was replaced with another one by the group that previously owned the press. Once the press arrived to the MML, two vertical guides were added in order to stiffen the system.
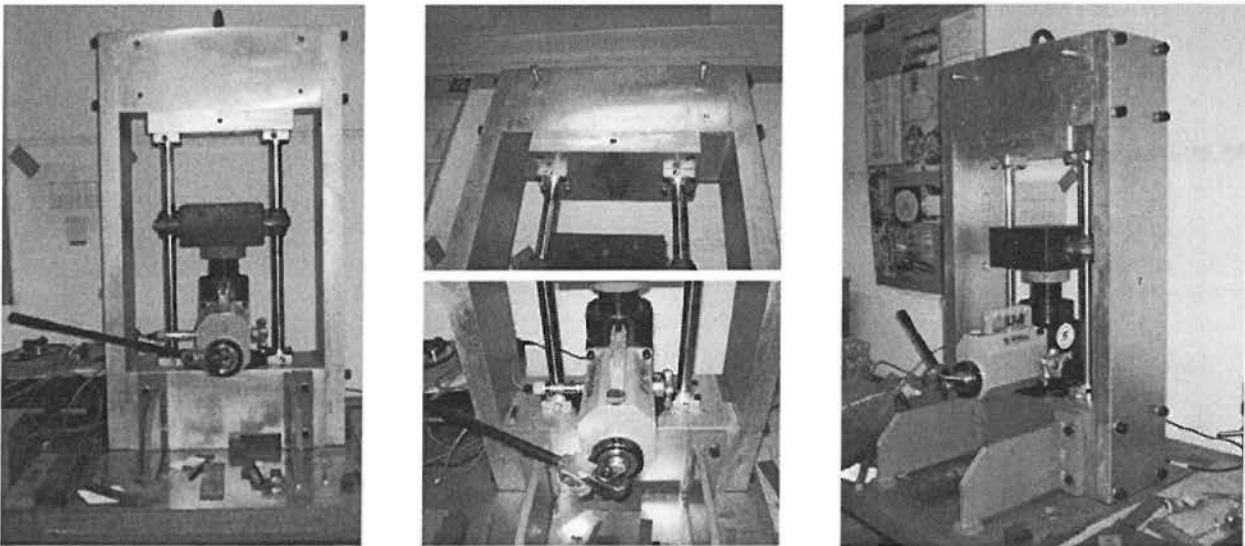
Figure 42: Old press – Calibration system.

All those studies came to a single conclusion. This particular press is not suited to fulfil the tests and calibration procedures planned for the capacitive gauges, accurately enough therefore a substitution is obligatory. A fast sum up of the conclusions derived from these studies is:

✓ Lack of parallelism between the pressing surfaces that lead to a shifted pressure distribution.

✓ Lateral deformations caused when the gauge is not placed centred on the pressing axis. This effect could be minimized by having more than one pressure axis.

✓   Unsymmetrical deformation is caused even when the block is placed centred on the axis. This effect can be induced by the lack of parallelism between plates, lack of perpendicularity and centring of the cylinder, and the clearances that exist in the joints of the frame.

✓   Apart from these problems, the manual pumping system causes lack of precision and control of the charge, and induces moments in the system that affect the measurements.

More information about these studies can be found in [Ref: 2]. After a wide market research, performed by two technical students, the MML purchased a state of the art materials testing machine in order not only to provide the beast means available for the development and testing of the capacitive gauges but to also expand the working possibilities of the laboratory in terms of mechanical properties measurements. This new machine offers:

- State of the art technology - High accuracy measurements.

- High Capacity Load Cell with insensitivity to parasitic forces (transverse, bending moments, torque).Grade 0.5 according to ISO 7500-1.

- Up to 400 KN Load Capacity for:

  ✓ Compression Tests
  ✓ Flexure Tests
  ✓ Buckling Tests
  ✓ Sensor Calibration Procedures

- Two testing areas offering the option of integrating the necessary tools to perform tensile tests (future plan) in parallel with the prementioned tests.
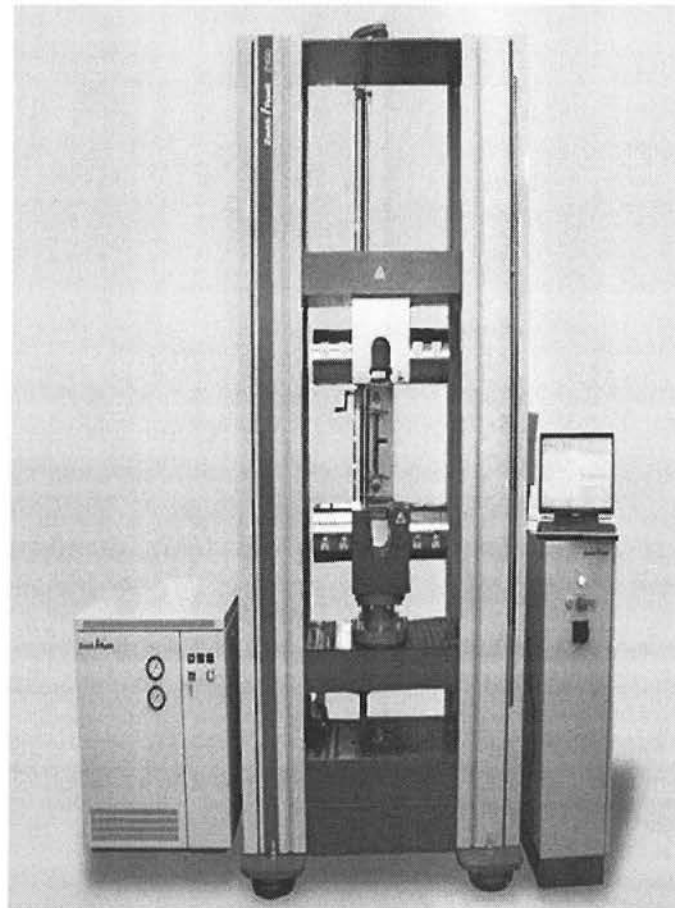
Figure 43: MML's new materials testing machine- Zwick / Roell Z400E

With the new machine more complicated and precise tasks can be performed automatically without having to adjust anything manually. This comes in handy when having to deal with operations such as capacitive gauges' calibrations in which precision is really important in order for the results to be as close as possible to an "error free" state. A demonstration of one capacitive gauge calibration cycle and a simple loading cycle performed on both machines can be observed in the next figures. The purpose of these figures is to present the gain gap of utility, control precision and accuracyacquired by this replacement.
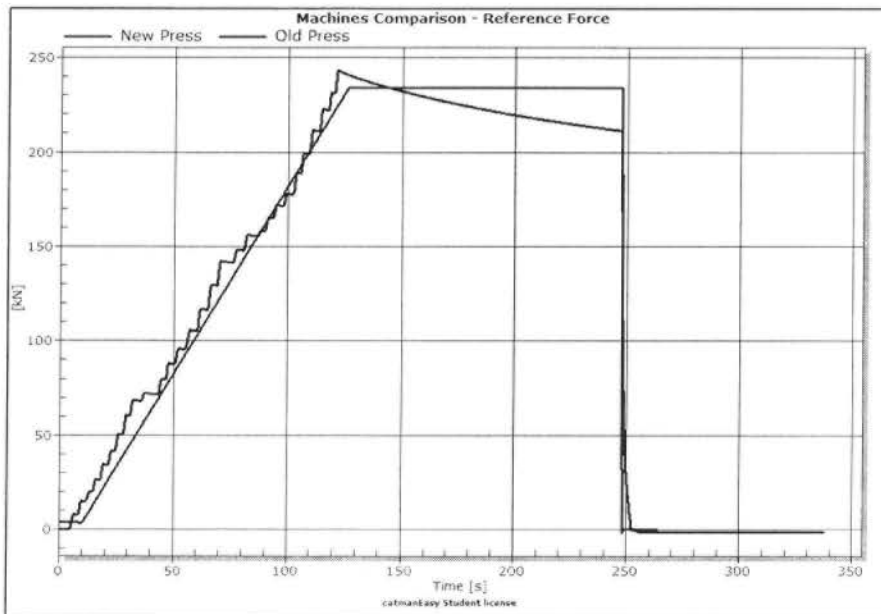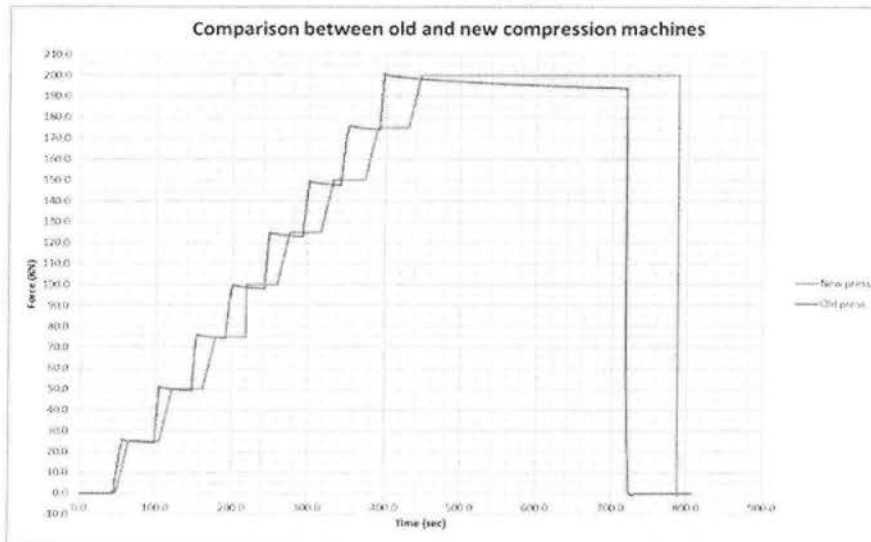

Figure 44: Machines comparison: Calibration steps top – Single loading step bottom.

From these figures it can become obvious that it is not possible to steadily stay at a given loading step while calibrating with the old system; an asset that is a prerequisite for a correct, "error free" calibration. Furthermore, by using the old setup it is impossible to run a creep test something that can become clear by observing the last loading step (200 KN of load for 300 seconds) for the very same reason. Even while performing a simple loading the differences in precision and accuracy are quite obvious something demonstrated better in the second figure.

Additionally, the new machine is offering the possibilities to:

- Expand the force range of the tests performed up to 400 KN which is almost an increase of a factor of 2.
- Mount a special made cryostat on to the machine in order to run calibrations in cryogenics using liquid nitrogen at 77K.

Cryogenics are the working environments that the capacitive gauges are being mainly used and their response is greatly affected by them thus performing a separate calibration procedure performed in cryogenics, mandatory.

The force application and the utilities a new machine offers are not sufficient enough alone to prove that the best means for the capacitive gauges' testing procedures are being provided. Various tests have been performed in order to compare the setups in depth and analyse the degree of this optimization. The next section of this thesis is dedicated to this comparison of testing set ups.

> ## *Pressure distribution on the capacitive gauges*

Cryostat integration summary:

A really important parameter that contributes to the real force value estimation obtained while measuring with the capacitive gauges is the pressure distribution on its surface. According to various tests performed by the mechanical measurements laboratory in the past, it has been made clear that a non-homogenously distributed pressure on the surface of the gauge can lead to significant measurement errors.

Figure 45: FEA analysis on the pressure distribution performed in the past by the lab.
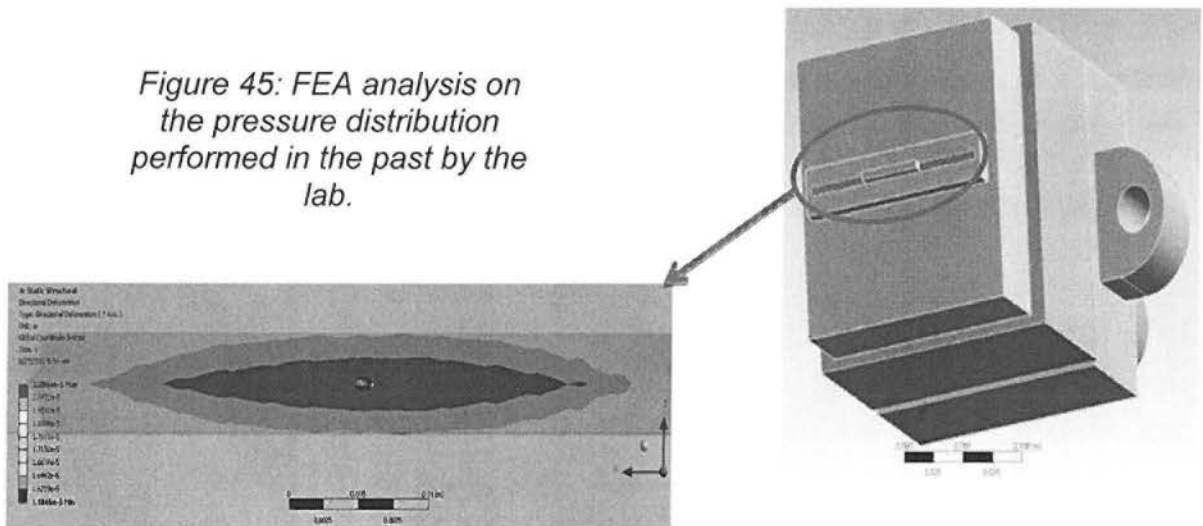
To minimize the error obtained specifically while testing and calibrating the gauges, a massive cryostat has been designed and manufactured in CERN. High stiffness, mass and volume can provide the best means for a homogenous pressure distribution and minimize relative deformations of the setup, meaning much more accurate testing and calibration procedures.
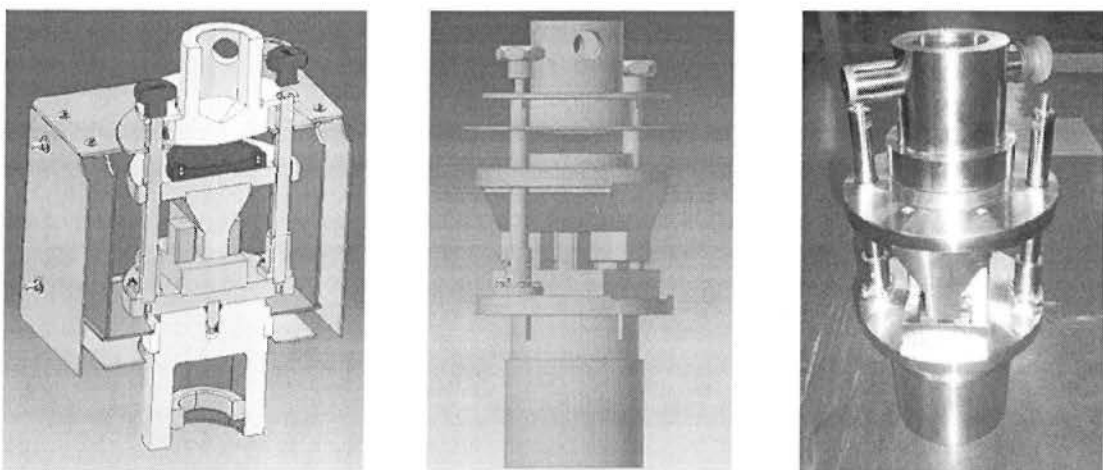
Figure 46: Laboratory's special made calibration cryostat.

Furthermore by using this cryostat the compression forces are being provided by a spherical contact, enabling automatic force centering to the main pressure axis of the machine. The cryostat has also been designed having strict mechanical tolerances and its horizontal surfaces can be used as reference planes. In theory the load application provided by the machine in which this cryostat has been integrated is homogenously distributed in the testing zone where the capacitive gauges are being compressed.

The first priority of the MML after the reception of the new machine was in fact the integration of the cryostat on the new machine. In order to do this, two flanges-supports have been studied and created keeping in mind that they are going to work under high loading forces and in cryogenic environments. Therefore, before the actual testing and comparison of the two set ups, a small section describing the procedures for these supports to be created has been included. The first thing of course to take under consideration is the existing geometry, which includes in fact the assembling cavities of the new machine and those of the cryostat.

Existing geometry:

The new supports need to be designed in accordance to the available space and geometry of the machine and the cryostat. This existing geometry has been divided into two parts namely the bottom and the top part. For each part the mechanical drawings for both the materials testing machine and the components of the cryostat assembly are being presented in the next series of figures. The designs of the machine's flanges have been provided by the manufacturing company "ZwickRoell" while the ones for the whole cryostat assembly can be found in CERN Drawings Directory (CDD: CRNHZMML0063 and forth).

Bottom:

Figure47: Component designs with the existing geometry of the new machine – Bottom part of the assembly.

Top:

Figure 48: Component designs with the existing geometry of the new machine – Top part of the assembly.

Given the existing geometry, prototype design models have been created and mechanically studied. In the next figures these CAD models are being presented.
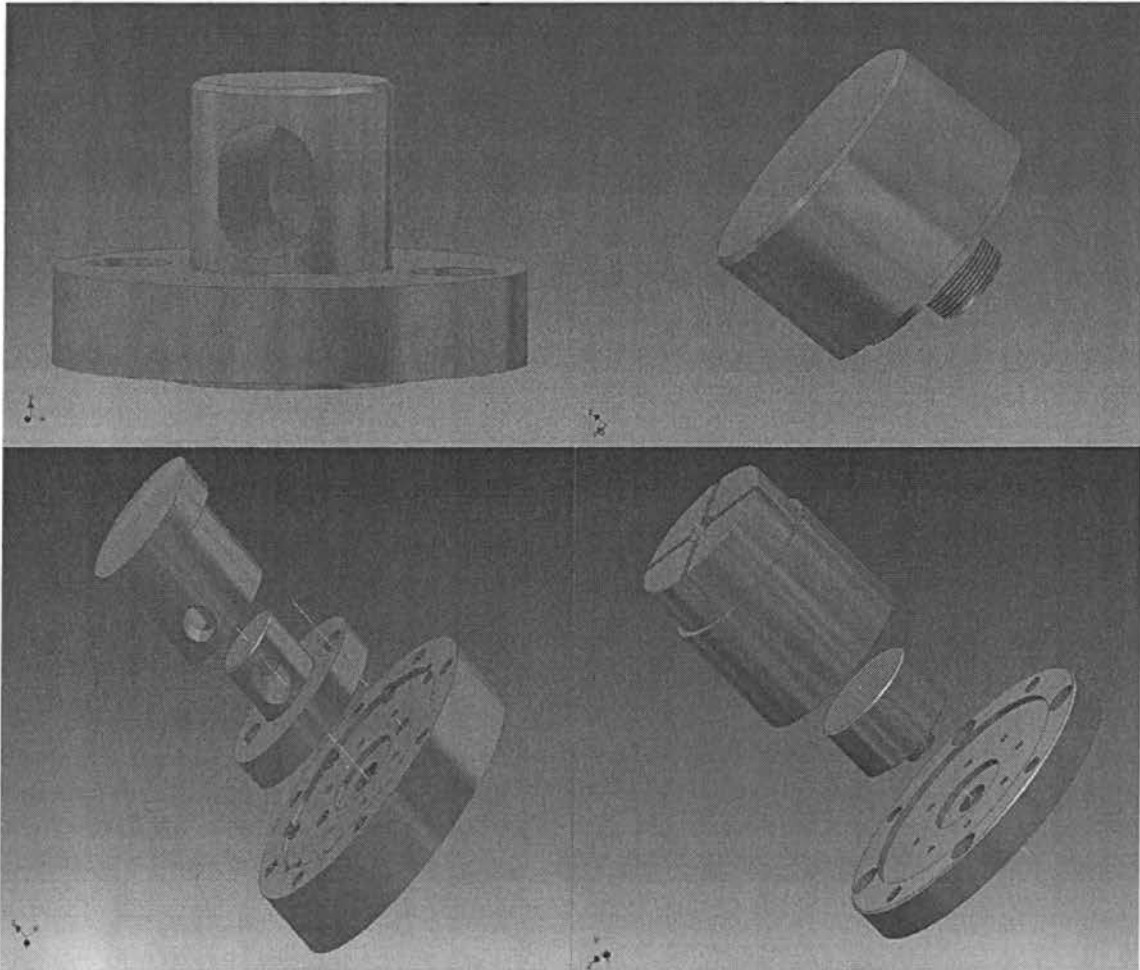
Figure 49: Prototype CAD models for the integration of the cryostat.

The next step is to ensure the mechanical integrity of the supports by choosing the right material and dimensioning. This is only necessary for the upper support since it is transferring the load from the machine to the cryostat. This is not the case with the lower support since its only role is to align the cryostat in the compression axis of the machine and prevent its relevant movement in all other directions, something ensured by the assembling tolerances chosen.

> *Mechanical integrity calculations*

Average Bearing Stress (p):

The average bearing stress for the given contact area (4110 mm^2) under 400 KN of force can be calculated by:

$$p = \frac{F}{A} = \frac{400000}{4110} \frac{N}{mm^2}$$

$$p = 97MPa < 0.75R_e = 135\ MPa$$

- Where F is the nominal force the support is being subjected to and R_e the yield strength of the material (minimum 180 MPa for stainless steel 304 according to the manufacturer).
- The safety factor 0.75 has been chosen according to the handbook [Ref:3] for static loading conditions.
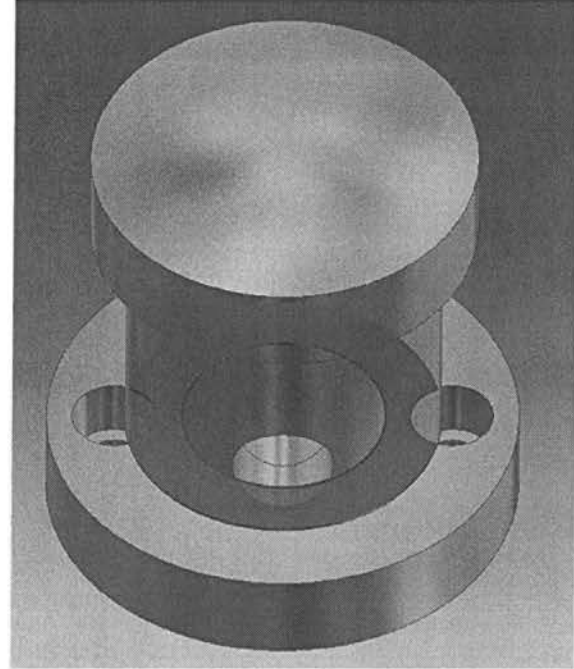
Figure 50: Loading transfer area.

As it can be seen, the loading criteria are being satisfied for this particular contact and no further calculation needs to be performed for the rest of the cryostat since it has been both studied during the designing and tested while performing calibrations on gauges in the past.

Buckling test:

Apart from the increased load that this new machine is possible to provide, by adding the height of the new supports, this assembly needs to be checked for buckling failure. In order to perform a buckling calculation in this complicated structure some simplifications need to be applied. Therefore in order to simplify it, the structure is being replaced by a tube and a bar having the same dimensions as the thinnest and most critical cross sections of the assembly (which in fact are the contact checked previously and the contact between the components directly compressing the capacitive gauges in the cryostat). The following figure and arrays contain the results of the calculations.
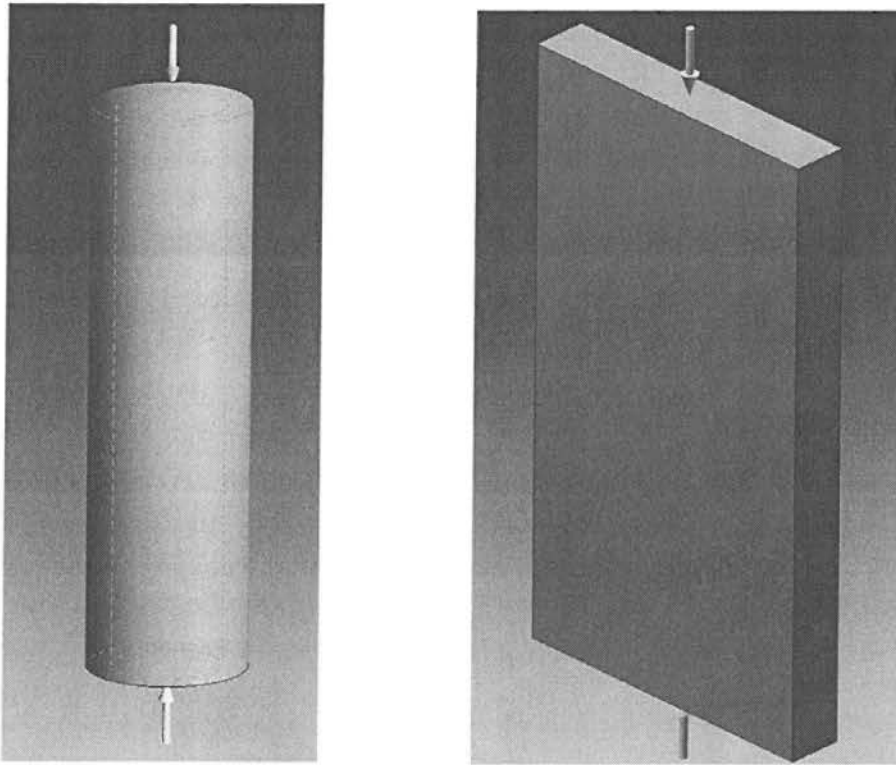
Figure 51: Geometry simplification for the buckling calculation of the assembly.

I	A	lk	i	λ
(mm^4)	(mm^2)	(mm)	(mm)	11.4
3.2*10^6	4110.26	319	28	

I	A	lk	i	λ
(mm^4)	(mm^2)	(mm)	(mm)	37
3.85*10^5	5269	319	8.55	

Figure 52: Buckling calculation arrays for the tube and rectangular bar

- Where I is the area moment of inertia, A the critical area, lk the column effective length (one pinned end and one fixed end), i the radius of gyration and λthe slenderness ratio.

With slenderness ratio less than 50 in both cases, there is no danger of buckling failure of the structure and it can be assumed that the cryostat from the mechanical integrity point of view is safe to be used while supported by the designed flanges.

> *Thermal integrity calculations*

According to the manufacturer, the load cell'soperating temperature threshold is -30 °C. While calibrating in cryogenic environments it is possible for the load cell to reach this temperature and stop providing correct load indications. Therefore a theoretical thermal calculation is needed to determine the time window available and to verify that the chosen dimensions for the new supports are providing enough material to maintain the load cell within the temperature range in the available time.

A simple approximation of the problem can be achieved by making some assumptions. First step is to define the system for which this time window will be calculated. Since the load cell is the critical part of the assembly, it will be left outside of the system while the rest of the assembly that is submerged in the nitrogen will be included. When the rest of the system has reached this temperature, then the load cell will be really close to this threshold. In the next figure the cryostat assembly and the defined system are presented.
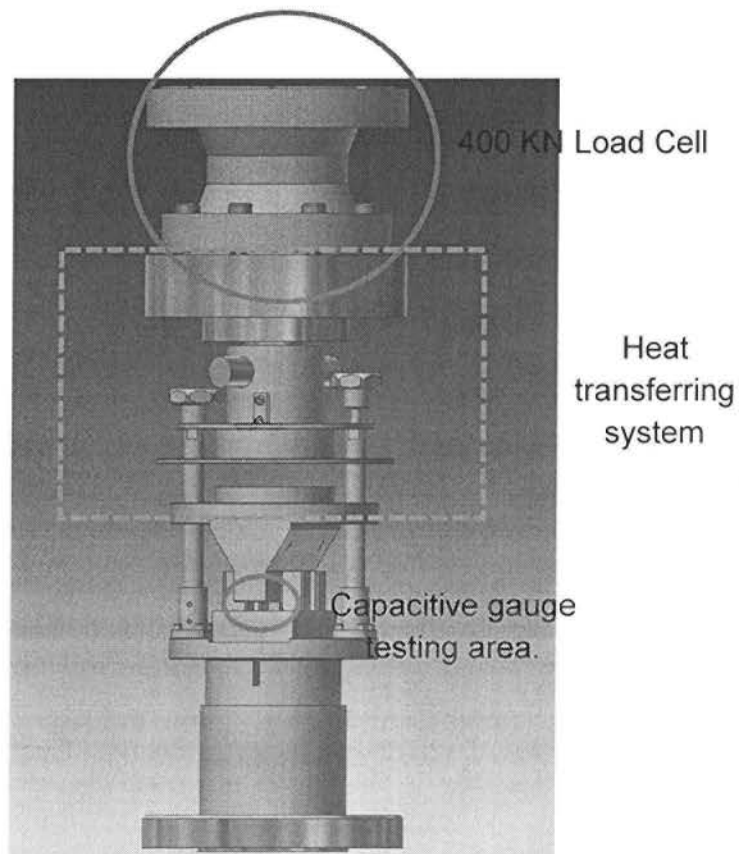
Figure 53: Cryostat assembly connected to the 400 KN load cell.
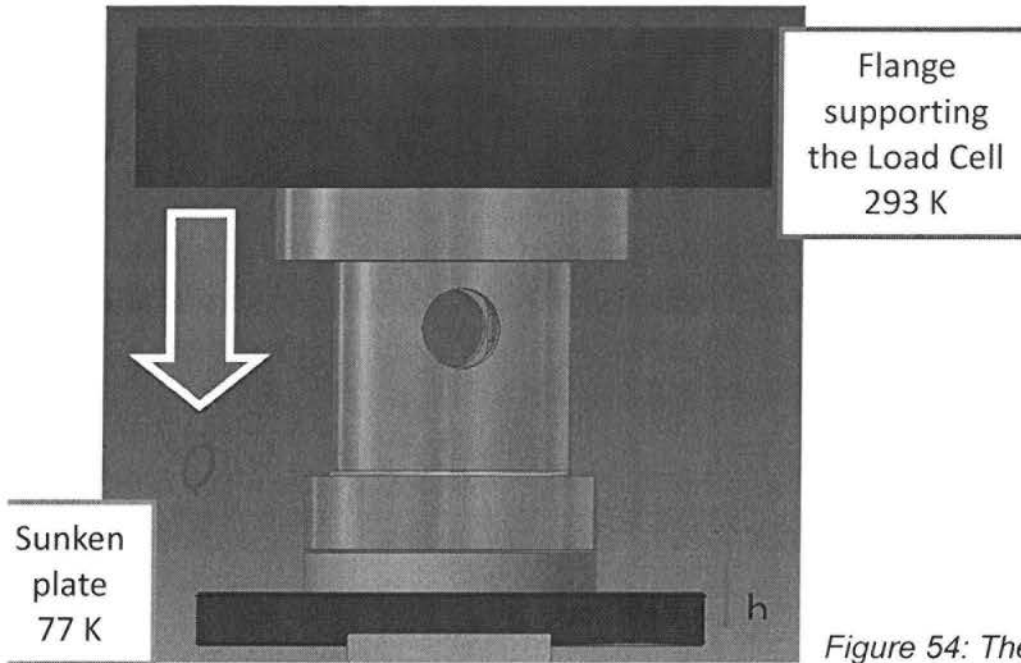
Figure 54: Thermal analysis system.

Assumptions:

- Heat transfer exclusively through conduction and in h direction. Convection's and radiation's contribution are negligible. Specifically for convection, the nitrogen (gas) is heavier than air therefore a direct contact with the load cell can be prevented.
- Bottom plate's T1(t)|0 = 77 K. Since convection is not considered in the calculation, it can be assumed that the sunken plate (blue plate in figure 54.) when put inside the liquid nitrogen, its temperature reaches directly 77K.
- Upper flange's T2(t)|0 = 293 K
- The system is treated as a single body (no contacts, no holes)
- Constant thermal conductivity of St steel 304: k = 16.2 W/(m*K)

The mass of the system is 35 Kg and the area (mm^2) normal to the heat transfer vector is described by the following equation:

$$A_{(h)} = \begin{cases} 31400, \ 0 < h \le 20 \\ 10382, \ 20 < h \le 63 \\ 4110, \ 63 < h \le 88 \\ 6936, \ 88 < h \le 143 \\ 15386, \ 143 < h \le 171 \\ 49063, \ 171 < h \le 231 \end{cases}$$

From the equation of thermidometry, in order for the body to reach -30 °C, the energy that must be "ejected" from the system equals to:

$$Q = m * C_p * (\Delta T) = 35 * 500 * 50 \leftrightarrow$$

$$Q = 875 \text{ KJ}$$

The maximum heat flux is occurring at $t_0=0$ s where the delta of the temperature has its maximum value (20 °C – (-30°C)=50 °C). For simplicity, it can be assumed that this flux is constant something that provides a safety factor in the calculation since this flux cannot have a higher value. From Fourier's law for heat transfer through conduction, the heat flux is:

$$\vec{q} = -k * \nabla T$$

Where: $\vec{q}$ is the local heat flux, W·m^{-2}

   k is the material's conductivity, W·m^{-1}·K^{-1}

   ∇T is the temperature gradient, K·m^{-1}

But since it has already been assumed that the flux is only in one direction (h) and k is constant, the equation becomes:

$$\dot{Q} * \frac{dh}{A_{(h)}} = k * dT \leftrightarrow \dot{Q} * \int_0^{231} \frac{dh}{A_{(h)}} = k * \int_{77}^{293} dT \leftrightarrow \dot{Q} = 180 \ W$$

The boundaries of integration are the total distance from the sunken plate to the interaction point of the top flange and the load cell as well as the two temperature values of these points.

Finally the critical time of the system to lose this thermal energy is:

$$\frac{dQ}{dt} = 180 \leftrightarrow \int_0^{875000} dQ = 180 \int_0^T dt \leftrightarrow$$

$$T = 81\ min$$

The time window is 81 min whereas the time for the calibration procedure is 90 min. It is clear that this time window is really close to the desired one that has been calculated keeping the heat flux constant at its maximum value. From this point on, either a more precise calculation or even a simulation can be performed or the experimental way can be followed. Since this is a mechanical measurements laboratory, it has been decided to do what the laboratory does best; measure and monitor the temperature while performing a cryogenic calibration.

For this measurement, two pt100 Resistance Temperature Detectors were installed on the newly manufactured supports (final designs included in Annex B). The pt100 detectors are sensors used to measure temperature by correlating the resistance of the RTD element with temperature. Most RTD elements consist of a length of fine coiled wire wrapped around a ceramic or glass core. The element is usually quite fragile, so it is often placed inside a sheathed probe to protect it. The RTD element is made from a pure material, typically platinum, nickel or copper. The material has a predictable change in resistance as the temperature changes; it is this predictable change that is used to determine temperature. They are slowly replacing the use of thermocouples in many industrial applications below 600 °C, due to higher accuracy and repeatability. More information about this kind of sensors can be found in the web.
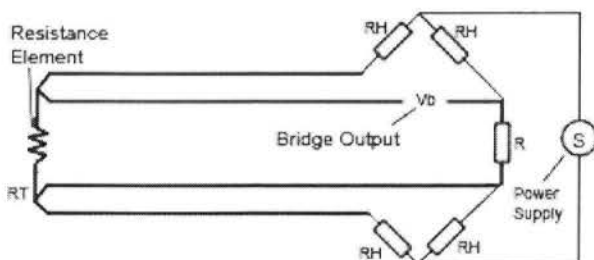
Figure 55: Four-wire Kelvin connection used to measure and calculate the temperature of a body on which a pt100 sensor has been mounted.
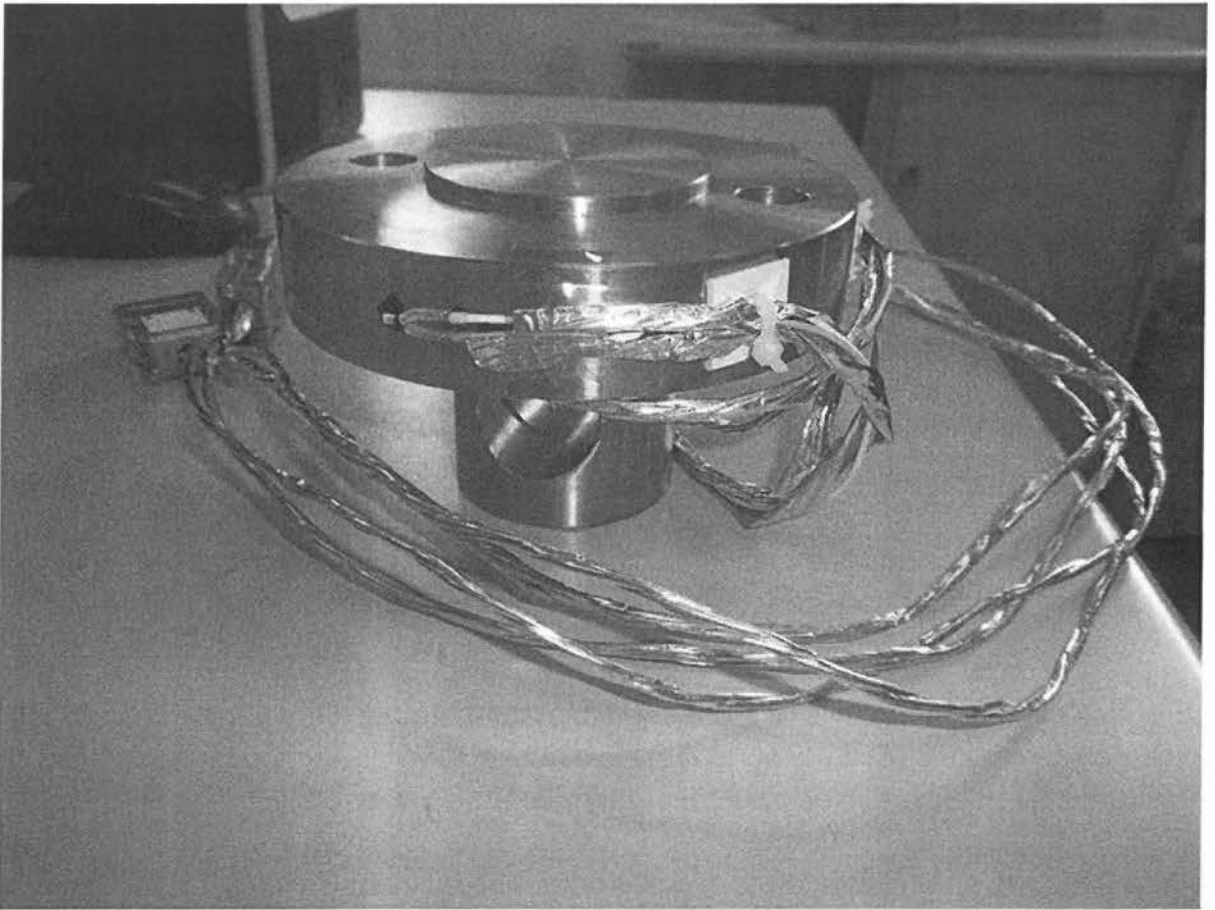
Figure 56: After the machining of the new support, two pt100 temperature sensors were connected to measure and monitor the temperature close to the 400 KN load cell.

While calibrating in cryogenics these sensors indeed verified that the time window available, before the load cell stops providing correct results, is more than the time a calibration lasts. Anaphorically, the lowest temperature the support reached in three cryogenic calibrations, was above 0 °C.

The last step before the comparison is possible, involves the creation of specific capacitive gauge adaptation and centering plates, which are located in the testing area of the cryostat and needed for what the name suggests. For every different geometry, a capacitive gauge may have, in order to centre it to the cryostat's main compression axis, a new specific plate must be created.

This plate has been designed for the purposes of this thesis and has been machined. The mechanical drawings have been included in [Annex B] and in the next figures the real piece after the machining is presented.
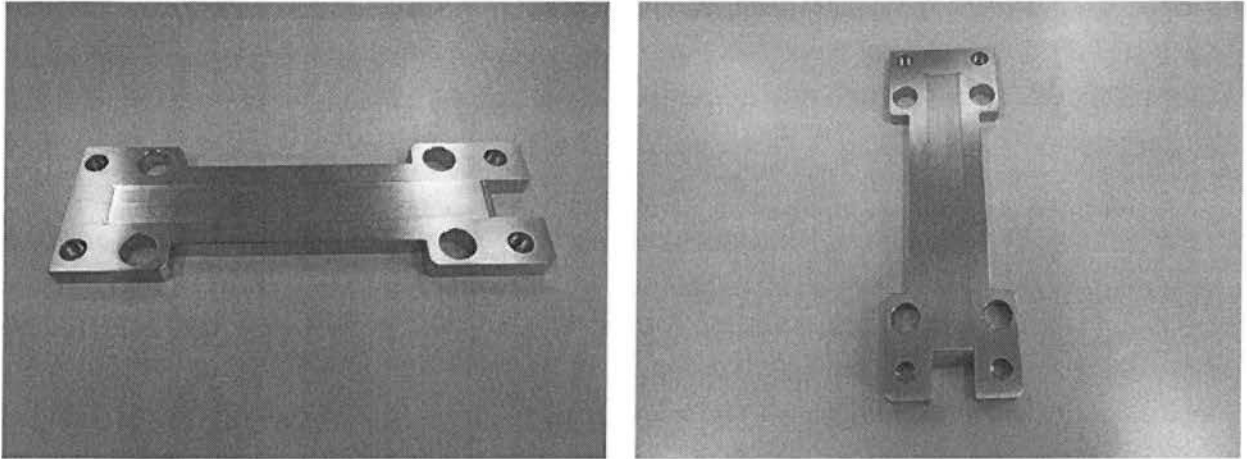
Figure 57: Capacitive gauge adaptation plate for 1800 mm² gauges.

With the new machine installed and ready to be used, the next step is to perform several compression cycles on both the new and old machines (cryogenic tests included) with and without the use of the cryostat and compare the two set ups in terms of pressure distribution and signal response. The next section of this chapter is aiming to present the results of these tests.

> ## *Comparison of the two compression machines:*

As explained before the two testing set ups will be compared both in terms of pressure distribution on the gauges and of signal response while performing loading cycles. In order to do so, three different capacitive gauges have been used. The first two gauges that will be used for this comparison have been manufactured recently with this test as their main creation purpose while the third one has been manufactured in the past for monitoring of the stress levels inside the 11 tesla prototype magnet and has been used repetitively in room and cryogenic temperatures since then.

Using the first gauge a Fujifilm paper measurement has been performed (more information to follow), resulting in a pressure distribution state overview and its signal response. The second gauge has been tested in both machines; more specifically for the new machine, using both the standard commercial compression plates that were purchased from the manufacturer and by using the special CERN made cryostat. Furthermore, this test includes a reversal of the gauge in the main pressing axis of the two machines (90° rotation), for reproducibility checking purposes. In addition a cryogenic loading curve from the same gauge has been included. Finally, for the second gauge a last Fujifilm paper test has been performed to have results for the pressure distribution estimation for all the three possible testing ways of a capacitive gauge. For the third gauge, a more focused testing on the reproducibility and loading of the machines has been performed. Different positioning has been tested (four different angle orientations), while using the old machine and the new machine with its commercial compression plates mounted on.

For all these three cases, all parameters (connection to the bridge, instrumentation, preparation of the measurements, DAQ system and environmental conditions), were kept constant to ensure the validity of the comparison.

All the results as well as the conclusions of the comparison between the machines can be viewed in the following pages.

Test preparation:

Just like the tests performed in the past in order to estimate the pressure distribution on the gauge, Fujifilm Prescale® pressure measurement film was used. Information about the film can be consulted in the manufacturer´s catalogue.

The first gauge will be tested under pressure in two different set ups. For this gauge the first test will be performed on the new compression machine, without the use of the special cryostat while the second test will be performed using the old compression machine. Both the electrical signal and the prints on the Fujifilm paper will be presented for comparison. An increasing pressure value of up to 130 MPa will be applied on the surface of the first gauge over a period of 2 minutes and when this value has been achieved it will be maintained for an additional 2 minutes. The load will be released directly after the 2 minutes of loading have been achieved.

First gauge - test results:

New machine – Compression tools installed.
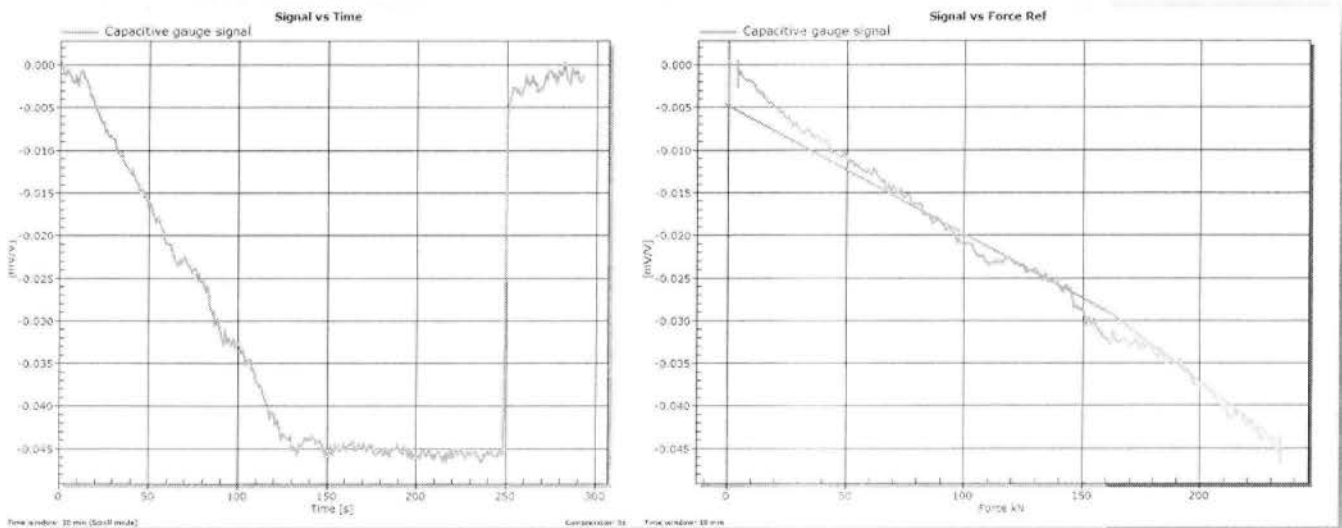
Figure 58: Signal response (new machine).
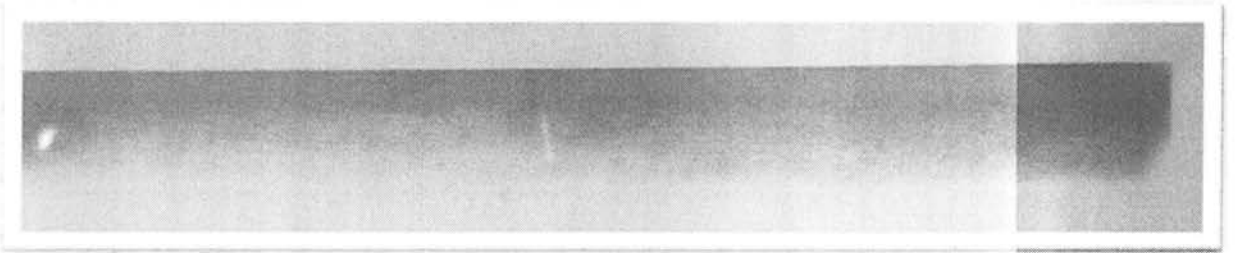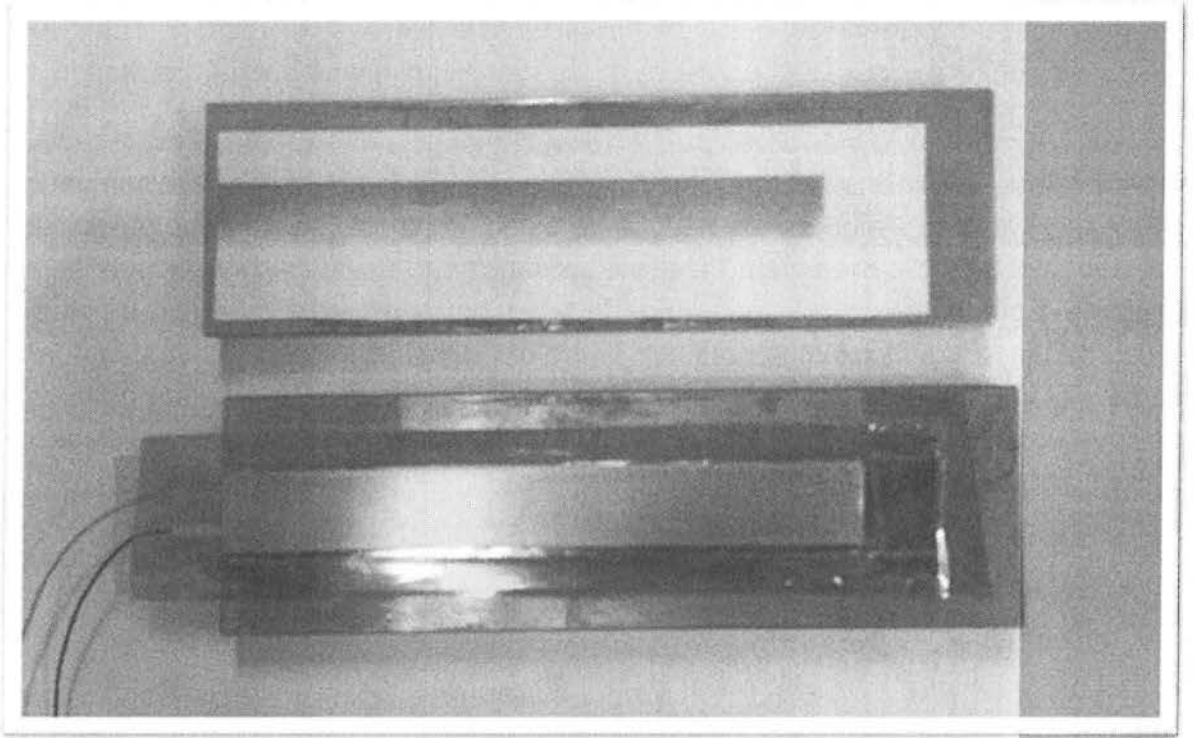
Figures 59,60: Pressure prints of the first test.

Old machine
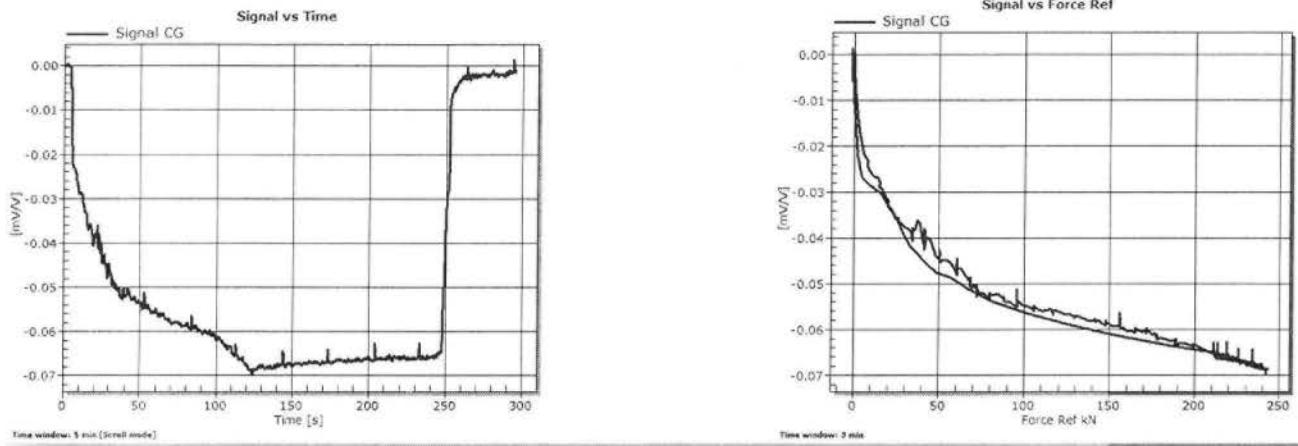
Figure 61: Signal response (old machine).
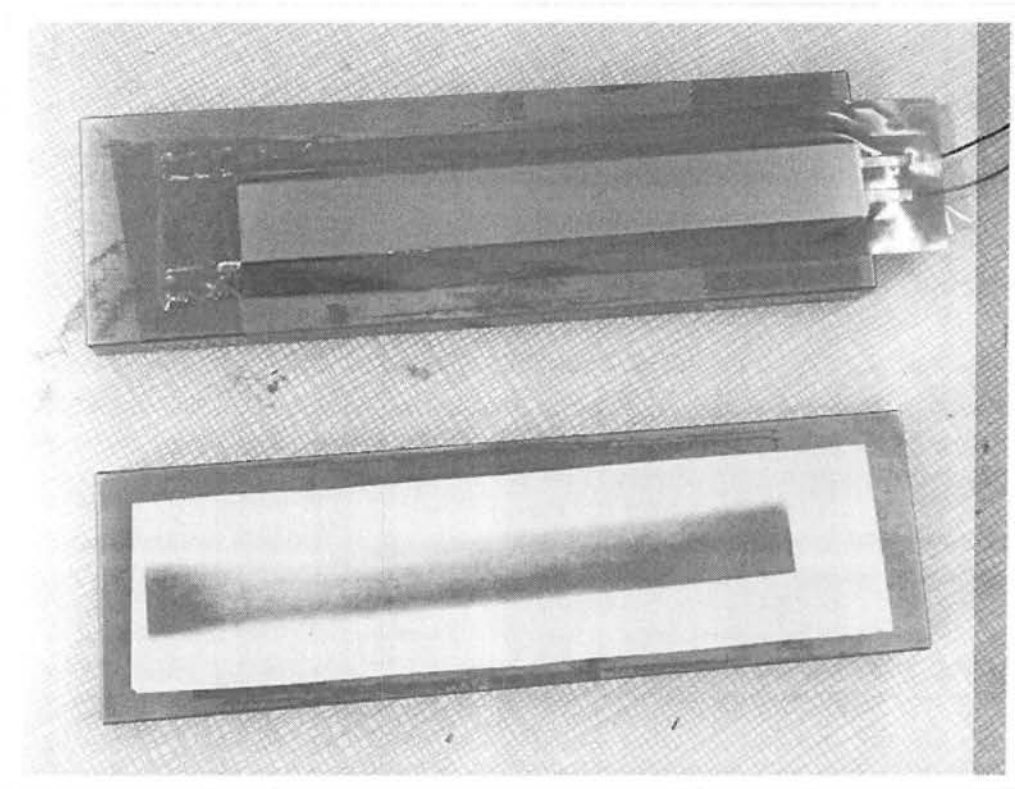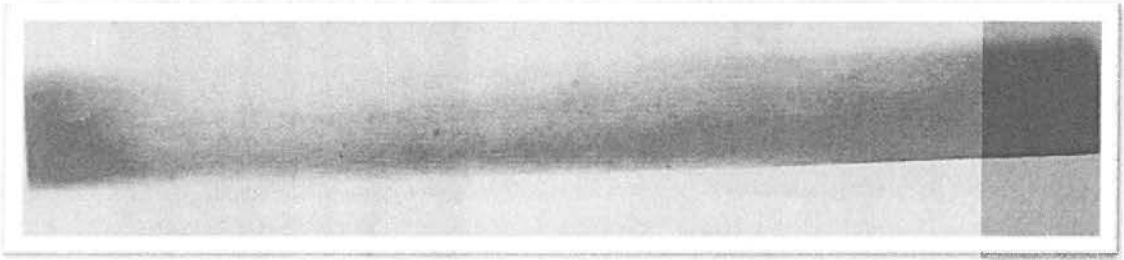
Figures 62,63: Pressure prints (second set up).

Conclusion of the first test:

These figures show the pressure distribution estimation over the surface of the same gauge in both machines. Even though in both cases the distribution does not appear to be equally distributed, a small improvement can be observed with the use of the new machine (synopsized results to follow after the completion of the third film measurement in the next test).The magnitude of theimprovement can become apparent from the signal response though. In the following figure the difference in the signal response is quitevisible.The same gauge tested on the new machine exhibits a better linearity and a much more consistent response overall.
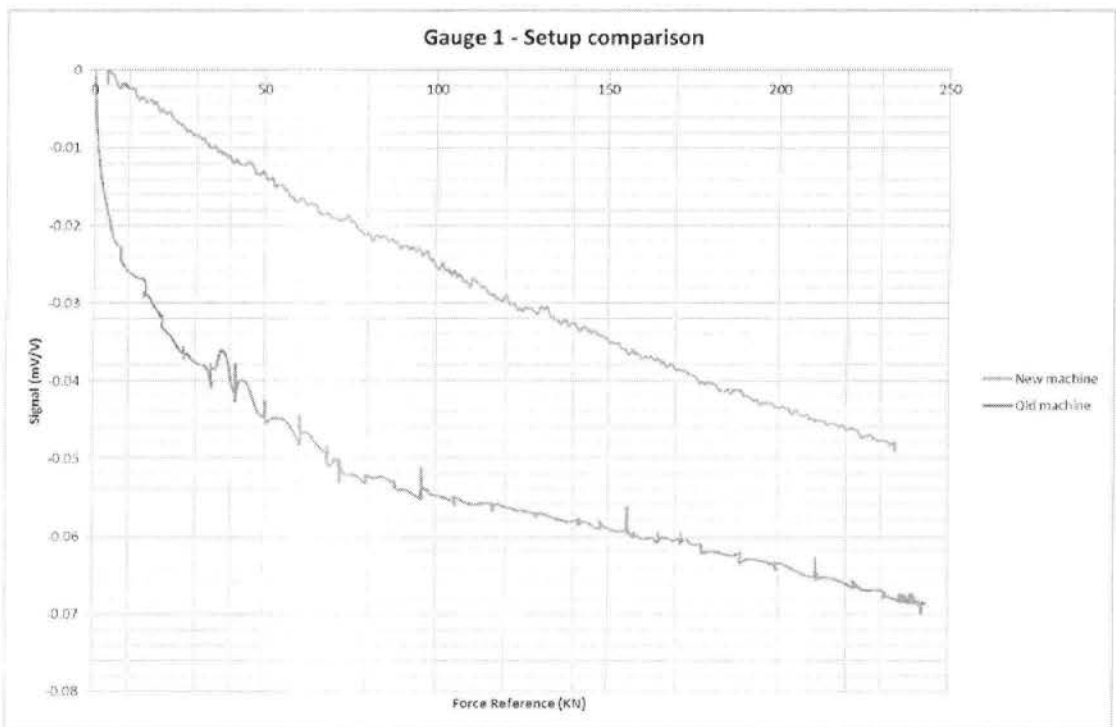
Figure 64: Response of gauge 1. Collected data from both setups (loading only).

Second gauge - test results:

The second gauge has been tested in various ways. Intergraded in both the old machine and the new one using the compression plates - prototype shims to apply the pressure and finally in the new machine with the use of the special cryostat for both room and cryogenic temperatures.In the next figures, the final Fujifilm paper print is presented for the pressure distribution estimation of the cryostat as well as the signal responses of the second gauge for this second comparison test.

Figure 65: Pressure prints (Cryostat on new machine).
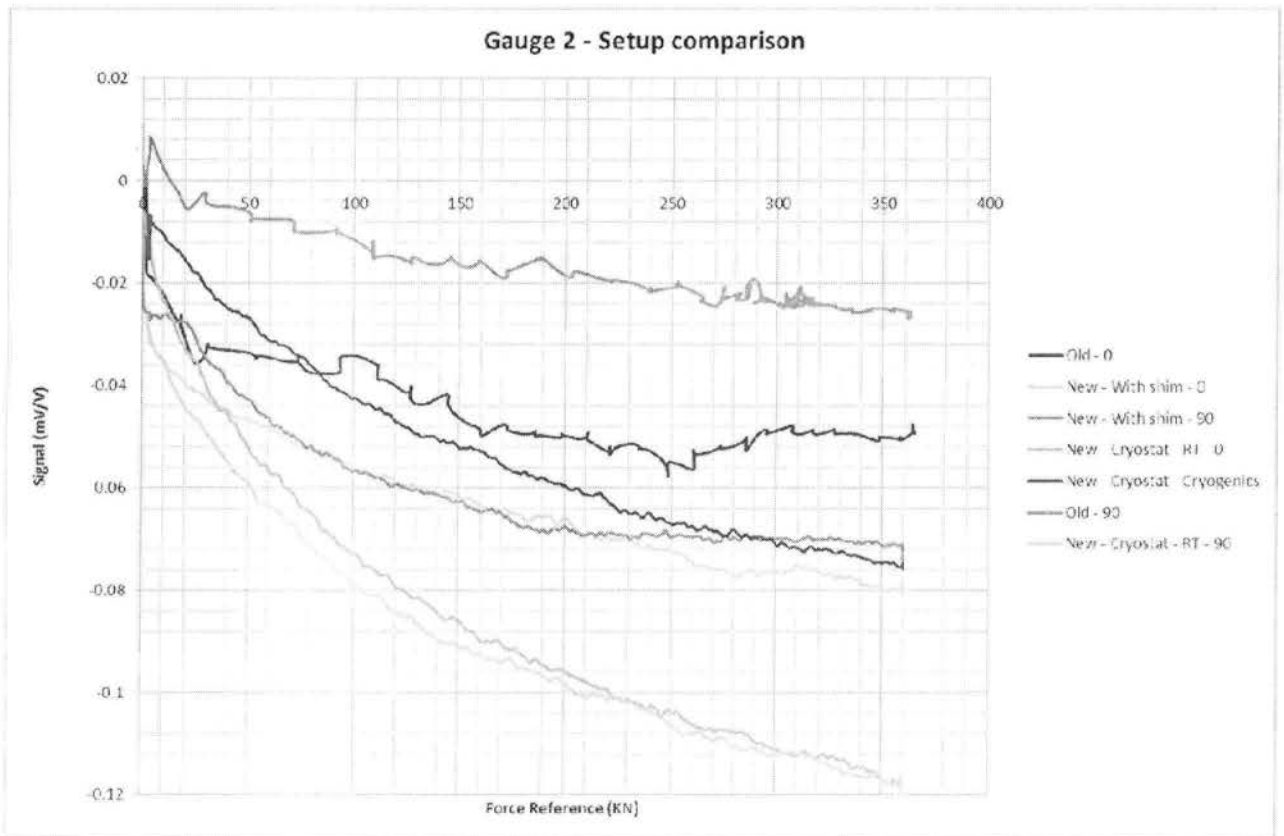
Figure 66: Results of the second test.

Conclusion of the second test:

From figure 66 several conclusions about the two machines can be derived. To begin with, it is clear that the signal response while the second gauge is being tested on the old machine presents no reproducibility while the only thing changed is its orientation on the machine (90° shift in the pressing axis). The signal gap between these curves is almost 50% of the signal's range. This is not the case with the new machine that exhibit good reproducibility behaviour. The range of the signal as well as its linearity in the case of the new machine has also being improved to a big extent. Apart from the small signal range in the case of the old machine, the 0° position appears to have a minimum value close to the loading value of 260 KN (3/4 of the loading width). Finally, the cryostat utilization appears to exhibit the best results with a wider, more linear and less noisy signal. The reproducibility of cryostat set up is also superior compared to the rest. Both the room temperature and cryogenic tests provided a trustworthy signal that can be used without problems in a real pressure monitoring measurement.

In addition to the signal response, the Fujifilm paper results confirmed that in the case of the cryostat usage, the pressure distribution on the gauge is more homogeneous with most of the gauge surface receiving roughly the same amounts of the loading, without being focused on one side like in the other two cases.
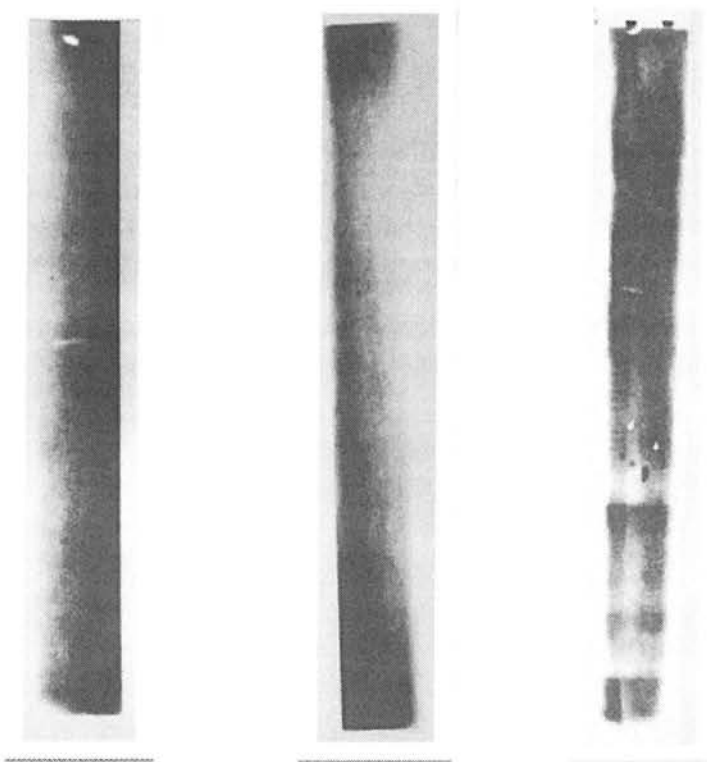
Figure 67: Gathered results of the Fujifilm measurement. New machine (left) – Old machine (middle) – New machine with cryostat (right).

Third gauge - test results:

For the final gauge, four angle orientations on the compression areas of both machines have been tested. The preloading force was set to 10 KN and before the actual recording of each signal curve, each gauge was subjected to a preloading cycle in order to set it ready for the measurement. In the following graph the results of this final measurement are being presented.

Figure 68: Results of the third comparison test.

Conclusion of the third test:

For the third gauge the reproducibility of the tests seem to be much better for both machines than the previous gauge. In all eight position curves, the slopes of the signal, while the loading force is increasing, seems to not be affected by the positioning. The range differences between the cycles and the machines are due to the zero drift errors of the gauge and the zero balancing of the DAQ systems. An interesting fact that can also be derived from this graph is that due to the steadily and precise application of the force, the new machine can achieve, a much more steady and smoother response is being resulted, making a polynomial curve fitting calibration much more precise and accurate.

Chapter Conclusion:

The optimization of the capacitive gauges in terms of testing procedures started directly after the reception of the new materials testing machine. The results of the machines comparison section proved this optimization and clearly displayed the extent of the improvement, this new machine brought to the capacitive gauges. The integration of this machine in the laboratory as well as the modifications that were implemented in order to use it for the capacitive gauges purposes,have also been included and described in this chapter. Finally with this new tool a new calibration procedure based on international standards is now possible. In the beginningof this chapter, the whole procedure has been thoroughly described having included a section presenting calibration examples of gauges that will be used in future measurements and a troubleshooting guide that might solve some problems with the software usage. Finally in this chapter of this thesis, a laboratory certificate template (according to the directions of ISO 376:2011) filled with a gauge's calibration results, has been prepared to match and finalize the new procedure.

Chapter III
Optimization in terms of manufacturing procedures

Section I
Pre-stressing of the steel foils

Summary

Prior to the assembly of a capacitive gauge, it is mandatory to pre-stress the steel foils in order to form the appropriate shape/roughness and create cavities required for the glue to be maintained. This procedure is performed by compressing each one of the five steel foils using a pair of sandblasted steel plates. This pair of plates is getting permanent plastic deformations every other gauge creation, something that is causing big problems in the manufacturing process. This problem eventually leads to the continuously need of sandblasting the surface of each plates in order to repair them over and over again.
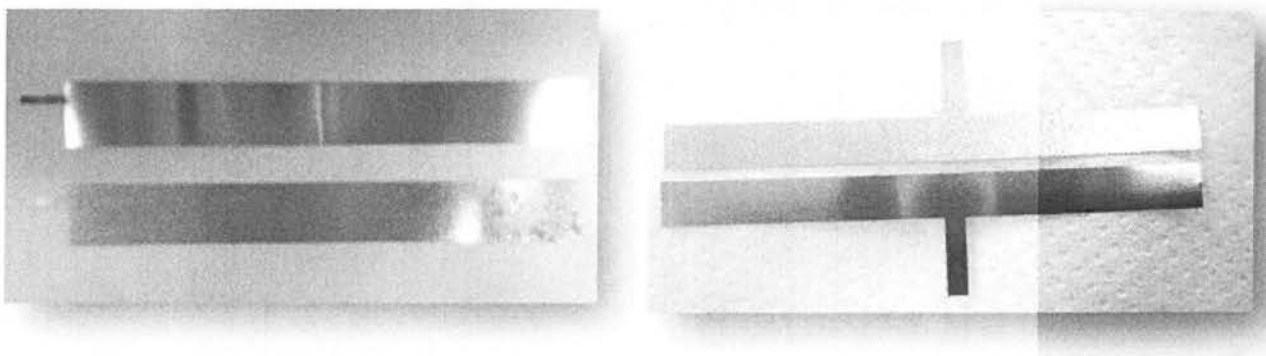
Figure 69: Steel foils before and after the pre stressing.

Problem solution:

Steps to solve this problem have been already performed. It is clear that this problem occurs due to the fact that the surface hardness of the plates is very low, that is why these steps are mainly focusing in replacing the plates with others having a higher surface hardness. Attempts have been performed to sandblast a material with higher surface hardness in the past but they failed because the sandblasting machine is not powerful enough to shape the hard surfaces of the pieces.

The step sequence that has been followed to solve this problem is to choose and acquire a new pair of steel plates, machine it having strict geometrical tolerances, sandblast it and finally perform a steel hardening.

> *Machining*

The material that has been chosen to be machined for this application is a steel alloy - DIN 14NiCr14. Its chemical composition (in weight %)and its physical properties are being summarized in the following figures:

C	Si	Mn	Cr	Mo	Ni	V	W	Others
0.17	max. 0.40	0.55	0.75	-	3.25	-	-	-

Figure 70: Chemical composition of DIN 14NiCr14 steel alloy.

Physical properties (avarage values) at ambient temperature
Modulus of elasticity [10^3 x N/mm^2]: 210
Density [g/cm^3]: 7.83
Thermal conductivity [W/m.K]: 34.0
Electric resistivity [Ohm mm^2/m]: 0.20
Specific heat capacity[J/g.K]: 0.46

Figure 71: Physical properties of DIN 14NiCr14 steel alloy.

The main reason for this alloy selection is that this particular steelcontains alloying elements that enhance itsability to be machined/sandblasted and in addition they simplify the hardening procedure.

Having acquired the material the first step is to machine it to the desired dimensions. In this case precision and accurate dimensions are not necessary and the only thing that really matters in terms of geometrical dimensioning and tolerancingis the flatness and the parallelism of the compressing surfaces.Several tries to pre-stress steel foils using various sets of plates in the past have failed because of these two parameters not being so strict.Eventually, keeping in mind that the machining will be performed in a compatible milling machine, these parametershave been set to 0.05 mm. In the next figure the results of this first step can be viewed.
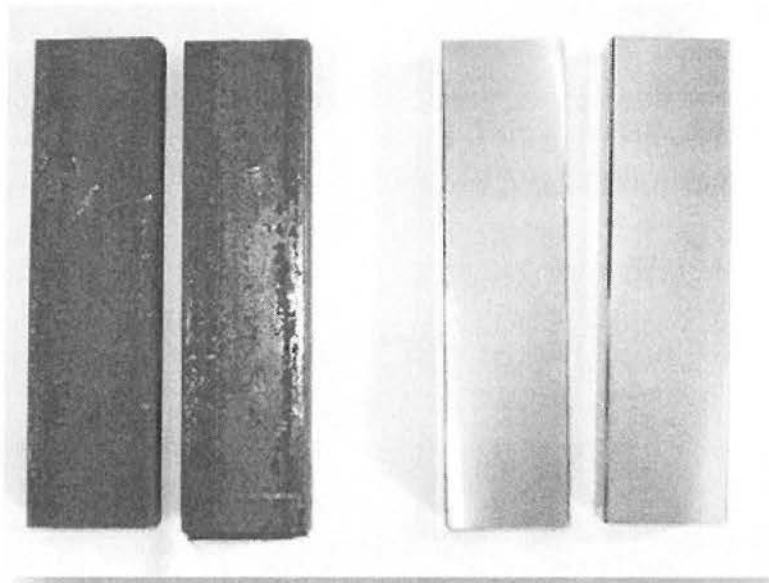
Figure 72: Machining of the new plates (before and after).

Before the sandblasting and the steel hardening steps, a Fujifilm paper test has been performed to estimate the pressure distribution these plates shall provide while in the process of pre-stressing. The test performed byintegrating the film located in-between the plates on the testing area of the new machine followed by a pressure applicationof 50 MPa on the plates, maintained for 2 minutes (50 MPa in this area corresponds to 261KN or 145 MPa in a common capacitive gauge of 1800 mm^2 compressing area). According to the instructions of the Fujifilm paper manufacturer, the time to reach the maximum load has been set to 2 minutes.
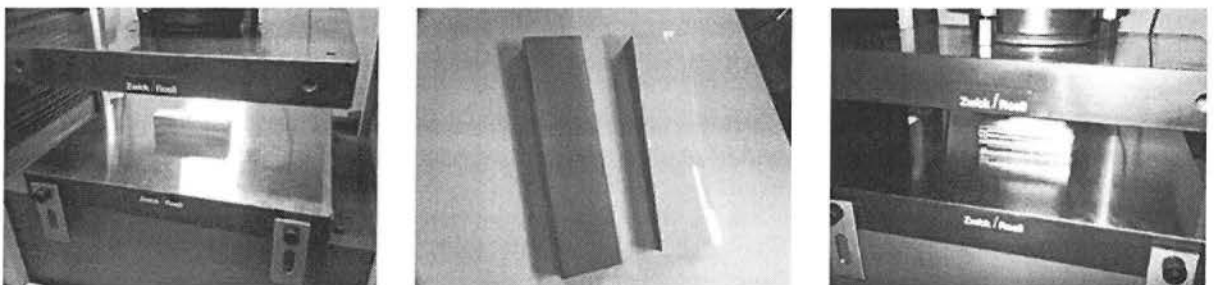
Figure 73: Fujifilm test preparation.

The results of the test can be seen in the next figure:
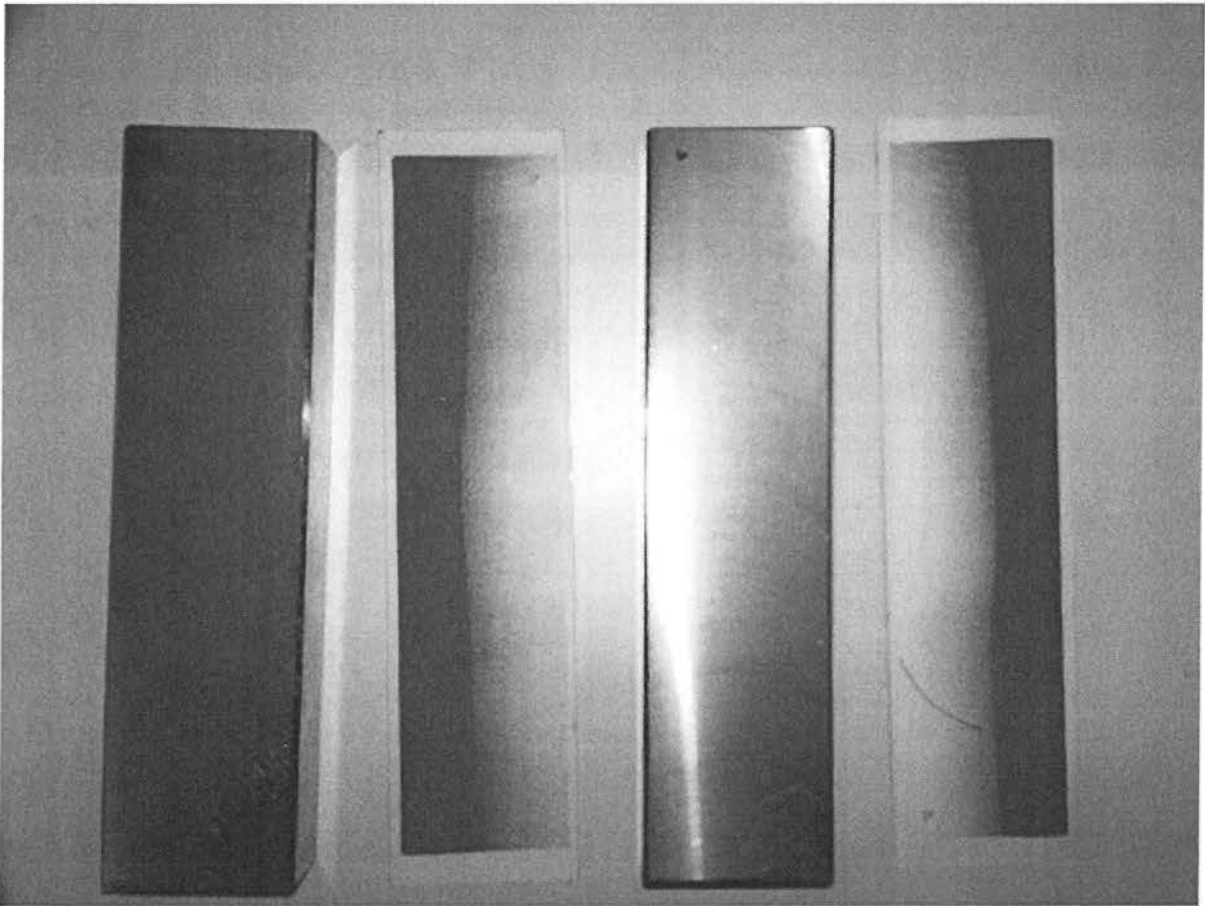
Figure 74: Test results

In addition to the Fujifilm measurement, the plates were given to the metrology sector of CERN to evaluate the flatness and parallelism of the plates after having being subjected to machining. Since no information exists about whether the selected tolerances of such a project request are enough, it would be good to know,for future references, if 0.05 mm flatness and parallelism tolerances are indeed sufficient.

The results of this evaluation are being summarized in the following certificate:
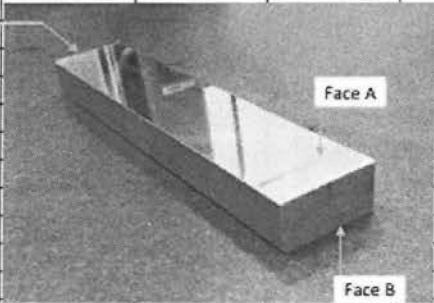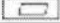
MÉTROLOGIE EN-MME-MM		
CERTIFICAT DE CONTRÔLE		

CONCLUSION CONTRÔLE		VISA MME	ACCEPTATION CLIENT
	OK	Nom :	Nom :
	Non conforme	Date :	Date :

NUMERO DE PLAN: ...
DESIGNATION: Blocs . Jauges capacitives
Nombre de pièces 2 x 2 cales spéciales
N° EDMS: 1312227

REQUERANTS: **BAKKER A.**
REYNARD Y.

CONTROLEUR: **RIGAUD J.Ph.**

page 1/1

résultat de mesure

	pièce 1		pièce 2	
	face A	face B	face A	face B
L x l	255.8 x 50		258.7 x 50	
⌷	0.063	0.024	0.041	0.052
// face A / B	0.052		0.033	
épaisseur	27.618 / 27.566		29.321 / 29.288	

2 plaques

2 plaques
149.3 x 38

	pièce 3		pièce 4	
	face A	face B	face A	face B
⌷	0.013	0.017	0.041	0.052
// face A / B	0.025		0.025	
épaisseur	19.085 / 19.110		19.081/19.06	

DATE	observations
09.09.2012	
APPROUVE PAR	
A.CHERIF	

Température : 20 °C	Moyens utilisés (incertitude de mesure estimée) :	Unités de mesure : mm

Colonne de mesure TRIMOS (±0,005mm) ; Comparateur à levier (±0,005mm) ; Comparateur numerique (±0,005mm)

Figure 75: Official certificate from CERN's Metrology section.

➢ *Machining conclusion*

According to figure 75, the requested tolerances from the machining procedure have been satisfied (apart from face B but since no CNC machine was used, the results cannot easily be improved).Still the Fujifilm paper results suggest that the design might need more demanding flatness and parallelism tolerancesfor better results (0.02 or even 0.01 mm), therefore CNC machining is advised to be usedfor similar future attempts.

Even though the results were not "ideal", no further machiningshall be performed on the new compression plates due to the fact thateven this "ideal" surface after the sandblasting, will possiblybe altered ending up having the same Fujifilm results. Additionally, the fact that the pressure is distributed in an area sufficient to cover the steel foils, has also contributed to this decision.

Figure 76: The area where the pressure levels are higher is enough for most of the commonly manufactured capacitive gauges.
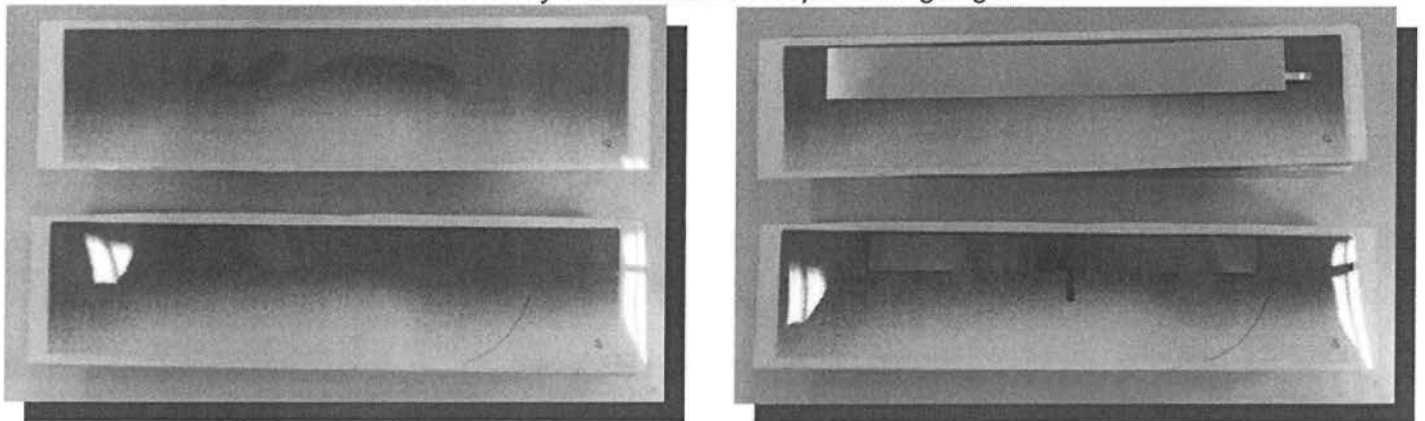
After their machining, the plates were sent to get sandblasted twice, first in the polymer section of CERN and due to the fact that the results were not matching the acceptance criteria, they were sent in an external company to obtain the desired results. The results of the sandblasting performed by the external company can be observed in the next figure.

A visible stamp print with the shape of
the steel foils indicates the plastic
deformation of the plates.
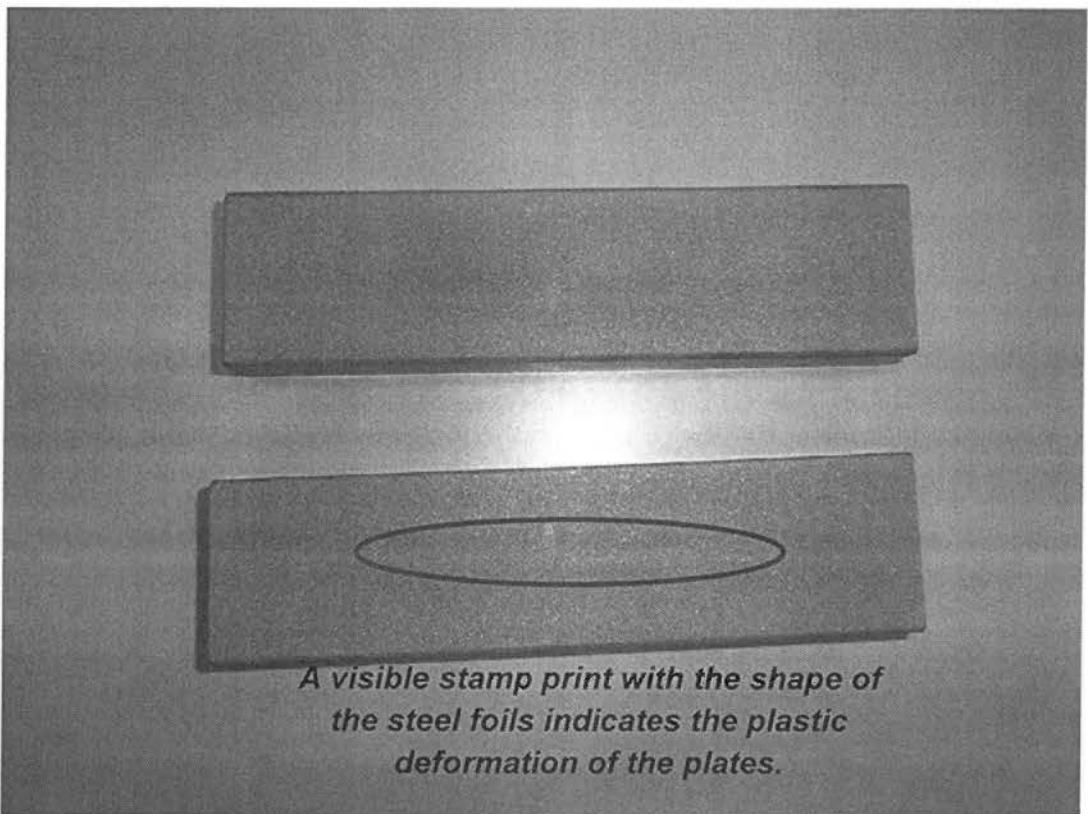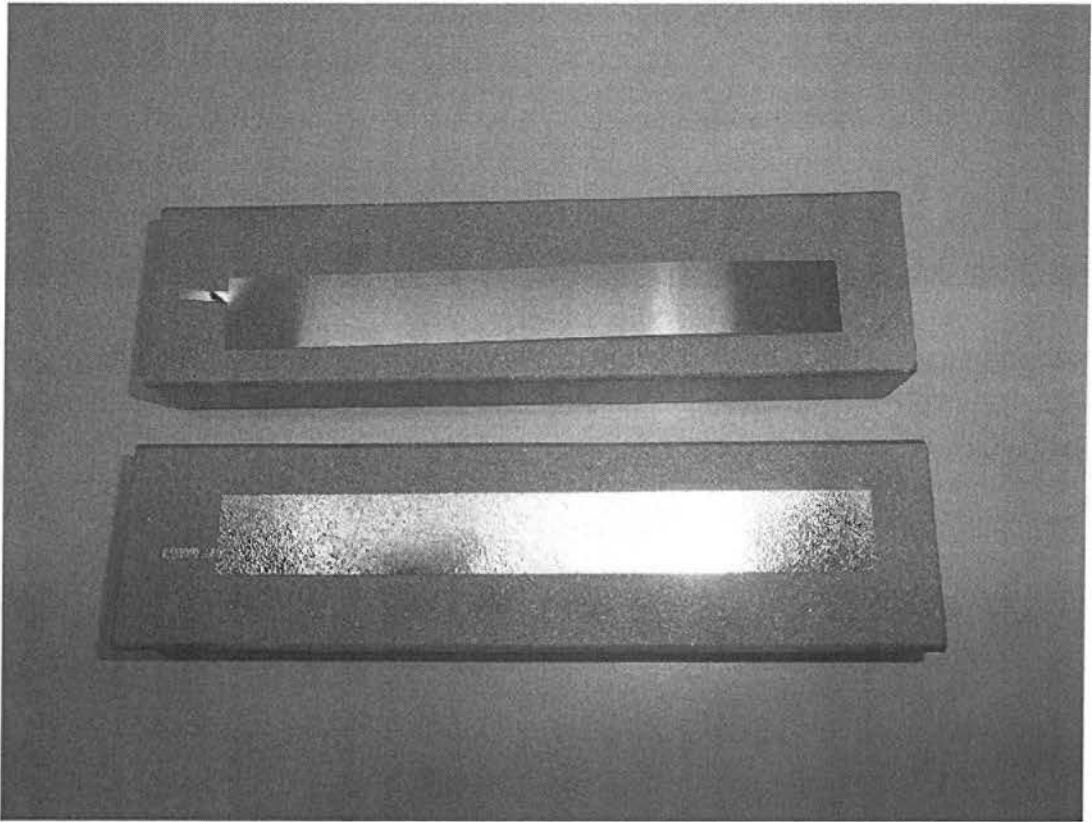
*Figures 77,78: Results of the sandblasting. In the lower figure the plastic deformation of
the plates after one gauge preparation is visible.*

The next step to the solution of this problem is to measure the surface hardness of the plates on the sandblasted area. The measurement was performed using a universal hardness test machine developed by "Otto Wolpert – Werke" (Fig: 79,80).

Figure 79: Universal hardness measuring machine.

Figure 80: Spec details of the machine.

The results of the hardness test have been synopsised in the following figure and table.
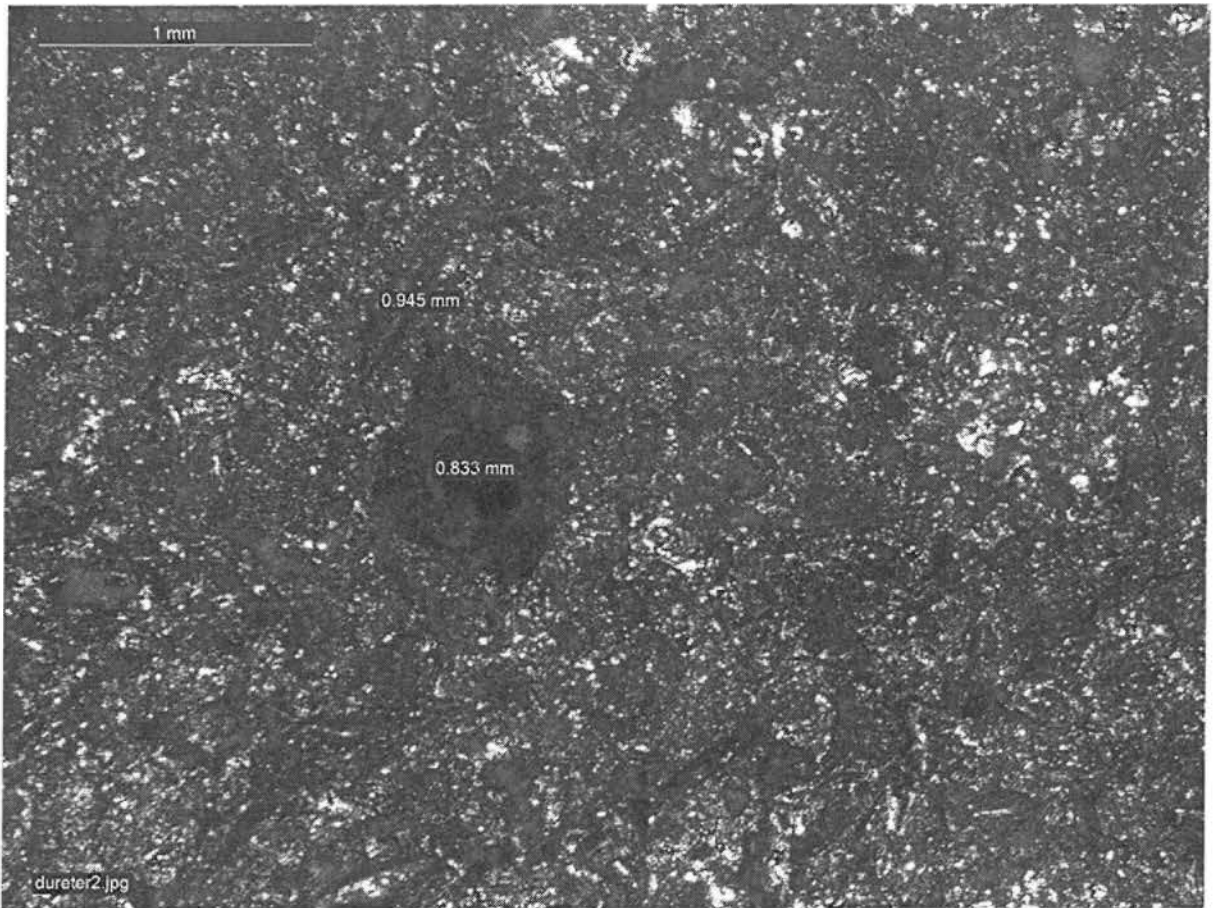
Figure 81: Vickers test results on the surface of the sandblasted plates.

According to the conversion table[Annex C] the surface hardness of the material is 235 HV for 100 KP of penetrating force. The last step to solve the pre-plastification problem of the steel foils in the capacitive gauges is to perform a steel hardening that will increase the hardness from 235 HV to around470 HV by following the steel's manufacturerinstructions[Ref: 4].

> *Steel Hardening*

The austenitizingprocedure of the ferrite phase, was performed by heating the plates at 880 °C for 30 minutes. The time in the oven was decided to be 30 minutes to avoid grain increasement, accepting the fact that this will lead to sole case hardening. The quenching was performed in an oil bath in room temperature followed by a tempering procedure that was performed in 150 °C for 30 minutes.

When the plates were delivered back after the hardening procedure, they were degreased and the oxidised surfaces were cleaned by using a metallic brush.

In order to check the results of the steel hardening procedure a second Vickers hardness test (100 Kp) was performed for which the results can be view in the next figure.
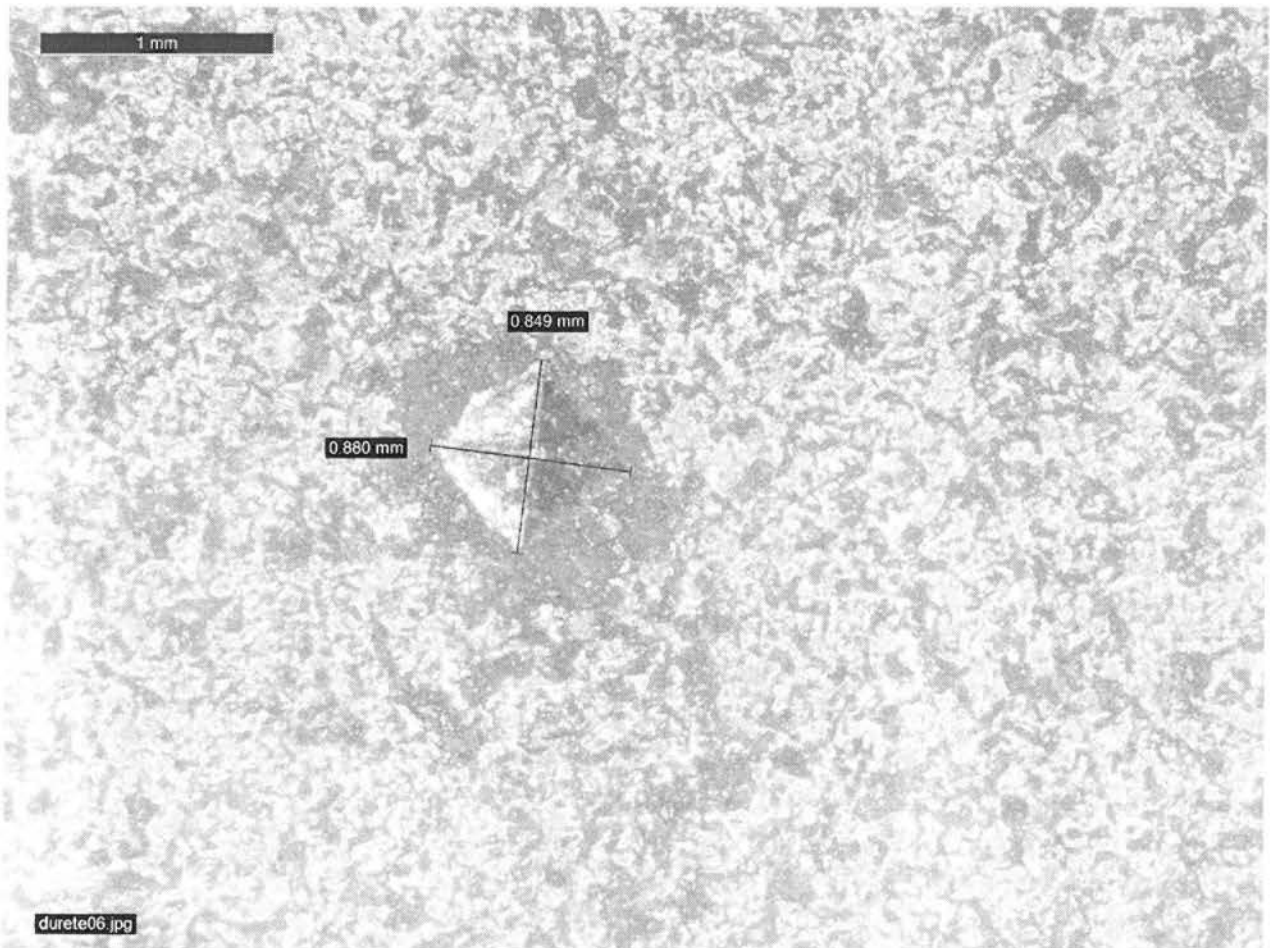
Figure 82: Vickers hardness test on the surface of the heat treated plates.

> ### *Hardening conclusion*

Based on the hardness conversion table the hardness obtained is 248 HV, a result that is unexpected. The sequence of the steps followed to perform this steel hardening was performed exactly like the instructions suggest with the only exception the temperature of the oil bath (room temperature instead of 160 °C) that should it affect the results, it would be by increasing the hardness. Based on the CCT diagram of the material (Fig: 83) and on the final hardness obtained, one can conclude that the cooling rate (around 0.014 °C/s) was not as fast as it should have been for the martensitic transformation.
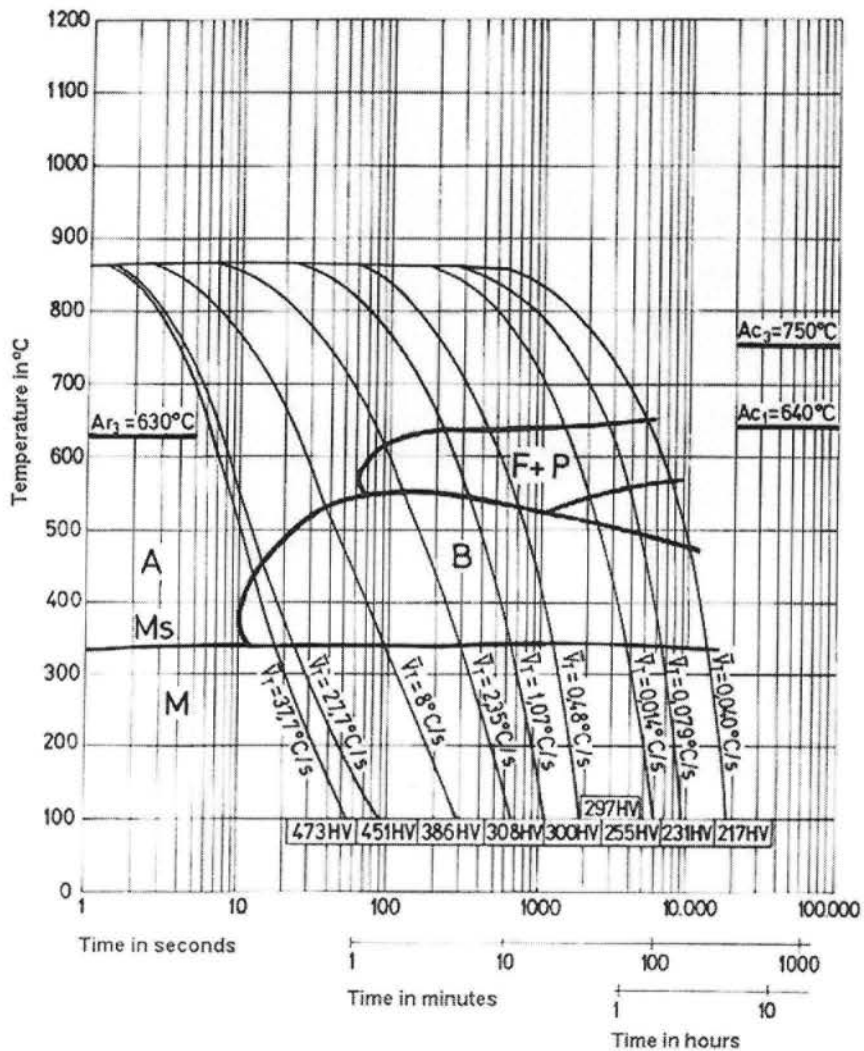
Figure 83: Continuous Cooling Transformation diagram of the material used.

➢ *Suggestions for solution*

In order to solve this problem it is suggested to increase the cooling ratio of the quenching phase. The way to increase this ratio is by performing the quenching procedure using water instead of oil. By doing so, the austeniticphase will not be given the chance to enter the perlite area resulting in a martensitic and bainiticstructure. The estimated hardness by following this suggestion is 470 HV. In case this value of hardness is still not high enough, either a different alloy of steel should be used having close to 1% carbon composition, which will result in a pure martensitic (with some remaining ferrite) structure or a carbonitriding surface heat treatment should be performed in order to diffuse carbon and nitrogen to the surface of this low carbon alloy steel and ultimately achieve high values of surface hardness that will solve the pre-plastification problem of the steel foils for the capacitive gauges.

Section II
Implementation of new ideas

Summary

Almost twenty years have passed since the first measurement implementation using capacitive gauges. Even though this kind of sensor has a lot of potentials, it is mainly used in parallel with strain gauges to validate their indications and the theoretical calculations,finally providing a rough approximation of the pressure levels in-between a contact.The main reason for this is that their response is not always as predictableas expected.

Overall, during the manufacturing procedure there are a lot of factors that contribute to the final results and affect them in a big extend (even determine their functionality). It is a manual procedure that requires the full attention of the technician assembling it and the results are dependent on the experience and the patience he possess. One of the biggest contributions to the response of the gauge is coming from the adhesive that is being used to hold the structure of the gauge in place and to maintain their alignment. This special glue is formulated specifically for bonding strain gauges and other special-purpose sensors such as the capacitive gauges and it is consisted by two components M-bond 43-B, 600 and 610 adhesive systems, two epoxy resins adhesives that have to be mixed together before use. More information about the adhesives can be found in their manufacturer's site [Ref: 7].

Figure 84: "Vishay Precision group" Adhesive systems for stain gage installation.

In fact the application of the glue and the thickness of the layers it forms is a factor that is random and uncontrollable due to the manual application. In the next figure a cross section of a gauge magnified under a microscope is presented.
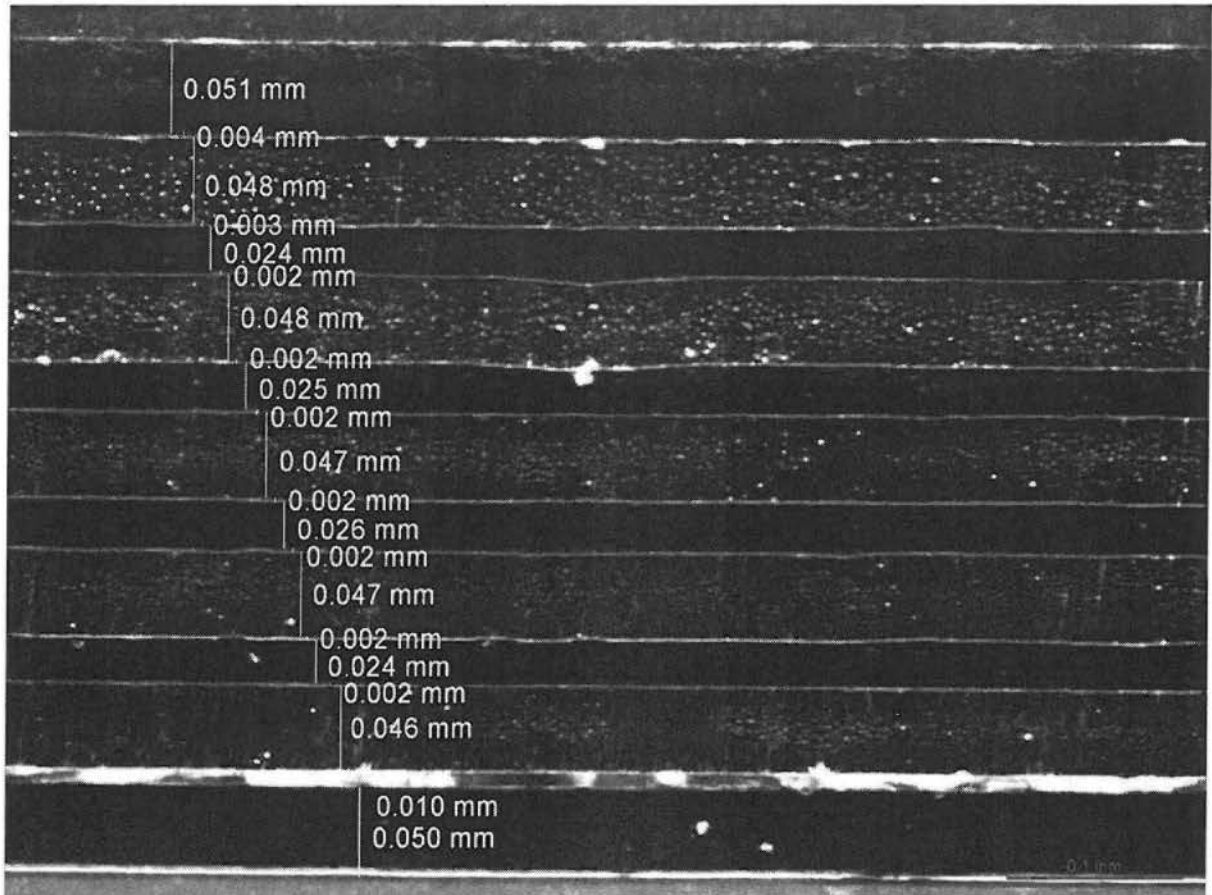
Figure 85: Cross section of a capacitive gauge. The various layers of the steel foils, kapton and adhesive have been measured and presented in the figure.

As it can be observed from the figure the glue's thickness can vary from 0.010 to 0.002 mmfor this specific vertical axis and for this specific cross section of the gauge.

In the past an experimental comparison test has been made using two gauges that only vary in the amount and thickness of the glue applied. This comparison was aiming in their signal response having as a sole variable the thickness of the glue. In the next figure the cross sections of this set of gauges are presented.
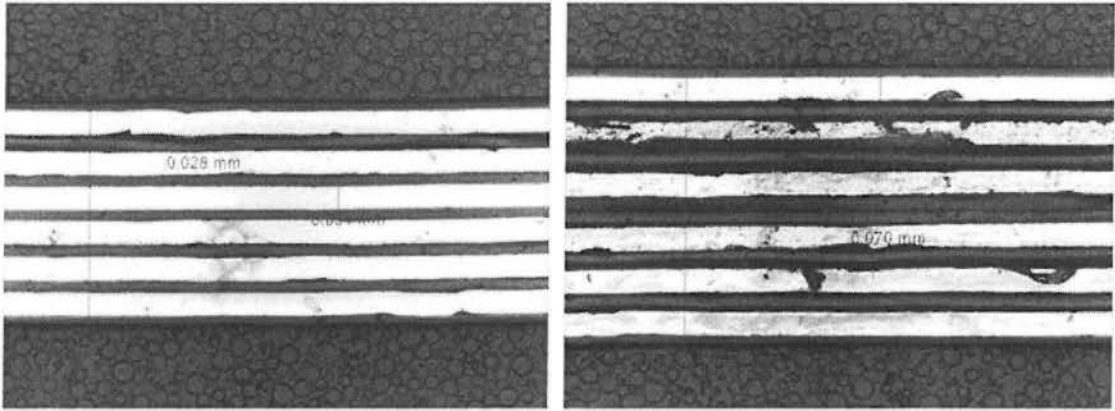
Figure 86: The set of capacitive gauges used to compare the impact of the glue (same scale).

As it can be observed from this figure the left gauge is much thinner that the one on the right and looks more consistent due to the fact that there is less amount of glue in between the various layers composing it.Just by only looking at these pictures, one can guess which gauge will provide the best results, in terms of signal response. The results of this particular test are synopsised in the following figure.

Impact of the glue thickness
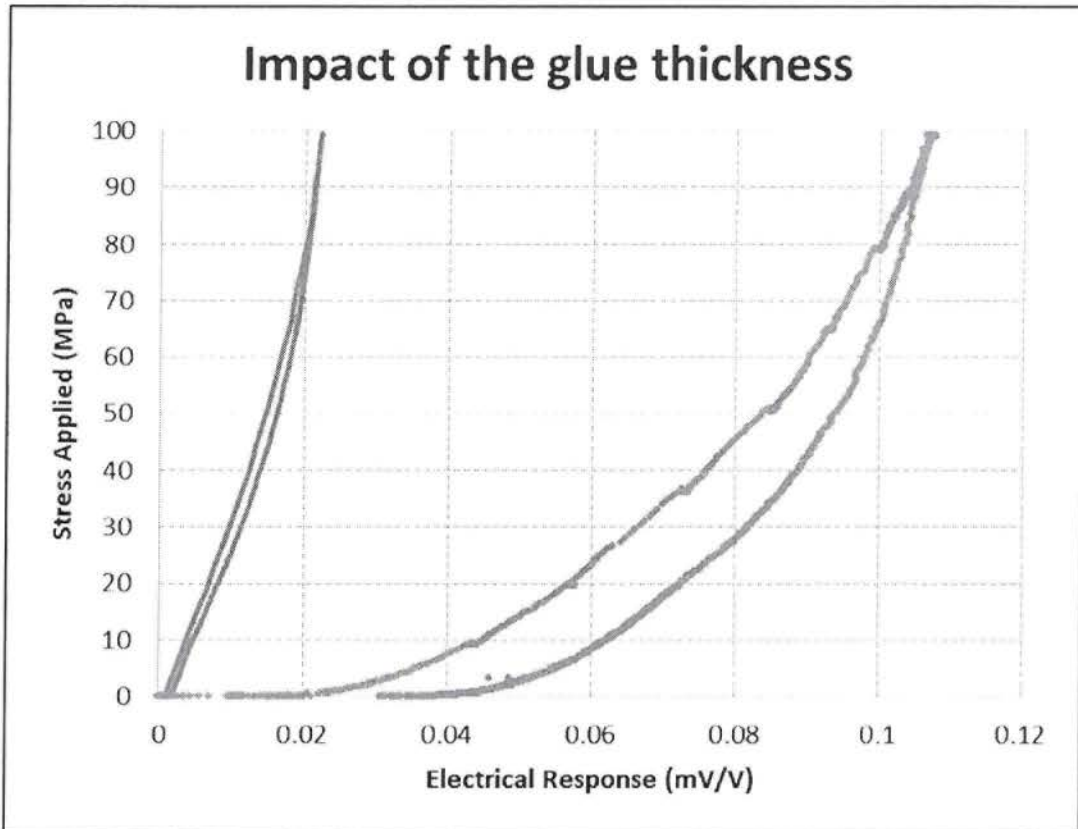
Figure 87: Comparison results.

In this figure the red curve represents the signal response of the gauge having the thinner and more consistent layer of glue. Not only its response is easier to be approximated by linear curve fitting but also the measuring uncertainties deriving from the hysteresis, the interpolation and the zero drift of this particular gauge are negligible in comparison with the other one. Truth be told, its electrical responserange is almost five times smaller but then again this is a typical fact for the capacitive gauges. In fact the range of the signal in most gauges is around 0.1 to 0.2 mV/V depending mainly on the area of each gauge, the apparent strain of the glue and the bridge that is connected to.

Finally the state of the adhesive existing in each gauge is contributing to its overall response. It is clear that between the various measurements a capacitive gauge is performing throughout its lifecycle, the state of the glue is constantly changing. Either its quantity is being decreased with every compression cycle performed or its quality is being degraded as time goes by. The degradation of the adhesive can actually result in huge signal "quality" changes and in some cases a gauge can even become unusable.

The effect of all these factors can become clear with an example which involves actual capacitive gauges that have been used in the monitoring of the stress levels on the eleven Tesla's (CERN's prototype magnet) dipole coils. For this particular measurement eight capacitive gauges had been manufactured and were installed in the interphase of the coils in order to monitor the bearing stress in the radial direction of the coil pack.
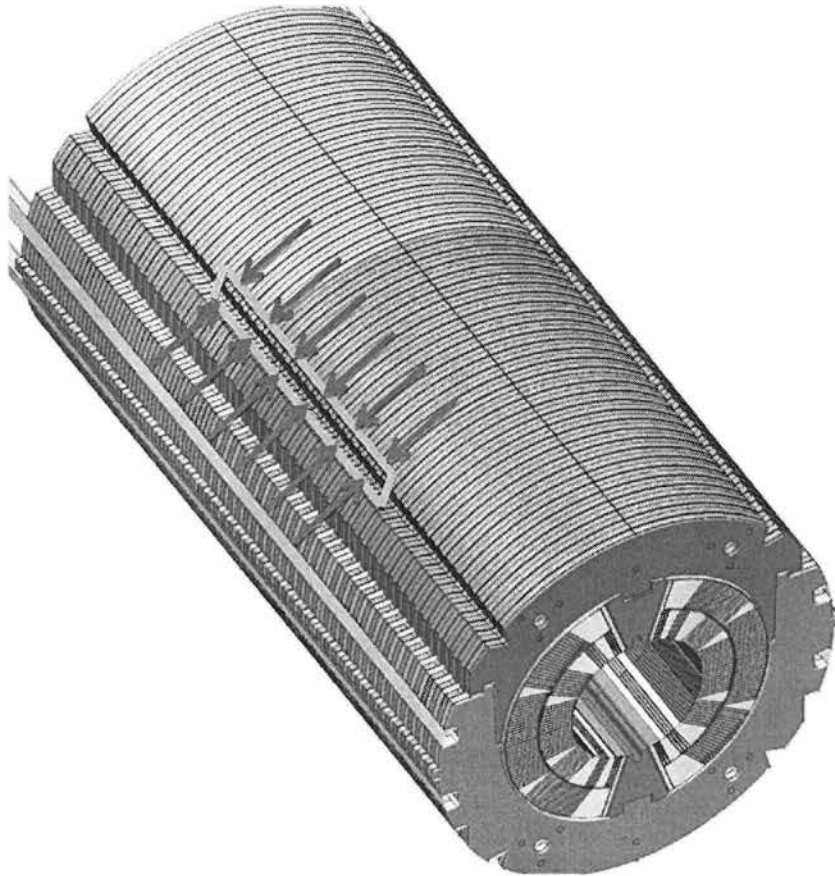
Figure 88: 11 Tesla coil pack monitoring with 8 capacitive gauges.

When the gauges were delivered back to the laboratory for recalibration after having been operating for almost a year, three of the gauges had to be replaced because of this signal change that was caused among other things by the degradation of the glue (the DAQ system used was the very same one and the connections were repaired more than once, in order to exclude those possibilities also). In the next series of figures the calibration curves performed in the past and the signal obtained when they were delivered back to the lab are presented.
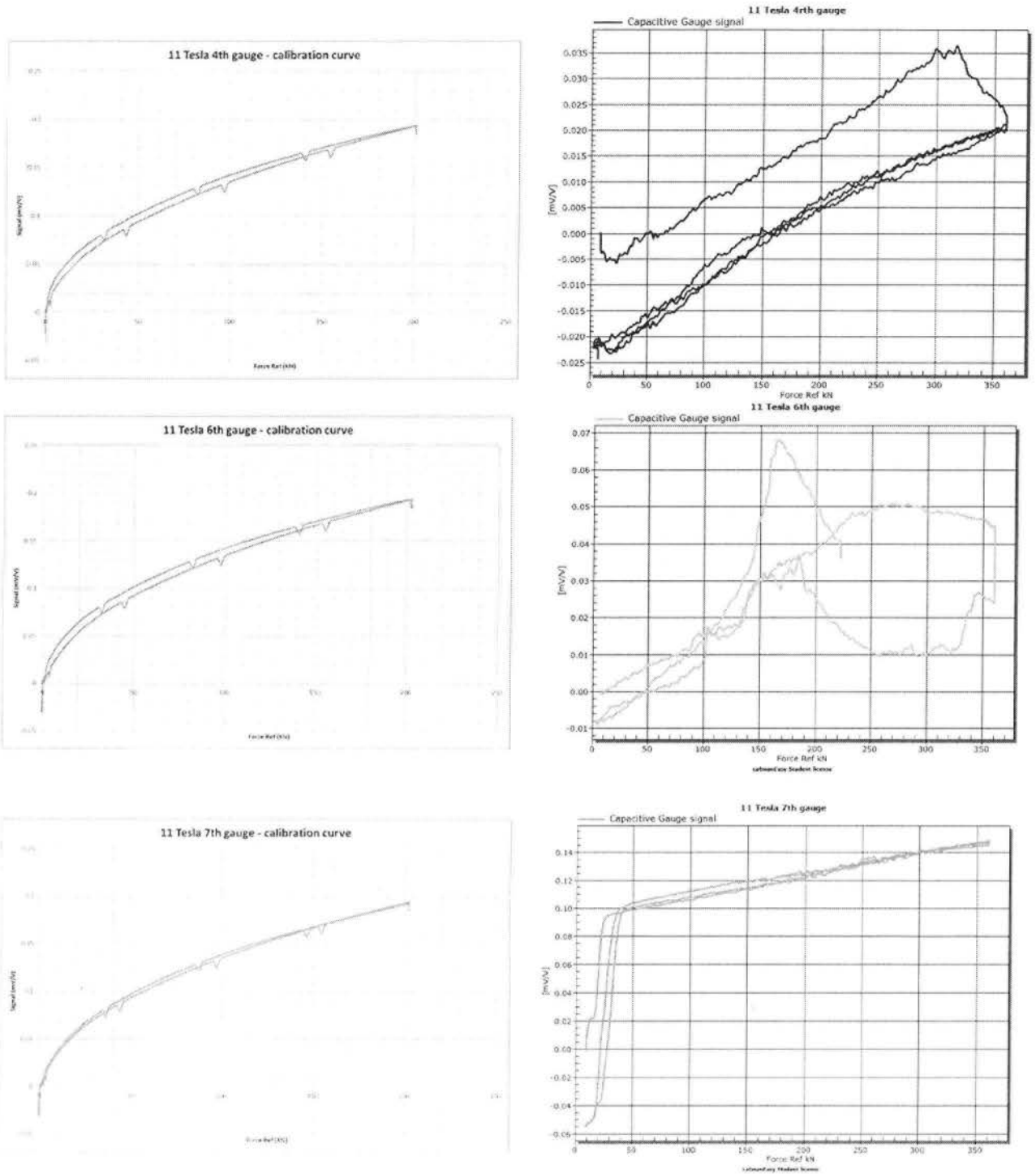
Figure 89: Results of the degradation of the glue (old calibration curves left column – new ones right column). All three gauges had to be replaced with new ones.

Figure 90: CG Connectors

Of course the glue is not always the sole thing to blame for this kind of signal change. In most cases, the state of the connectors that connect the gauge with the measuring bridge as well as the state of the bridge itself can among other things be the reason for this signal deterioration. The glue problem is more apparent with the last gauge shown in figure89 where this signal gap occurring in low values of loading, can be explained by the gradually replacement of the glue, in a portion of the gauge, with air.

At the beginning of the loading, since there is some air existing inside the gauge where the glue was supposed to be, the deformation is quite big (causing the signal step) as opposed to the more stiff behaviour observed while the loading is increasing. At that point the air has evacuated the gauge and the elastic deformation of both the glue and the dielectric (with young's modulus around 200 GPa) arecausing the change in the capacitance of the gauge as explained in the working principals section.

Finally it has to be mentioned that the rest of the 11 tesla gauges were properly working and still provide some of the best results the laboratory has ever obtained using this kind of sensors. By accepting the fact that the glue degradation does indeed contributes to this signal alternation, eventually leads to the uncertainty of whether the working conditions for such a long time of these three particular gauges caused them to cease working correctly (small possibility since all eight gauges were working in the same conditions) or is it the amount and the manual application of the glue during the manufacturing thathas to do with it.

As a conclusion to this section summary, just like the people previously in charge of the R&D of the capacitive gauges suggested[Ref: 2], a change in the way the gauges are being bonded should be considered. In that particular document the concluding suggestions were focused in trying different types of adhesives with different properties such as lower viscosity, lower young's modulus, higher relative capacitance or even change the way the glue is being applied on the metallic foils by trying for example spraying it. Even though these suggestions might actually work and improve the results obtained, the fact is that the presence of the glue will always play an important role to the gauge's performance. That's why in the last pages of this thesis a new glue-free model is being presented that aims to simplify things and if able to provide a good alternative to the baseline model.

> *New design idea*

In the theoretical model of a capacitor there is only one dielectric material in between its plates separating them, keeping them in place and increase the overall capacitance. In the case of the capacitive gauges, there is a layer of kapton acting as the dielectric material plus two more layers of glue on each one of its sides. In various attempts to better approach this theoretical model and to try to simplify the manufacturing process, a new model has been tested having no glue at all.

In the beginning of the implementation of this idea, many difficulties encountered especially with how the metallic foils would be maintained in position and how they would keep their alignment. Initially alcohol was used to remove the air between the foils and the kapton pieces, in order for the atmospheric pressure to maintain the assembly. The idea was to let the alcohol (not a good insulator of electricity) dry and then while the difference in pressure between the kapton and metallic foils would keep everything aligned and bonded, a final external (not active part of the gauge) piece of tape would be applied to seal the gauge. Even though the removal of the air from the gauge and the sealing of the gauge worked quite well, the problem with this attempt was that even with the alcohol evaporated, there was still some current passing through the foils (3 KΩresistance between them) and therefore the idea of alcohol was abandoned.

Eventually after plenty of tries focused in the use of kapton tape (having a silicone adhesive on one side) to maintain the assembly, applied only in the external layers of the gauge (therefore not an active part of the gauge), the first "good" results started to be acquired. To make it more clear, what was done was that in between the metallic foils, simple kapton without adhesive was used in order to avoid the same problems with the glue being in the gauge, while the last two layers were bonded with kapton tape that seals the gauge and keeps the structure aligned.Initially in order to keep the foils aligned while preparing the "sandwich", the connectors (Fig: 90) were soldered together before the installation of the kapton. These "good" results obtained can be observed in the next figure.
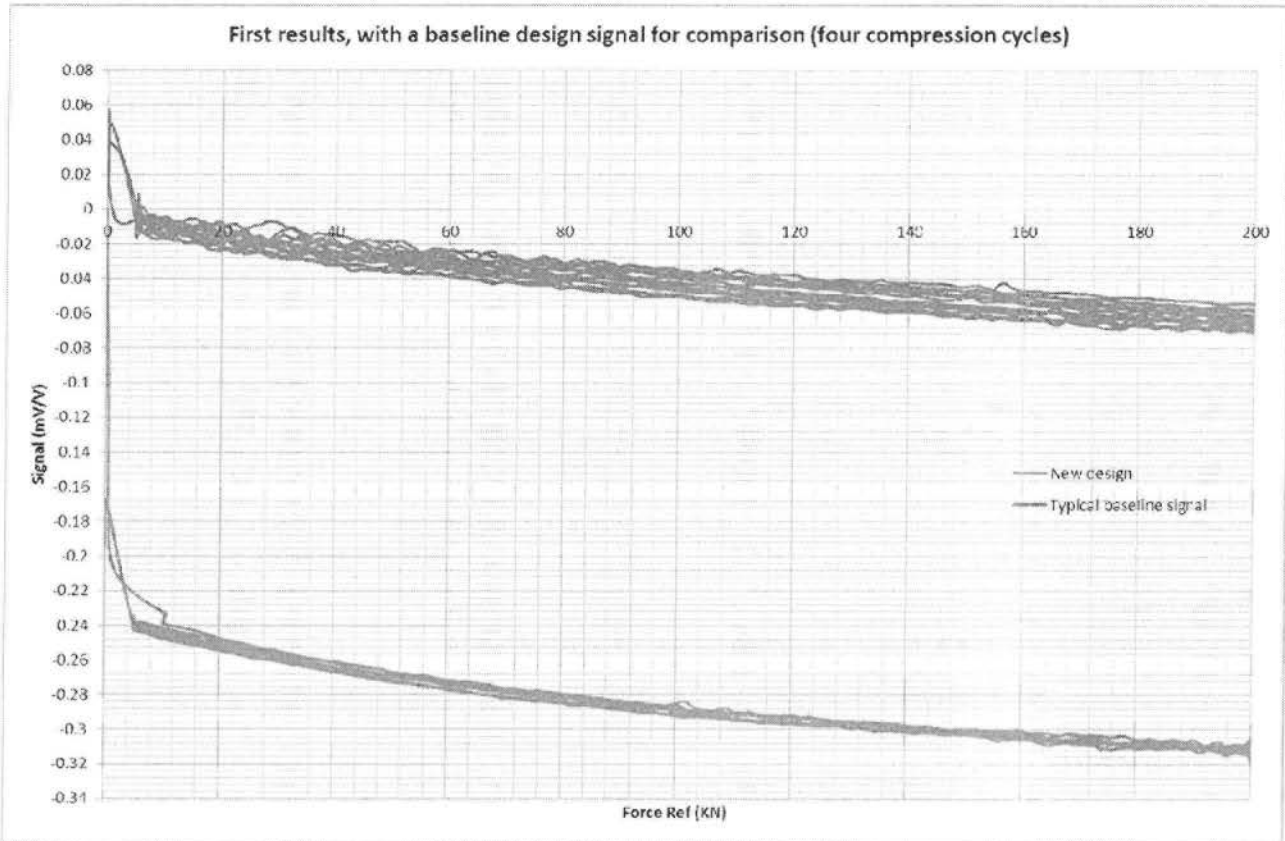
Figure 91: First results without the use of glue. Also a typical signal from a gauge with glue is presented for comparison.

The signal coming from the glue-free model appears to be less noisy meaning a less significant interpolation error and results with better repeatability. In addition, the hysteresis of this model is almost non-existent something quite logical since the glue that presents a higher plasticity in respect to the steel foils, can be assumed to act as a dumper dissipating energy while the gauge is operating thus creating this hysteresis gap in between the increasing and decreasing loading curves.

On the other hand, the prementioned initial step that was caused due to the air existing in between the plates has been amplified. Since there is no glue and air has infiltrated inside the gauge, the stress strain ratio is dramatically changing when the air is being removed after a small amount of load has been applied. Also the zero drift error with this model is considerably big compared to the baseline model. The reason behind this is that after the load has been removed the atmospheric pressure is maintaining the deformation since there is no air anymore inside the gauge. Eventually, at some point while in unload conditions the air is infiltrating causing the restoration of the gauge to its initial state. The problem is that since the connectors had been soldered beforehand to keep the alignment while assembling the gauge, unavoidably there was still some air trapped inside, not to mention that due to the soldering of the connectors the sealing wasfar from being considered airtight.

This problem of the air trapped inside causing this gap is not so major. In fact, it can be partiallyavoided by the DAQ system itself. While using the capacitive gauges it is quite common to have a small initial load applied during the installation of the sensor inside the magnets. Since this load is negligible but enough to cause this step, a software balancing zero of the bridge can be performed at that point indirectly resolving the problem.What is actually not acceptable is the lack of an airtight sealing. Since air can infiltrate inside the gauge it is quite sure that the same can happen with liquid nitrogen or even liquid helium resulting in the destruction of the gauge while the warm up phase of the magnets.

After the evaluation of these results what can be concluded is that:

1. Producing a capacitive gauge without the use of an adhesive is possible.
2. By doing so, not only the sensor presents better results in terms of repeatability and linearity, but also avoids all the downsides of the usage of the glue explained in the beginning of this section.
3. In order for the sensor to be usable and therefore to replace the baseline model, the problem with the sealing needs to be resolved.
4. The signal step and the big zero drift error of this model could be avoided if a vacuum could be created before sealing the gauge. By creating this vacuum the gauge's layers would also be maintained together better with the atmospheric pressure actively contributing to this bonding.

Even though creating a vacuum and hermetically sealing a gauge is quite difficult to achieve manually (if not impossible), a few more ideas were implemented in this direction. The one that was proven to provide the best results was in fact the most simple. Instead of pre soldering the connectors (and thus avoid a big volume that makes the sealing more complicated), align the sandwich with nothing actually fixing it in position and then apply tape on the connectors to keep the assembly in position. After this, one can apply the last layer of kapton tape(having the glue) and removing the air with pressure caused by him. The step sequence in order to manufacture such a gauge is being described in detailsin the next few paragraphs. Also figure 92 helps visualizing the process.

5) Trimming boarder	6) Final trimming boarders	4) Tape

7) Alcohol

Figure 92: Glue-free model explanation

1) One external kapton layer

3) Five steel foils

2) Four internal kapton layers serving as the dielectric
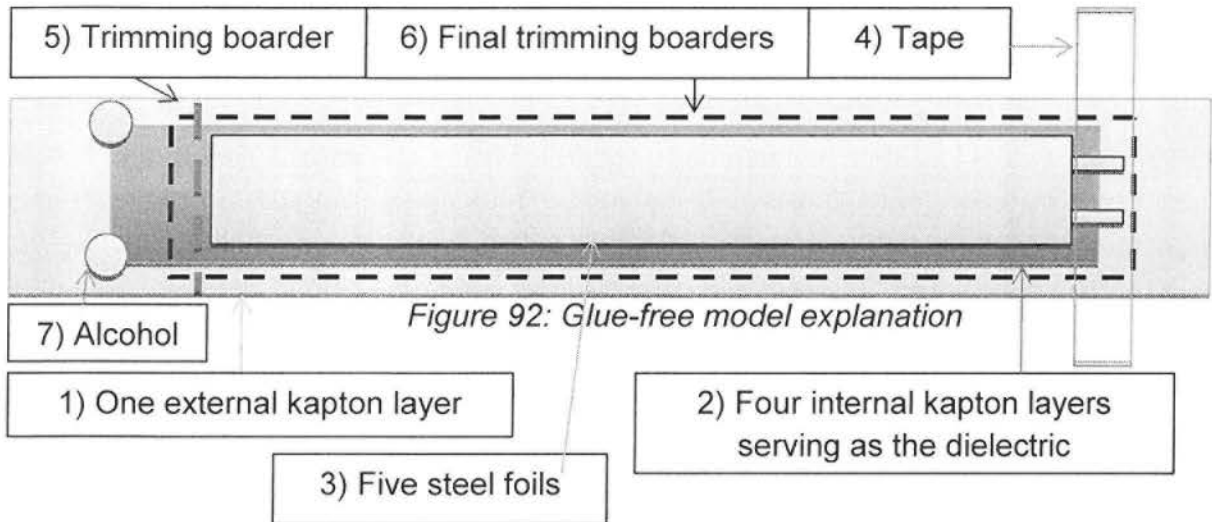
- The first step is to prepare the four internal kapton layers (2) by cutting them having slightly bigger dimensions than the steel foils (3). The smaller and closer to the steel foil dimensions they have the better it is (since the space inside the magnets is limited) and the more difficult to assemble it as well. The side where the alcohol is applied according to the figure (opposite side of the connectors if the geometry is different) should be bigger and will be trimmed at the end of the procedure.
- Apart from the internal kapton layers, an additional one should be prepared having the biggest dimensions according to figure92. For example, for a typical 15x120 mm capacitive gauge, the dimensions of the four kapton layers can be 17x130 mm (the length will be reduced at the end of the procedure) and for the final external layer it doesn't really matter since it will be trimmed as well, as long as the dimensions are bigger than the others.
- The cleaning is performed only with alcohol since the surfaces need to be smooth and homogenous unlike the baseline model in which the application of acid is partially a contributor to the final roughness of the foils.
- Starting with the big external kapton layer (1), the assembly is performed like a normal capacitive gauge with the only difference that there is no glue application thus making it a bit more difficult to keep the alignment and to make sure that there is no contact between the metallic foils (3). A trick to keep the alignment is to apply a small quantity of alcohol (7) with every layer of kapton (2) application. The alcohol should by nomeans infiltrate the final trimming boards (6). Since the connectors will not be covered entirely by the kapton according to figure 92, the alignment of the metallic foils can be adjusted by them.
- When five layers of kapton (including the big one) have been stacked and aligned with five metallic foils, the connectors need to be fixed in position with tape (that will be scratched later much like the kapton in the baseline model).

- The next step is to start applying the adhesive kapton tape (not included in figure 92), from the side of the connectors. The application can be performed using Teflon and by applying pressure with the fingers to remove the air from the assembly.This kapton tape must have dimensions big enough, to overlap the final trimming boarders.
- When the trimming boarder (5) has been approached, trim the extremities according to the figure and seal the gauge. What holds the assembly together is the interaction surface between the big kapton layer and the kapton tape.
- Finally cut the remaining kapton (final trimming boarders (6)), scratch the kapton and the tape to reveal the connectors and connect the gauge to the bridge.

The procedure is simple and if done once or twice it is easy to get used to it and both improve the time and way to perform it. Since this procedure is still fresh and within the R&D procedures of the MML, new modifications and improvements can still be implemented.

The most important asset of producing such a gauge is without any doubt the time it takes to manufacture it. To begin with, no more pre-plastification of the foils is required something which saves several minutes. The cleaning procedure prior to the assembly is performed much faster as well since there is no need to use acid and base anymore. The assembling itself, while it's still quite tricky to align and maintain everything in position correctly, is faster due to the fact that the manufacturer is not required to be so perfectly focused while carefully applying the glue. Furthermore, even if a mistake is performed while assembling a gauge, the procedure can easily be restarted (which is not the case with the baseline model). The installation of the gauge in between plates that homogenously compress it all over its surface before the insertion in the oven is no longer an issue and finally the oven itself. A capacitive gauge must be maintained inside an oven at 150 °C for two to three hours for the curing procedure of the glue. It goes without saying that this is not a requirement for this model. Overall the time needed to manufacture this new gauge in comparison with the baseline model, has gone from a few hours to several minutes or an hour maximum, depending on the experience and skills of the manufacturer.

The improvements in the zero drift error and in the initial big step of the signal that were brought to the new design model (Fig:91), by making some simple modifications in the manufacturing procedure, can be observed in the next two following figures.
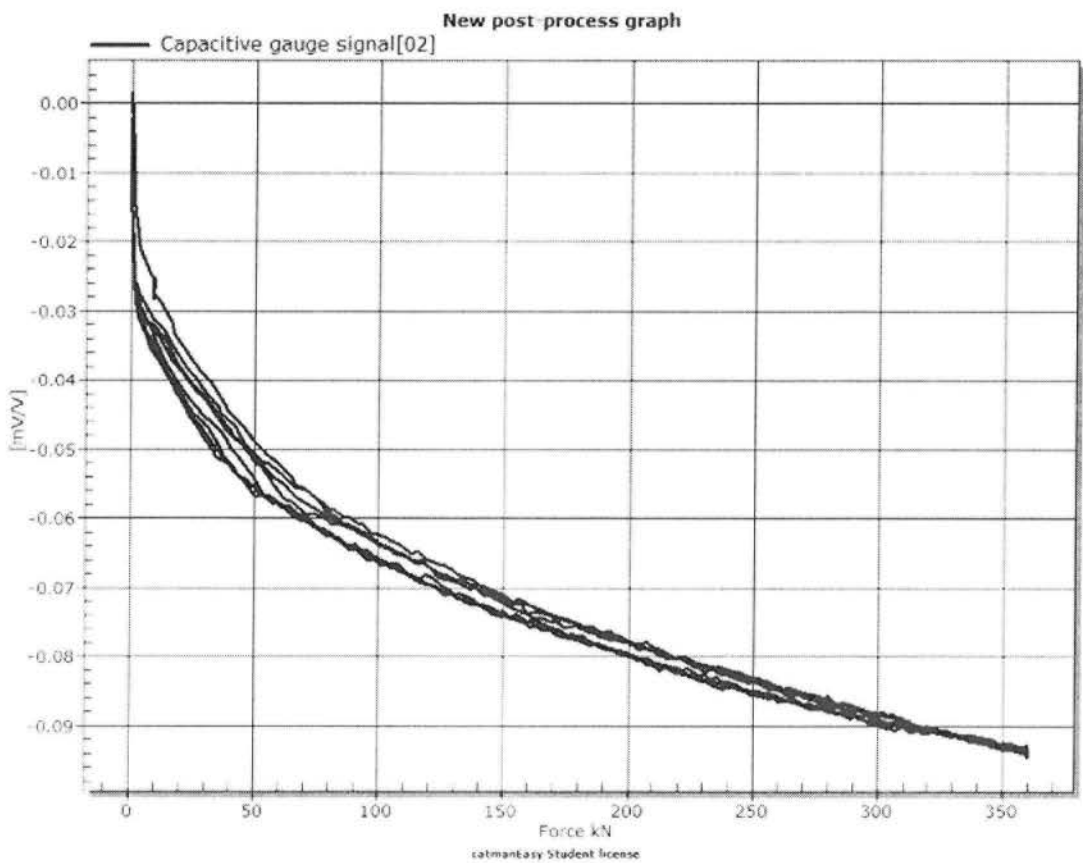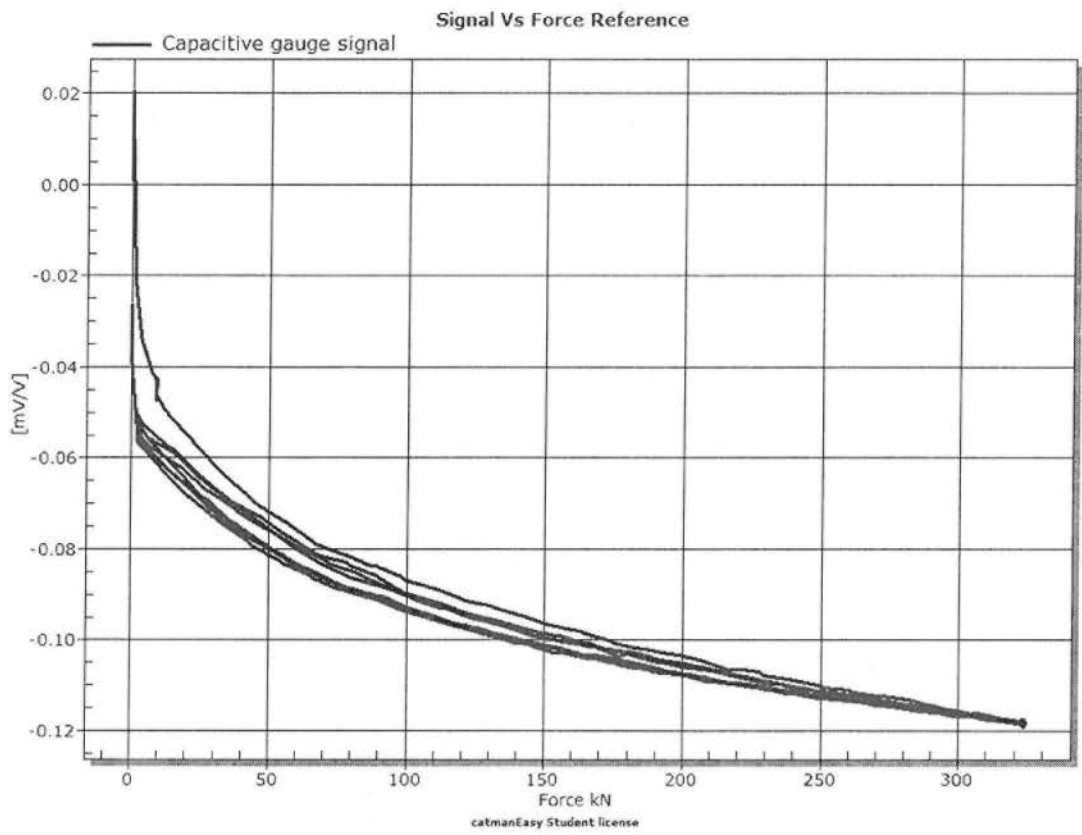
Figure 93: Continuous improvement of the new gauge model.

By following the manufacturing procedure explained before, the gauges that are being produced,presenta considerably big improvement in the two problems that were explained before. The initial signal step, while the loading is being applied, has been decreased from 0.24 mV/V to 0.07 mV/V (Fig:91) to even less as shown in figure 93. Also a direct result to this improvement is the reduction of the zero drift error that the gauge presents, something that is quite logical and visible in the prementioned plots.

Having presented these results, it has to be mentioned that even though the problems have been minimized, they have not been totally extinct. Since there is still air existing inside the gauges and the sealing is not perfect, this attempt cannot be considered complete and the perfect substitute to the baseline capacitive gauges model. Even if the results seem to be good and usable in room temperature conditions, the case with the cryogenic temperatures might be different. In the final section of this chapter a conclusion will be madebased onthe results obtained by the signal comparison between the new and the baseline models including all the pros and cons of this new model. These results have been collected forthe new calibration procedure explained in chapter 2 and include information for both environmental conditions.
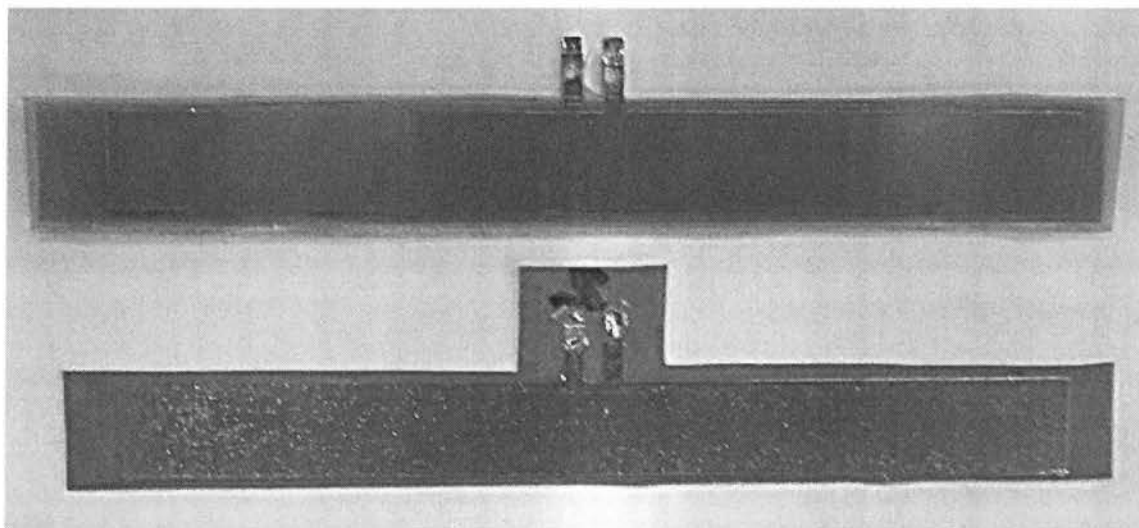
Figure 94: Capacitive gauges - New model (top) Baseline model (bottom).

> ➢ *Comparison of the results between the two models*

Figure 95: The difference between the external and internal layers of Kapton is more visible with the first manufacturing attempts. The interaction point of the external layers is what holds the assembly together.

The results that are presented in the following figures 96 and 97, have been gathered fromtwo calibration procedures performed ontwo gauges; one according to the new manufacturing procedure and one according to the baseline. Data for both room temperature and cryogenics have been included. For both cases, the gauge that has been chosen to be presentedis the one that provided the best overall results, during this last year of continuous testing and calibrating.

The most interesting results to compare are their performance in terms of accuracy and precision that both contribute to the combined standard uncertainty of the outcome values. This information has been derived directly from their calibration results, located in the "calculated values" sheets in their corresponding certificates (arrays according to figure 24). The purpose of these arrays is to display in which fields one gauge is better from the other.

NEW MODEL								
Force (KN)	u1 (Load cell)	u2 (reprodu - cibility)	u3 (repeatability)	u4 (resolution)	u5 (creep)	u6 (zero drift)	u7 (intepo - lation)	uc
0	0.00	2.29	0.00	0.00	0.00	0.00	0.00	2.29
45	0.01	20.75	0.08	0.00	0.23	2.04	7.42	22.13
90	0.02	19.95	0.16	0.00	0.47	4.08	0.03	20.37
135	0.03	17.87	0.63	0.00	0.70	6.12	6.20	19.90
180	0.04	15.57	0.72	0.00	0.93	8.16	6.23	18.68
225	0.05	14.89	0.60	0.00	1.16	10.20	0.88	18.11
270	0.05	13.52	0.81	0.00	1.40	12.24	6.78	19.52
315	0.06	12.83	0.65	0.00	1.63	14.28	8.34	21.00
360	0.07	11.01	0.69	0.00	1.86	16.32	7.43	21.13

BASELINE MODEL								
Force (KN)	u1 (Load cell)	u2 (reprodu - cibility)	u3 (repeatability)	u4 (resolution)	u5 (creep)	u6 (zero drift)	u7 (intepo - lation)	uc
0	0.00	1.19	0.00	0.00	0.00	0.00	0.00	1.19
45	0.01	13.42	0.66	0.00	0.41	0.95	5.01	14.37
90	0.02	12.35	0.49	0.00	0.81	1.89	0.19	12.54
135	0.03	9.42	0.42	0.00	1.22	2.84	2.72	10.29
180	0.04	5.96	2.44	0.00	1.62	3.79	5.27	9.28
225	0.05	6.86	0.34	0.00	2.03	4.73	0.76	8.61
270	0.05	4.28	2.80	0.00	2.44	5.68	4.31	9.11
315	0.06	3.48	0.59	0.00	2.84	6.63	6.11	10.09
360	0.07	2.51	0.78	0.00	3.25	7.57	5.23	10.10

The left side of both tables is labeled vertically: Room Temperature Results

Figure 96: Uncertaintyresults (in KN)for the two gauges in room temperature conditions.

NEW MODEL								
Force (KN)	u1 (Load cell)	u2 (reprodu - cibility)	u3 (repeatability)	u4 (resolution)	u5 (creep)	u6 (zero drift)	u7 (intepo - lation)	Uc
0	0.00	6.97	0.00	0.00	0.00	0.00	0.00	6.97
45	0.01	14.64	1.84	0.00	1.89	4.34	4.00	16.00
90	0.02	16.34	0.26	0.00	3.77	8.69	0.00	18.88
135	0.03	16.71	0.47	0.00	5.66	13.03	0.66	21.95
180	0.04	11.16	0.03	0.00	7.54	17.37	4.87	22.51
225	0.05	13.89	0.39	0.00	9.43	21.71	0.43	27.45
270	0.05	9.81	0.05	0.00	11.31	26.06	3.07	30.21
315	0.06	5.40	2.70	0.00	13.20	30.40	1.98	33.74
360	0.07	6.02	0.83	0.00	15.09	34.74	2.23	38.43

BASELINE MODEL								
Force (KN)	u1 (Load cell)	u2 (reprodu - cibility)	u3 (repeatability)	u4 (resolution)	u5 (creep)	u6 (zero drift)	u7 (intepo - lation)	Uc
0	0.00	2.08	0.00	0.00	0.00	0.00	0.00	2.08
45	0.01	12.36	0.79	0.00	0.29	1.81	4.98	13.47
90	0.02	21.65	0.15	0.00	0.58	3.62	0.67	21.96
135	0.03	22.54	1.24	0.00	0.87	5.43	3.36	23.48
180	0.04	17.00	1.15	0.00	1.16	7.24	2.20	18.68
225	0.05	17.80	0.93	0.00	1.46	9.05	0.47	20.05
270	0.05	14.55	0.69	0.00	1.75	10.86	3.12	18.52
315	0.06	9.20	0.01	0.00	2.04	12.67	3.05	16.08
360	0.07	7.95	0.73	0.00	2.33	14.48	2.91	16.95

The left side of both tables is labelled vertically: "Cryogenic Results"

Figure 97: Uncertainty results (in KN) for the two gauges in cryogenic conditions.

➢ *Results - Conclusion:*

Based on the combined standard uncertainty results (u_c) these two gauges provide, one can conclude that the baseline model provides more accurate and precise results. This is the case for both environmental conditions where in both cases the values taken from the "glue free" model are almost double. This is to be expected though, due to the fact that the contribution of the zero drift error to the overall uncertainty of the "glue free" model is way much higher. More specifically,its contribution to the u_c results is more than 50% for both cases.One thing that is clear from these results is that if the problems with the sealing and the vacuum creation inside the gauge are solved, then the new model gauges will present even better results, possiblysurpass the baseline model in terms of accuracy and precision.

Last thing that needs to be mentioned is that based on the instructions of the international standards for the calibration procedure that the MML has adopted (chapter 2 "Classification and assessment of the gauge"), the capacitive gauges have been listed as case c sensors. Themeaning of this, is that data concerning the creep of each gauge calibrated are being included in the uncertainty analysis, replacing information about the hysteresis each gauge presents. The reason for this is that in most of the measurements performed with a capacitive gauge, the measuring components are being mechanically loaded and then they are inserted in cryogenic environments (cryostats). The sensor is providing crucial information about the stress levels inside the cavities of the measuring components during the assembling, the cool down, the warm up and finally the load releasing phases. Since most of these phases last several hours, the creep contribution is higher than the hysteresis leading to the case c classification. The main reason of this paragraph is to remind thateven though the hysteresis is not being considered, the improvement of the gauge in this direction is quit considerable. Before the closure on this subject and the final conclusions on this new model gauges, a last plot (Fig: 98) is presented proving what this and displays the future possibilities and potentials this new gauge has.
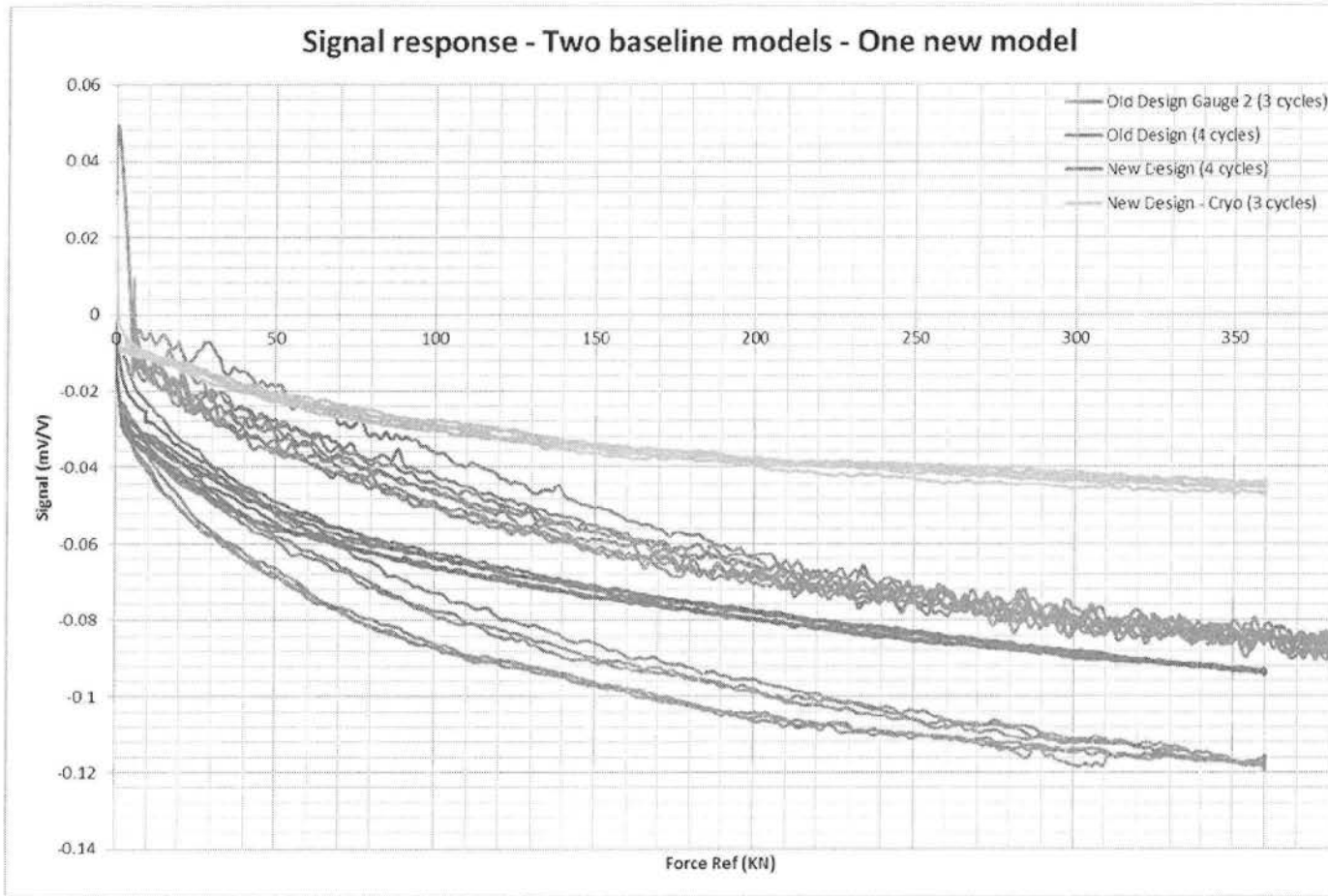
Figure 98: Display of the measured signal of the gauges that were compared in the previous paragraphs (red and purple curves). Additionally the curve in green displays the cryogenic response of the same "glue free" gauge while the blue curve displays the typical response a baseline gauge usually has.

Epilogue

This last section of this thesis has begun by explaining various problems and difficulties the capacitive gauges manufactured with the use of glue are presenting. The fact that has been reported in other MML documents as well in the past is that thethickness of the glue layers and their manual application, have a great impact on the response of the gauge. In order to minimize this dependence various propositions and suggestions have been proposed, including ideas such as replacing the adhesive with a different one having different properties and even change the way it is applied.Within this thesis the idea of not using glue at all has been tested and proved to be working. Even though the results are not satisfactory enough yet, by finding a more efficient way to seal the new gauges, a real optimization in every way will be achieved either it is from the manufacturing or the response point of view. Synopsizing the results and conclusions, the pros and cons of these gauges are:

Pros:

- Simplified, faster and much easier manufacturing procedure.
- The process of manufacturing can be restarted if an assembling mistake is made.
- No alternation or degradation of the sensor after repetitive measurements.
- A smaller number of random factors affect the outcome.
- Almost non existing hysteresis error, with a much smoother and stable signal.
- Decreased thickness due to the lack of the glue layers.

Cons:

- Increased non active area due to the way they are bonded together. Having an extra surface as interaction point by using bigger external layers of kapton to seal the gauge, might be a problem with the limited space available inside the cavities of the magnets.
- Two yet unsolved problems that have to do with the way these gauges are being manufactured.
- Due to these problems the response is not matching the best made baseline gauges.
- The stiffness of the gauge has been decreased. Their endurance in harsh environments has not been tested in real measurements yet,although the fact that after several cold cycles they still faction perfectly, is promising.

Concluding, for further optimization of the capacitive gauges in the future, the people from the MML should focus in two directions. One of these directions has already been explained before and has to do with finding a way to create vacuum inside the gauge to avoid the initial and sudden signal step, reduce the zero drift error and better maintain the assembly by using the atmospheric pressure. Mutually related to this activity is the sealing of the gauge that needs to be hermetic and airtight.

The second direction is to find an alternative way to connect the gauges with the Wheatstone bridge. When a capacitive gauge is connected to a different Wheatstone bridge, its response dramatically changes (even if the circuit is having the same value resistors) and needs recalibration in both room temperature and cryogenic conditions. Furthermore, the long cables that are being used to connect the gauges to the bridges playing an active part to the circuit, during the cool down and warm up phases of the magnets, they greatly unbalance the bridge and introduce significant random errors to the measurements. Therefore, a permanent connection to the resistors of the bridge is being suggested that will be in direct contact with the connectors of the gauges avoiding long cables and even soldering connections that most probably are the weakest points of a capacitive gauge, both mechanically and electrically speaking.

References

1. Karl Hoffmann, "An Introduction to Stress Analysis and Transducer Design using Strain Gauges", 2nd ed, Hottinger Baldwin Messtechnik GmbH, Darmstadt, 1989.

2. Raul MoronBallester, "Study for the improvement of the capacitive pressure gauges' performance and the design of an automated compressing system for the calibration of force sensors at the Mechanical Measurements Lab at CERN, Master Thesis, 2012.

3. Ιωάννης Κ. Στεργίου & Κωνσταντίνος Ι. Στεργίου, "Στοιχείαμηχανών Ι", Σύγχρονη Εκδοτική, Αθήνα, 2003.

4. www.metalravne.com/selector/steels/steels/ecn35.html

5. www.HBM.com

6. http://en-dep.web.cern.ch/en-dep/Groups/MME/DEO/MECHANICAL-LAB/default.asp

7. http://www.vishaypg.com/micro-measurements/installation-accessories/adhesives

Annex A - Matlab code for the calibration analysis.

%%%Capacitive Gauge Calibration Algorithm%%%

%For information, questions or modifications about this algorithm, please

%contact "Kostas Velissaridis" at kostakis86@yahoo.gr

%!!!!!!!!!!!NOTE!!!!!!!!!!%

%Green text starting with % do not affect the algorithm and is being used for

%notes and directions like this one.


```matlab
clear all

clf

formatshortE

clc

%Starting commands that clear the memory of matlab

ctf=('\\cern.ch\dfs\Workspaces\m\MechanicalMeasurement\Data\2013\EDMS_13
04901\Calibration Tools');

df=(input('Input the directory of the export list excel file: ','s'));

%Requests the user to provide the defined folder where normally the

%exported raw Catman data from RT and Cryocalibrations, are located.

cd(ctf);

copyfile('xlsPasteTo.m',df,'f')

cd(df);

if exist('Certificate.xlsx','file')

cd(df);

else

cd(ctf);

copyfile('Certificate.xlsx',df)
```

```
end

cd(df);
```

%Sets the current Matlab folder to the defined one. Also creates

%the necessary files needed for the procedure to be completed.

```
IRD=importdata(input('Input the full name (ending with .XLSX) of the exported list
EXCEL file: ','s'));
```

%Imports all the raw data coming from Catman's export-list. This command requests from the user the name of the raw data XLSX file.

```
RD=IRD.data;
```

%Separates numerical and string data.

```
SV1=0:25:200;
```

```
SV=SV1';
```

%Inputs the Calibration Loading Steps - Stress values in MPa.

```
Area=input('Input the area of the gauge in (mm^2): ');
```

%The area of the gauge is being requested from the user with this command.

```
FV=SV*Area;
```

%Calculates the Calibration Loading Steps - Force values in N

```
X1=RD(161:191,1:10);
```

```
X2=RD(161:191,11:20);
```

```
X3=RD(161:191,21:30);
```

```
X4=RD(161:191,31:40);
```

```
X5=RD(161:191,41:50);
```

```
X6=RD(161:191,51:60);
```

```
i300=zeros(31,10);
```

```
i300(:,1)=RD(1501:1531,60);
```

%Separates and stores into a matrix all the useful signal values meaning from the 32nd to the 38th second (creep test values as well).

if X1 > -10000 & X2 > -10000 & X3 > -10000 & X4 > -10000 & X5 > -10000 & X6 > -10000 & i300 > -10000

STX1=[std(X1(:,1));std(X1(:,2));std(X1(:,3));std(X1(:,4));std(X1(:,5));std(X1(:,6));std(X1(:,7));std(X1(:,8));std(X1(:,9));std(X1(:,10))];

STX2=[std(X2(:,1));std(X2(:,2));std(X2(:,3));std(X2(:,4));std(X2(:,5));std(X2(:,6));std(X2(:,7));std(X2(:,8));std(X2(:,9));std(X2(:,10))];

STX3=[std(X3(:,1));std(X3(:,2));std(X3(:,3));std(X3(:,4));std(X3(:,5));std(X3(:,6));std(X3(:,7));std(X3(:,8));std(X3(:,9));std(X3(:,10))];

STX4=[std(X4(:,1));std(X4(:,2));std(X4(:,3));std(X4(:,4));std(X4(:,5));std(X4(:,6));std(X4(:,7));std(X4(:,8));std(X4(:,9));std(X4(:,10))];

STX5=[std(X5(:,1));std(X5(:,2));std(X5(:,3));std(X5(:,4));std(X5(:,5));std(X5(:,6));std(X5(:,7));std(X5(:,8));std(X5(:,9));std(X5(:,10))];

STX6=[std(X6(:,1));std(X6(:,2));std(X6(:,3));std(X6(:,4));std(X6(:,5));std(X6(:,6));std(X6(:,7));std(X6(:,8));std(X6(:,9));std(X6(:,10))];

%Since there are 30 values for each step in each cycle, a mean value is being used to fill the measurement values table (Figure 23).

%With the previous commands the standard deviation (SD) of these values is being calculated.

%These values are not included in the results and certificate.

%If the SD is needed for a cycle it can be called by typing in the command window STX1, STX2 (capital letters) and so on for all 6 cycles accordingly.

X1=[mean(X1(:,1));mean(X1(:,2));mean(X1(:,3));mean(X1(:,4));mean(X1(:,5));mean(X1(:,6));mean(X1(:,7));mean(X1(:,8));mean(X1(:,9));mean(X1(:,10))];

X2=[mean(X2(:,1));mean(X2(:,2));mean(X2(:,3));mean(X2(:,4));mean(X2(:,5));mean(X2(:,6));mean(X2(:,7));mean(X2(:,8));mean(X2(:,9));mean(X2(:,10))];

```matlab
X3=[mean(X3(:,1));mean(X3(:,2));mean(X3(:,3));mean(X3(:,4));mean(X3(:,5));me
an(X3(:,6));mean(X3(:,7));mean(X3(:,8));mean(X3(:,9));mean(X3(:,10))];


X4=[mean(X4(:,1));mean(X4(:,2));mean(X4(:,3));mean(X4(:,4));mean(X4(:,5));me
an(X4(:,6));mean(X4(:,7));mean(X4(:,8));mean(X4(:,9));mean(X4(:,10))];


X5=[mean(X5(:,1));mean(X5(:,2));mean(X5(:,3));mean(X5(:,4));mean(X5(:,5));me
an(X5(:,6));mean(X5(:,7));mean(X5(:,8));mean(X5(:,9));mean(X5(:,10))];


X6=[mean(X6(:,1));mean(X6(:,2));mean(X6(:,3));mean(X6(:,4));mean(X6(:,5));me
an(X6(:,6));mean(X6(:,7));mean(X6(:,8));mean(X6(:,9));mean(X6(:,10))];

    %Begins the calculation of the measurement values (Figure 23). It fills each
cell with the mean value of the 30 gathered in the calibration process.

    i300=mean(i300(:,1));

    i30=X6(10,1);

    %Calculated the values i30 and i300

MeasurementValues=[X1 X2 X3 X4 X5 X6];

SDMeasurementValues=[STX1 STX2 STX3 STX4 STX5 STX6];

    %These commands gather the measuring values for easy display.

Xr=(X1+X3+X5)/3;

    %Calculates the values Xr

subplot(2,1,1)

set(gcf, 'Units', 'centimeters');

set(gcf, 'PaperPositionMode', 'auto');

set(gcf,'Position',[12 12 2.3*4 9])

title('Calibration curve')

ylabel('Resulting Force (KN)')

xlabel('Gauge Signal (mV/V)')

grid on
```

hold on

    %Prepares the dimensions, titles, and label names of the plot results.

    p=polyfit(FV/1000,Xr(1:9),1);

slope=p(1,1);

    %Calculates the slope of the gauge (assuming linear correlation) in (mV/V)/KN.

disp('The curve fitting shall be linear or 3rd degree?')

deg=input('Type 1 for linear or 3 for a 3rd degree polynomial curve fitting:','s');

disp('Is this a Room temperature or a cryogenic calibration analysis?')

temp=input('Type 1 for RT or 2 for cryo:','s');

ifdeg=='1'

    p4=polyfit(Xr(1:9),FV/1000,1);

    p3=p;

disp('The coefficients of the linear fitting curve F(s)=a*s+b (Where s is signal and F the Force) are:')

disp(p4)

elseifdeg=='3'

    p4=polyfit(Xr(1:9),FV/1000,3);

    p3=polyfit(FV/1000,Xr(1:9),3);

disp('The coefficients of the third degree polynomial fitting curve F(s)=a*s^3+b*s^2+c*s+d (Where s is signal and F the Force) are:')

disp(p4)

else

disp('Error: It is only possible for now to use linear or 3rd degree polynomial fitting, please restart the program and type either 1 or 3 when asked again')

end

    %With these commands the user has the option to either use a linear or a 3rd degree polynomial curve fitting.

    %Also returns the coefficients of the curve fitting trend line.

```
XA1=polyval(p4,Xr(1:9));
```

%Interpolates the measured values in the curve fitting trend line created before.

```
Xa=polyval(p3,FV/1000);
```

%Calculates the Xa values.

```
fig1=plot(Xr(1:9,1),FV/1000,'r*',Xr(1:9),XA1,'g-');
```

%Plots the measuring values in a Force VS Signal diagram. The points measured are displayed as red *.

```
Xwr=(X1+X2)/2;
```

%Calculates the Xwr values.

```
Xmax=zeros(9,1);

Xmin=zeros(9,1);
```

%Fills 2 arrays, Xmax and Xmin, with zeros to speed the process while filling them with the real values.

```
A=zeros(9,3);

for i=1:9

A(i,1:3)=[(X1(i,1)) (X3(i,1)) (X5(i,1))];

Xmax(i,1)=max(A(i,1:3));

Xmin(i,1)=min(A(i,1:3));

end

clear A

clear i
```

%Calculates the values Xmax, Xmin.

```
b=abs((Xmax-Xmin)./Xr(1:9,1))*100;

b1=abs((X2-X1)./Xwr)*100;

b1=b1(1:9,1);
```

%Calculation of the values b, b1.

```
fc=(Xr(1:9,1)-Xa)./Xa.*100;
```

```matlab
XN=[X1(9,1);X2(9,1);X3(9,1);X4(9,1);X5(9,1);X6(9,1)];

XN=max(XN);

c=abs((i300-i30)/XN)*100;

%Calculation of the values fc XN and c

If=[X1(10,1);X2(10,1);X3(10,1);X4(10,1);X5(10,1);X6(10,1)];

lo=[X1(1,1);X2(1,1);X3(1,1);X4(1,1);X5(1,1);X6(1,1)];

f0=abs((If-lo)/XN*100);

f0=max(f0);

%Calculation of the values If, lo and f0

r=abs(5/2^24/slope);

%Calculation of the resolution of the gauge in KN.

%5 is the range of the output signal of the bridge (mV/V) while 2^24 stands for
the bit resolution of the DAQ system.

u1=0.0002*FV/1000;

u1=u1(1:9,1);

u2=FV(9)/1000/abs(XN)*sqrt((1/6)*((X1-Xr).^2+(X3-Xr).^2+(X5-Xr).^2));

u2=u2(1:9,1);

u3=b1.*FV(1:9,1)/100000/sqrt(3);

u4=r/sqrt(6);

u4(1:9,1)=u4;

u5=c.*FV/100000/sqrt(3);

u6=f0*FV/100000;

u7=abs((Xr(1:9,1)-Xa)./Xr(1:9,1)).*FV/1000;

%Calculation of the values from u1 to u7 in KN

uc=sqrt(u1.^2+u2.^2+u3.^2+u4.^2+u5.^2+u6.^2+u7.^2);

%Calculation of the combined standard uncertainty uc

p1=polyfit(FV/1000,uc,1);
```

```matlab
ucFV=polyval(p1,FV/1000);

    %Interpolates the values of the linear curve fitting that will be used for the
combined standard uncertainty uc.

hold off

subplot(2,1,2)

    fig2=plot(FV/1000,uc,'r*',FV/1000,ucFV,'g-');

xlabel('Force Reference (KN)')

ylabel('uc (KN)')

title('Combined standard uncertainty "uc" vs Force range')

grid on

    %Creates the second graph with the uc VS Force reference and also displays
the linear curve fitting.

disp('The coefficients a,b belonging to the function: uc(F)=a*F+b accordingly
are:')

disp(p1)

    %Returns the coefficients of the uncertainty's linear trend line

disp('Please wait for the Certificate...')

    CalcValues1=[FV/1000 Xr(1:9,1) Xwr(1:9,1) Xmax(1:9,1) Xmin(1:9,1) b(1:9,1)
b1(1:9,1) Xa(1:9,1) fc(1:9,1)];

    CalcValues2=[u1 u2 u3 u4 u5];

    CalcValues3=[u6 u7 uc];

%Gathering of all the data for easier display in the certificate.

if temp=='1'

xlswrite('Certificate.xlsx',MeasurementValues,'Measured values - RT','C5:H14')

xlswrite('Certificate.xlsx',FV/1000,'Measured values - RT','A5:A13')

xlswrite('Certificate.xlsx',i30,'Measured values - RT','A17:A17')

xlswrite('Certificate.xlsx',i300,'Measured values - RT','E17:E17')

xlswrite('Certificate.xlsx',CalcValues1,'Calculated values - RT','A3:I11')
```

```
xlswrite('Certificate.xlsx',FV/1000,'Calculated values - RT','A13:A21')

xlswrite('Certificate.xlsx',XN,'Calculated values - RT','B13:B13')

xlswrite('Certificate.xlsx',f0,'Calculated values - RT','C13:C13')

xlswrite('Certificate.xlsx',c,'Calculated values - RT','D13:D13')

xlswrite('Certificate.xlsx',CalcValues2,'Calculated values - RT','E13:I21')

xlswrite('Certificate.xlsx',FV/1000,'Calculated values - RT','A23:A31')

xlswrite('Certificate.xlsx',CalcValues3,'Calculated values - RT','B23:D31')

else

xlswrite('Certificate.xlsx',MeasurementValues,'Measured values - Cryo','C5:H14')

xlswrite('Certificate.xlsx',FV/1000,'Measured values - Cryo','A5:A13')

xlswrite('Certificate.xlsx',i30,'Measured values - Cryo','A17:A17')

xlswrite('Certificate.xlsx',i300,'Measured values - Cryo','E17:E17')

xlswrite('Certificate.xlsx',CalcValues1,'Calculated values - Cryo','A3:I11')

xlswrite('Certificate.xlsx',FV/1000,'Calculated values - Cryo','A13:A21')

xlswrite('Certificate.xlsx',XN,'Calculated values - Cryo','B13:B13')

xlswrite('Certificate.xlsx',f0,'Calculated values - Cryo','C13:C13')

xlswrite('Certificate.xlsx',c,'Calculated values - Cryo','D13:D13')

xlswrite('Certificate.xlsx',CalcValues2,'Calculated values - Cryo','E13:I21')

xlswrite('Certificate.xlsx',FV/1000,'Calculated values - Cryo','A23:A31')

xlswrite('Certificate.xlsx',CalcValues3,'Calculated values - Cryo','B23:D31')

end

%Creation of the Certificate.

ifdeg=='3'

if temp=='1'

xlswrite('Certificate.xlsx',p4(1),'Certificate','A20')

xlswrite('Certificate.xlsx',p4(2),'Certificate','B20')

xlswrite('Certificate.xlsx',p4(3),'Certificate','C20')
```

```
xlswrite('Certificate.xlsx',p4(4),'Certificate','D20')

xlswrite('Certificate.xlsx',p1(1),'Certificate','F20')

xlswrite('Certificate.xlsx',p1(2),'Certificate','H20')

xlsPasteTo('Certificate.xlsx','Certificate',2.26*4,9,'A27')

else

xlswrite('Certificate.xlsx',p4(1),'Certificate','A23')

xlswrite('Certificate.xlsx',p4(2),'Certificate','B23')

xlswrite('Certificate.xlsx',p4(3),'Certificate','C23')

xlswrite('Certificate.xlsx',p4(4),'Certificate','D23')

xlswrite('Certificate.xlsx',p1(1),'Certificate','F23')

xlswrite('Certificate.xlsx',p1(2),'Certificate','H23')

xlsPasteTo('Certificate.xlsx','Certificate',2.26*4,9,'F27')

end


else

if temp=='1'

xlswrite('Certificate.xlsx',p4(1),'Certificate','J20')

xlswrite('Certificate.xlsx',p4(2),'Certificate','L20')

xlswrite('Certificate.xlsx',p1(1),'Certificate','O20')

xlswrite('Certificate.xlsx',p1(2),'Certificate','Q20')

xlsPasteTo('Certificate.xlsx','Certificate',2.26*4,9,'J27')

else

xlswrite('Certificate.xlsx',p4(1),'Certificate','J23')

xlswrite('Certificate.xlsx',p4(2),'Certificate','L23')

xlswrite('Certificate.xlsx',p1(1),'Certificate','O23')

xlswrite('Certificate.xlsx',p1(2),'Certificate','Q23')

xlsPasteTo('Certificate.xlsx','Certificate',2.26*4,9,'O27')
```

end

end

%The if command was used to fill the coefficients of either the 1rst or the 3rd deg polynomial fitting that the user chose before.

%Also the secondary "if" commands were used so the program will locate the correct positions of the

%coefficients in the certificate, either they are for RT or Cryo temps.

hgexport(1,'Calibration - Figure')

hgexport(1,'-clipboard')

%Saves the figure (".eps" file in the defined folder) and transfers it to the clipboard.

disp('The Certificate is ready inside the defined folder and the figure results are also in the clipboard')

disp('If you want to have them in the clipboard at any time, copy/paste below: hgexport(1,"-clipboard")')

disp('Repeat the algorithm to fill information both for cryo and RT calibrations (in case it is needed)')

%This is the end of the procedure and the certificate is now completed unless a short circuit was detected in the raw data.

%The next commands check and display the position of the short circuited values (if any exist).

else

for i=1:10

for j=1:31

if X1(j,i)< -10000

disp('The value in cycle 1, row and loading step accordingly:')

disp(209+j)

disp(i)

```matlab
disp('is a short circuit')
end
end
end
clear i
clear j
for i=1:10
for j=1:31
if X2(j,i)< -10000
disp('The value in cycle 2, row and loading step accordingly:')
disp(209+j)
disp(i)
disp('is a short circuit')
end
end
end
clear i
clear j
for i=1:10
for j=1:31
if X3(j,i)< -10000
disp('The value in cycle 3, row and loading step accordingly:')
disp(209+j)
disp(i)
disp('is a short circuit')
end
end
```

```
end

for i=1:10

for j=1:31

if X4(j,i)< -10000

disp('The value in cycle 4, row and loading step accordingly:')

disp(209+j)

disp(i)

disp('is a short circuit')

end

end

end

clear i

clear j

for i=1:10

for j=1:31

if X5(j,i)< -10000

disp('The value in cycle 5, row and loading step accordingly:')

disp(209+j)

disp(i)

disp('is a short circuit')

end

end

end

clear i

clear j

for i=1:10

for j=1:31
```

```matlab
        for j=1:31

            if X6(j,i)< -10000

                disp('The value in cycle 6, row and loading step accordingly:')

                disp(209+j)

                disp(i)

                disp('is a short circuit')

            end

        end

    end

    clear i

    clear j

    for i=1:10

        for j=1:31

            if i300(j,i)< -10000

                disp('The value while performing the creep test in cycle 6, in row')

                disp(1519+j)

                disp('is a short circuit')

            end

        end

    end

    clear i

    clear j

    disp('It is suggested to manually fix these values in the ".XLSX" or if there are
plenty, the gauge is not working properly and therefore it should be disposed.')

end

%Checks for potential short circuits and warns - guides the user if any exists.
```
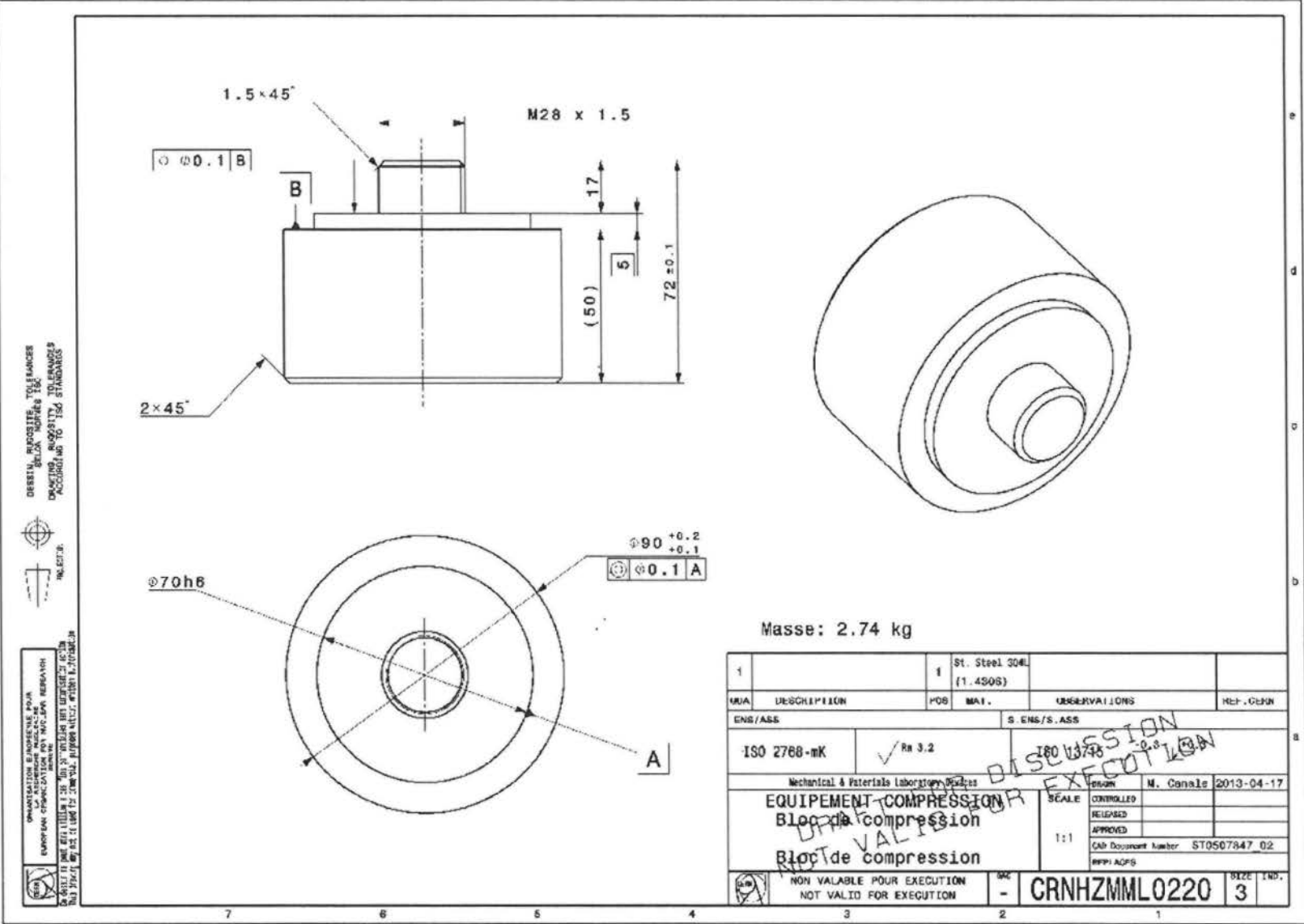
1.5×45°

M28 x 1.5

⌖ ⌀0.1 B

B

17

(50)

5

72 ±0.1

2×45°

⌀90 +0.2 +0.1

◎ ⌀0.1 A

⌀70h6

A

Masse: 2.74 kg

1			1	St. Steel 304L (1.4306)		
QUA	DESCRIPTION		POS	MAT.	OBSERVATIONS	REF.CERN

ENS/ASS   S.ENS/S.ASS

ISO 2768-mK   √ Rn 3.2   ISO 1302   -0.3

Mechanical & Materials Laboratory Service

EQUIPEMENT COMPRESSION	SCALE	DRAWN	M. Canale	2013-04-17
Bloc de compression		CONTROLLED		
		RELEASED		
Bloc de compression	1:1	APPROVED		
		CAD Document Number	ST0507847_02	
		RFP: ACFS		

NON VALABLE POUR EXECUTION
NOT VALID FOR EXECUTION   -   CRNHZMML0220   3

B-B

$30^{+0.2}_{+0.1}$

2×R15

$\phi 60^{+0.1}_{0}$

$\oslash \phi 0.005\ B$

2×45°

10

R0.5

87

48

$\parallel 0.1\ A$
0.05

20

28

ϕ $\phi 0.2\ A$

3.9

1×45°

f 0.05

A

$\phi 70$ h6

B

$\phi 140$

2×$\phi 31$
$\phi 0.5\ A\ B$

$\phi 100$

2×$\phi 17$
$\phi 0.2\ A\ B$

B

B
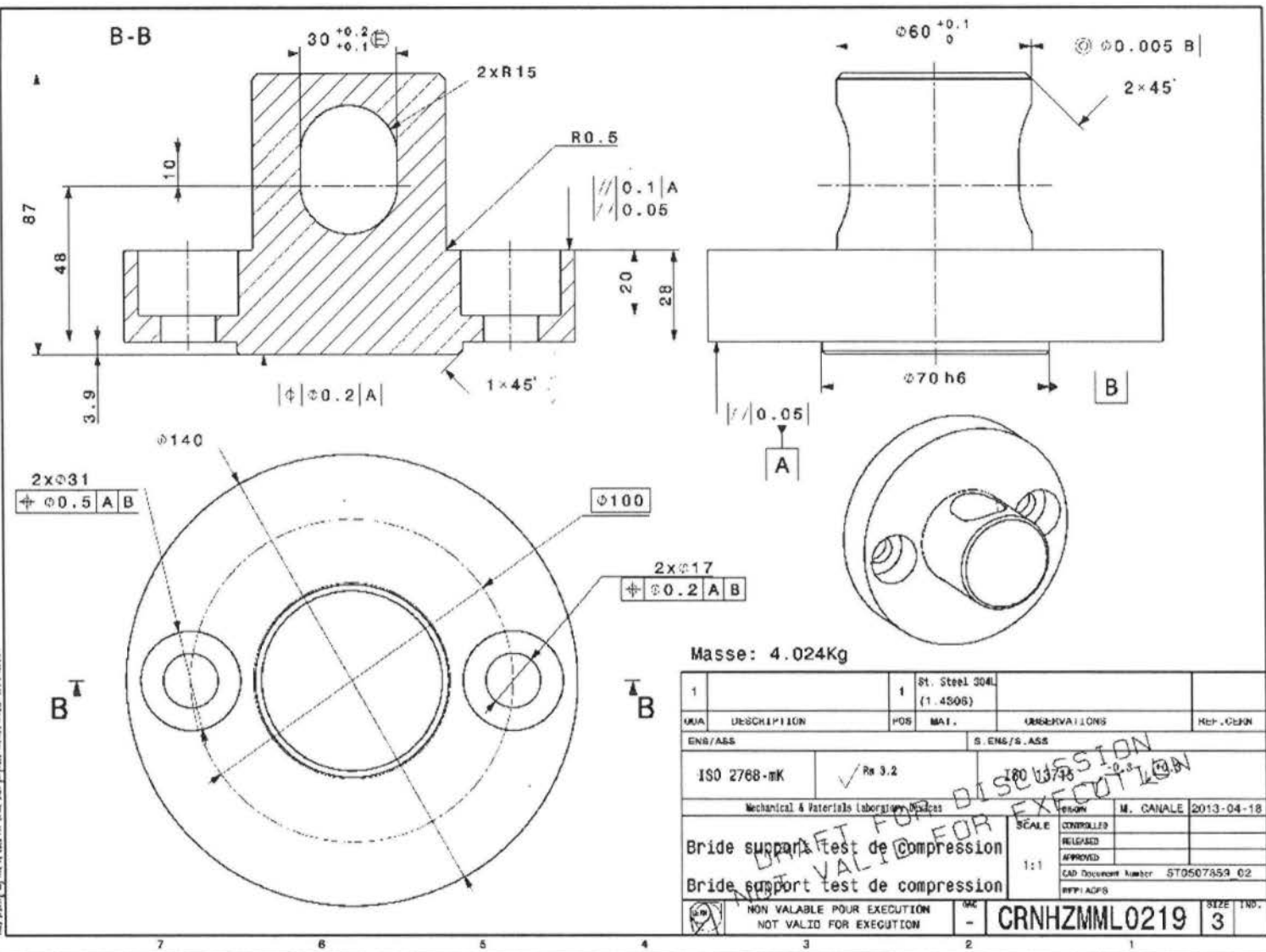
Masse: 4.024Kg

1		1	St. Steel 304L (1.4306)		
QUA	DESCRIPTION	POS	MAT.	OBSERVATIONS	REF.CERN
ENS/ASS				S.ENS/S.ASS	

ISO 2768-mK	Ra 3.2	ISO 1370

Mechanical & Materials Laboratory Services		DESIGN	M. CANALE	2013-04-18
		SCALE	CONTROLLED	
Bride support test de compression			RELEASED	
			APPROVED	
Bride support test de compression		1:1	CAD Document Number	ST0507859 02
			REF: AOFS	

NON VALABLE POUR EXECUTION
NOT VALID FOR EXECUTION

CRNHZMML0219

SIZE 3 IND.

Section view C-C

Section view A-A
Scale: 2:1

Detail B
Scale: 4:1

Detail D
Scale: 5:1

Masse=0.349kg

EQUIPMENT COMPRESSION
BOTTOM TOOL 15mm
OUTILLAGE COMPRESSION
Outillage inferieur 15mm

NON VALABLE POUR EXECUTION
NOT VALID FOR EXECUTION

CRNHZMML0223

C-C (1 : 1)   D (4 : 1)

B-B (1 : 1)

50

(4x) Ø11,00

⊕ Ø0,2 A B

(6x) 2 X 45°

(4x) R1

80,4 +0,2 -0,0

35,2 +0,1 -0,0

10 MAX

100

150

156

39,8 ± 0,1

(4x) Ø8,00

30

10

⊕ Ø0,2 A B

(4x) Ø4,50

10,5

35

(2x) M3

⊕ Ø0,05 C B

10

5 ± 0,1

Mass=0.362 kg

0,4

0,3

⊘ 0,01
// 0,02 C

⊘ 0,01
// 0,02 C

⊕ 0,1 A B
= 0,1

A-A (2 : 1)

31,6 ± 0,1

⊕ 0,2 C

8

1,6 / (√)

Designed by	Checked by	Approved by	Date	Date	
K.Velissaridis				18/09/2013	
CERN			small support		Edition	Sheet 1 / 1

Annex C – HV hardness conversion table.

Tabelle Nr. 25

| Vickershärtezahlen Hv | | | | Diamantpyramide 136° | | | | | | Prüfkraft |

Diagonale mm	0	1	2	3	4	5	6	7	8	9
0,30	2060	2047	2033	2020	2007	1993	1980	1968	1955	1942
0,31	1930	1917	1905	1893	1881	1869	1857	1845	1834	1822
0,32	1811	1800	1788	1777	1766	1756	1745	1734	1724	1713
0,33	1703	1693	1682	1672	1662	1652	1643	1633	1623	1614
0,34	1604	1595	1585	1576	1567	1558	1549	1540	1531	1522
0,35	1514	1505	1497	1488	1480	1471	1463	1455	1447	1439
0,36	1431	1423	1415	1407	1400	1392	1384	1377	1369	1362
0,37	1355	1347	1340	1333	1326	1319	1312	1305	1298	1291
0,38	1284	1277	1271	1264	1258	1251	1245	1238	1232	1225
0,39	1219	1213	1207	1201	1195	1189	1183	1177	1171	1165
0,40	1159	1153	1147	1142	1136	1131	1125	1119	1114	1108
0,41	1103	1098	1092	1087	1082	1077	2072	1067	1061	1056
0,42	1051	1046	1041	1036	1031	1027	1022	1017	1012	1008
0,43	1003	998	994	989	985	980	975	971	967	962
0,44	958	953	949	945	941	936	932	928	924	920
0,45	916	912	908	904	900	896	892	888	884	880
0,46	876	873	869	865	861	858	854	850	857	843
0,47	839	836	832	829	825	822	818	815	812	808
0,48	805	802	798	795	792	788	785	782	779	775
0,49	772	769	766	763	760	757	754	751	748	745
0,50	742	739	736	733	730	727	724	721	719	716
0,51	713	710	707	705	702	699	696	694	691	688
0,52	686	683	681	678	675	673	670	668	665	663
0,53	660	658	655	653	650	648	645	643	641	638
0,54	636	634	631	629	627	624	622	620	617	615
0,55	613	611	609	606	604	602	600	598	596	593
0,56	591	589	587	585	583	581	579	577	575	573
0,57	571	569	567	565	563	561	559	557	555	553
0,58	551	549	547	546	544	542	540	538	536	535
0,59	533	531	529	527	526	524	522	520	519	517
0,60	515	513	512	510	508	507	505	503	502	500
0,61	498	497	495	493	492	490	489	487	486	484
0,62	482	481	479	478	476	475	473	472	470	469
0,63	467	466	464	463	461	460	458	457	456	454
0,64	453	451	450	449	447	446	444	443	442	440
0,65	439	438		435		432	431	430	428	427
0,66	426	424	423	422	421	419	418	417	416	414
0,67	413	412	411	409	408	407	406	405	403	402
0,68	401	400	399	398	396	395	394	393	392	391
0,69	389	388	387	386	385	384	383	382	381	380
0,70	378	377	376	375	374	373	372	371	370	369
0,71	368	367	366	365	364	363	362	361	360	359
0,72	358	357	356	355	354	353	352	351	350	349
0,73	348	347	346	345	344	343	342	341	340	340
0,74	339	338	337	336	335	334	333	332	331	331
0,75	330	329	328	327	326	325	324	324	323	322
0,76	321	320	319	319	318	317	316	315	314	314
0,77	313	312	311	310	310	309	308	307	306	306
0,78	305	304	303	302	302	301	300	299	299	298
0,79	297	296	296	295	294	293	293	292	291	290
0,80	290	289	288	288	287	286	285	285	284	283
0,81	283	282	281	281	280	279	278	278	277	276
0,82	276	275	274	274	273	272	272	271	270	270
0,83	269	269	268	267	267	266	265	265	264	263
0,84	263	262	262	261	260	260	259	258	258	257
0,85	257	256	255	255	254	254	253	252	252	251
0,86	251	250	250	249	248	248	247	247	246	246
0,87	245	244	244	243	243	242	242	241	241	240
0,88	239	239	238	238	237	237	236	236	235	235
0,89	234	234	233	233	232	231	231	230	230	229
0,90	229	228	228	227	227	226	226	225	225	224
0,91	224	223	223	222	222	221	221	221	220	220
0,92	219	219	218	218	217	217	216	216	215	215
0,93	214	214	213	213	213	212	212	211	211	210
0,94	210	209	209	209	208	208	207	207	206	206
0,95	205	205	205	204	204	203	203	202	202	202
0,96	201	201	200	200	200	199	199	198	198	197
0,97	197	197	196	196	195	195	195	194	194	193
0,98	193	193	192	192	192	191	191	190	190	190
0,99	189	189	188	188	188	187	187	187	186	186

Die am WOLPERT-Härteprüfer DIA TESTOR 2 Rc vorhandene Laststufe für 100 kg dient zur Prüfung nach Rockwell B und ergibt nur mit Vorlast einschl. Meßuhr 100 kg Belastung.

Für Vickersprüfungen ist daher diese Laststufe nur anwendbar, wenn die Prüfung wie eine Rockwellprüfung ausgeführt, der Eindruck aber an der Mattscheibe ausgewertet wird.

Beim DIA TESTOR 2n (ohne Rockwelleinrichtung) trifft dies nicht zu und es kann die Tabelle ohne Einschränkung benutzt werden.

100 kp